ROLE OF ADVANCED MRI SEQUENCES IN THE CHARACTERISATION OF ADNEXAL MASSES

A THESIS SUBMITTED TO THE BABA FARID UNIVERSITY OF

HEALTH SCIENCES, FARIDKOT (PUNJAB)

FOR THE AWARD OF DEGREE OF

MD

IN

RADIODIAGNOSIS

BY

DR SURYAVEER SINGH

SUPERVISOR

DR KAVITA SAGGAR

DEPARTMENT OF RADIODIAGNOSIS
DAYANAND MEDICAL COLLEGE AND HOSPITAL
LUDHIANA
(MAY, 2021)

DECLARATION

I declare that the thesis entitled "**ROLE OF ADVANCED MRI SEQUENCES IN THE CHARACTERISATION OF ADNEXAL MASSES**" has been prepared by me under the guidance of **Dr. Kavita Saggar**, Professor & Head, Department of Radiodiagnosis, Dayanand Medical College and Hospital, Ludhiana. No part of this thesis has formed the basis for the award of any degree previously.

_____

Dr. Suryaveer Singh
Department of Radiodiagnosis
Dayanand Medical College & Hospital
Tagore Nagar
Ludhiana-141001
Punjab.

Date:

CERTIFICATE

I certify that **Dr. Suryaveer Singh** has prepared his thesis entitled "**ROLE OF ADVANCED MRI SEQUENCES IN THE CHARACTERISATION OF ADNEXAL MASSES**" for the award of degree of MD in Radiodiagnosis, under my guidance. He has carried out the work at the Department of Radiodiagnosis, Dayanand Medical College & Hospital, Ludhiana.

Supervisor

Dr. Kavita Saggar
Professor & Head
Department of Radiodiagnosis
DMCH, Ludhiana

Co-Supervisor(s)

Dr. Ritu Dhawan Galhotra
Professor
Department of Radiodiagnosis
DMCH, Ludhiana

Dr. Ashima Taneja
Professor & Head
Department of Obst. & Gynae
DMCH, Ludhiana

Date:

ENDORSEMENT BY THE HEAD OF THE DEPARTMENT AND PRINCIPAL

This is to certify that the thesis entitled "**ROLE OF ADVANCED MRI SEQUENCES IN THE CHARACTERISATION OF ADNEXAL MASSES**" is a bonafide research work done by **Dr. Suryaveer Singh** under the guidance of **Dr**. **Kavita Saggar**, Professor & Head, Department of Radiodiagnosis, Dayanand Medical College & Hospital, Ludhiana.

HEAD OF DEPARTMENT

DR. KAVITA SAGGAR
Professor and Head
Department of Radiodiagnosis
DMCH, Ludhiana

PRINCIPAL

DR. SANDEEP PURI
Principal and Professor
Department of Medicine
DMCH, Ludhiana

Date:

COPYRIGHT

Declaration by the Candidate

I hereby declare that the Baba Farid University of Health Sciences, Faridkot, shall have the rights to preserve, use and disseminate this thesis in print or electronic format for academic / research purpose.

Dr. Suryaveer Singh
Department of Radiodiagnosis
Dayanand Medical College & Hospital
Tagore Nagar
Ludhiana-141001
Punjab.

Date:

© Baba Farid University of Health Sciences,

Faridkot

Dedicated

to

my Family

&

Teachers

ACKNOWLEDGEMENT

It is not a mere formality to write an acknowledgement but it is my sacred duty to pay my debt of gratitude from the depth of my heart to my teachers, who have encouraged and inspired me at every step.

Words are insufficient to express my gratitude with great reverence to my supervisor **Dr. Kavita Saggar**, Professor & Head of Radiodiagnosis, DMC&H, Ludhiana who not only served as my mentor, but also encouraged and advised me throughout the study. All her constant support, constructive criticism and indelible help at all stages have helped me immensely in the completion of this project. Her academic excellence, commitment to the subject as well as the department and readiness to teach is an example to all. I take great pride in expressing my gratitude to her.

I wish to express my profound gratitude to my Co-Supervisors **Dr. Ritu Dhawan Galhotra**, Professor of Radiodiagnosis and **Dr. Ashima Taneja**, Professor & Head of Obstetrics & Gynaecology, DMC&H, Ludhiana for their encouragement and guidance throughout the venture.

I wish to offer my sincere thanks to **Dr. Devinder Pal Singh Dhanota**, Assistant Professor, and **Dr. Chandan Kakkar**, Associate Professor, Department of Radiodiagnosis, DMC&H, Ludhiana, who have been valuable guides and teachers in the true sense of the word.

Many sincere thanks to my teachers Dr. Archana Ahluwalia, Dr. Kamini Gupta and Dr. Siddharth Prakash for their guidance and encouragement throughout my post-graduation.

I am extremely thankful and indebted to my beloved wife **Dr. Mehak Munjal**, whose constant love and encouragement keep me motivated. I am blessed to have someone as supportive as her as my companion.

Words are woefully inadequate to express my sense of gratitude to my parents, **Mr. Neeraj Jeet Munjal** and **Mrs. Amita Munjal**, for their eternal guidance, immense love, and blessings that have made me whatever I am today.

I wish to thank all of my seniors, batchmates and juniors for their unfailing help and constant support.

My special thanks to the MRI technicians in the Department of Radiodiagnosis, DMC&H who provided me all the valuable help.

I am extremely thankful to all the patients and volunteers who participated in this study. This project would have been unthinkable without their contribution.

I am also indebted to Ms. Namita and Mr. Naveen Bhatia for diligently helping me with the thesis.

Dr. Suryaveer Singh

ABBREVIATIONS

MRI: Magnetic Resonance Imaging

US: Ultrasonography

TVS: Transvaginal Sonography

DWI: Diffusion-Weighted Imaging

ADC: Apparent Diffusion Coefficient

DCE: Dynamic Contrast-Enhanced MRI

T2WI: T2-Weighted Image

T1WI: T1-Weighted Image

VIBE: Volume Interpolated Breath-hold Examination

SI: Signal intensity

ROI: Region of Interest

TIC: Time-Intensity Curve

CT: Computed Tomography

PET-CT: Positron Emission Tomography

PPV: Positive Predictive Value

NPV: Negative Predictive Value

KEY TO MASTERCHART

K/c/o: Known case of

US: Ultrasonography

B/L: Bilateral

NA: Not applicable

SI: Signal Intensity

DWI: Diffusion-Weighted Imaging

ADC: Apparent Diffusion Coefficient

TIC: Time-Intensity Curve

e/o: Evidence of

Rt: Right

Lt: Left

ABSTRACT

Introduction: A large number of complex adnexal masses cannot be accurately characterized as benign or malignant on Ultrasonography. Evaluation with MRI, in particular with advanced sequences such as Diffusion-Weighted Imaging and Dynamic Contrast-Enhanced MRI is crucial in confidently characterizing the indeterminate masses.

Objective: To assess the role of advanced MRI sequences (DWI and DCE) in the characterisation of adnexal masses, into benign and malignant, with reference to histopathological examination wherever possible.

Materials and Methods: It was a prospective study of patients undergoing an MRI Pelvis for previously detected adnexal masses, referred to the Department of Radiodiagnosis, during a one-year period. Patients were imaged using a 3-Tesla MRI unit (Magnetom Skyra, Siemens, Germany) and the protocol included T1 weighted images with and without fat suppression in axial plane, T2 weighted images in all 3 planes, Diffusion-weighted images in axial plane in b-values of 50,400 and 800 s/mm^2 and Dynamic Contrast-Enhanced images.

Results: A purely cystic lesion, hypointense signal within the solid component on T2WI, absence of diffusion restriction, and Type I TIC on DCE were found to be statistically significant for the diagnosis of benignity ($p<0.05$). A predominantly cystic lesion with some solid component, predominantly solid lesion, intermediate SI within solid component on T2WI, presence of papillary projections, presence of diffusion restriction, and Type III TIC on DCE were proven to be statistically significant for the diagnosis of malignancy ($p<0.05$). While the accuracy of conventional MRI parameters based on solid-cystic nature of lesions ranged from 80.9% to 82.98%; that of T2 signal intensity within the solid component and presence of papillary projections were 78.95% and 87.1% respectively, diffusion restriction and TIC analysis on DCE yielded higher accuracies of 89.5% and 93.1%, respectively, with improved sensitivity and specificity as compared to the conventional MRI parameters.

Conclusion: Addition of DWI and DCE to the conventional MRI protocol seems to have significantly improved the accuracy of adnexal mass characterization, thereby playing a crucial role in determining the surgical strategy or feasibility of conservative management.

Keywords: Magnetic Resonance Imaging, Diffusion-Weighted Imaging, Dynamic Contrast-Enhanced, Apparent Diffusion Coefficient, Time-Intensity Curve, Ultrasonography.

TABLE OF CONTENTS

S. NO.	TOPIC	PAGES
I	INTRODUCTION	1-16
II	AIMS AND OBJECTIVES	17
III	REVIEW OF LITERATURE	18-31
IV	MATERIALS AND METHODS	32-39
V	OBSERVATIONS AND RESULTS	40-88
VI	DISCUSSION	89-103
VII	SUMMARY AND CONCLUSIONS	104-106
VIII	BIBLIOGRAPHY	107-118

APPENDICES - I

- PROFORMA
- MASTER CHART

APPENDICES - II

- APPROVAL LETTER OF THESIS PLAN
- THESIS PLAN

LIST OF TABLES

Table No.	Title	Page No.
1	MRI acquisition parameters	33
2	Age Distribution of Patients	40
3	Final diagnosis	42
4	Age distribution of patients with benign and malignant lesions	43
5	Presenting complaints	44
6	Mean CA-125 levels in benign and malignant lesions	46
7	Final diagnosis: Subtypes	47
8	Size comparison of benign and malignant lesions	49
9	Bilaterality in benign and malignant lesions	50
10a	Solid/cystic nature of lesions	51
10b	Comparison of solid/cystic nature in benign and malignant lesions	52
11a	T2 signal intensity of solid component	53
11b	Comparison of T2 signal intensity of solid component in benign and malignant lesions	54
12a	Marked T1 hyperintensity in cystic component	55
12b	Marked T1 hyperintensity in cystic component in benign and malignant lesions	56
13a	T2 shading	57
13b	T2 shading in benign and malignant lesions	58
14a	Thickened septa	59
14b	Thickened septa in benign and malignant lesions	60

15a	Hemorrhage	61
15b	Hemorrhage in benign and malignant lesions	62
16a	Papillary projections	63
16b	Papillary projections in benign and malignant lesions	64
17a	Ascites	65
17b	Ascites in benign and malignant lesions	66
18a	Diffusion restriction within solid component	67
18b	Comparison of Diffusion restriction within solid component in benign and malignant lesions	69
19a	Diffusion restriction in cystic component	70
19b	Comparison of Diffusion restriction in cystic component in benign and malignant lesions	71
20a	Low ADC signal in solid component	72
20b	Comparison of low ADC signal in solid component in benign and malignant lesions	73
21	Mean of mean ADC values in solid component in benign and malignant lesions	74
22a	Low ADC signal in cystic component	75
22b	Low ADC signal in cystic component in benign and malignant lesions	76
23	Mean of mean ADC values in cystic component in benign and malignant lesions	77
24a	Type of curve (TIC)	78
24b	Type of curve (TIC) in benign and malignant lesions	80
25a	Combination of intermediate T2 SI and presence of	81

	diffusion restriction in solid component	
25b	Combination of intermediate T2 SI and presence of diffusion restriction in solid component in benign and malignant lesions	82
26a	Combination of intermediate T2 SI, diffusion restriction and Type III TIC in solid component	83
26b	Combination of intermediate T2 SI, diffusion restriction and Type III TIC in solid component in benign and malignant lesions	84
27	Statistically significant parameters for the diagnosis of benignity	85
28	Statistically significant parameters for the diagnosis of malignancy	87

LIST OF FIGURES

Figure No.	Title	Page No
1	ROI placement on ADC maps	36
2a	ROI placement in DCE-MRI	37
2b	Time-Intensity Curve analysis	37
3	Types of Time-Intensity Curves	38
4	Age Distribution of Patients	41
5	Final diagnosis	42
6	Age distribution of patients with benign and malignant lesions	43
7	Presenting complaints	45
8	Mean CA-125 levels in benign and malignant lesions	46
9a	Final diagnosis: Benign lesions	48
9b	Final diagnosis: Malignant lesions	48
10	Size comparison of benign and malignant lesions	49
11	Bilaterality in benign and malignant lesions	50
12a	Solid/cystic nature of lesions	51
12b	Comparison of solid/cystic nature in benign and malignant lesions	52
13a	T2 signal intensity of solid component	53
13b	Comparison of T2 signal intensity of solid component in benign and malignant lesions	54
14a	Marked T1 hyperintensity in cystic component	55
14b	Marked T1 hyperintensity in cystic component in benign and malignant lesions	56
15a	T2 shading	57
15b	T2 shading in benign and malignant lesions	58
16a	Thickened septa	59
16b	Thickened septa in benign and malignant lesions	60

17a	Hemorrhage	61
17b	Hemorrhage in benign and malignant lesions	62
18a	Papillary projections	63
18b	Papillary projections in benign and malignant lesions	64
19a	Ascites	65
19b	Ascites in benign and malignant lesions	66
20a	Diffusion restriction within solid component	68
20b	Comparison of Diffusion restriction within solid component in benign and malignant lesions	69
21a	Diffusion restriction in cystic component	70
21b	Comparison of Diffusion restriction in cystic component in benign and malignant lesions	71
22a	Low ADC signal in solid component	72
22b	Comparison of low ADC signal in solid component in benign and malignant lesions	73
23	Mean of mean ADC values in solid component in benign and malignant lesions	74
24a	Low ADC signal in cystic component	75
24b	Low ADC signal in cystic component in benign and malignant lesions	76
25	Mean of mean ADC values in cystic component in benign and malignant lesions	77
26a	Type of curve (TIC)	79
26b	Type of curve (TIC) in benign and malignant lesions	80
27a	Combination of intermediate T2 SI and presence of diffusion restriction in solid component	81
27b	Combination of intermediate T2 SI and presence of diffusion restriction in solid component in benign and malignant lesions	82
28a	Combination of intermediate T2 SI, diffusion restriction and Type III TIC in solid component	83

28b	Combination of intermediate T2 SI, diffusion restriction and Type III TIC in solid component in benign and malignant lesions	84
29a	Statistically significant parameters for the diagnosis of benignity	86
29b	Accuracy of various MRI parameters for the diagnosis of benignity	86
30a	Statistically significant parameters for the diagnosis of malignancy	88
30b	Accuracy of various MRI parameters for the diagnosis of malignancy	88

INTRODUCTION

Adnexal masses represent a heterogeneous spectrum of conditions from gynecologic as well as nongynecologic origins and may be either benign or malignant. They are fairly common among women of all ages, but are more prevalent in the reproductive age group. The goal of radiological evaluation is to differentiate between benign and more serious conditions such as ovarian cancer.[1]

Adnexal mass lesions, in general, have a prevalence of 0.17% to 5.9% in asymptomatic women and 7.1% to 12% in symptomatic women.[2] Ovarian cancer is the seventh most common cancer worldwide. In fact, India has the 2nd highest incidence of ovarian cancer globally and the figures have been escalating [3] Five-year survival rates decrease dramatically from 90% in patients with stage I to 30-40% in stage III and IV disease. The near absence of symptoms in early stage and the lack of effective screening tools, both contribute to the poor overall survival.[4]

Anatomy

The adnexa includes the ovaries and certain other structures—paired fallopian tubes, broad and other parametrial ligaments, and the associated vascular structures. Pathology in this area may also be related to the uterus, bowel, retroperitoneum, or metastatic disease from other sites.[5]

Each ovary is ovoid in shape, measures approximately 5-15cc in volume and is composed of T2 hyperintense medulla and T2 hypointense peripheral cortex with multiple small follicles seen in the cortex. Ovaries are usually located in close proximity to the iliac vessels, near their bifurcation. Medially, the ovaries are adherent to fallopian tubes and the proper ovarian ligament, caudally to the broad ligament, and superolaterally to the suspensory ligament, which contains the ovarian vessels.[6]

Imaging Modalities

Accurate characterization of adnexal mass lesions is of utmost importance for deciding appropriate management and also in preoperative planning,

as it enables the surgeon to anticipate possible ovarian malignancy.[7] Masses felt to be benign can be managed expectantly or with minimal-access surgery.[8]

Several diagnostic modalities, including Ultrasonography (US), Computed Tomography (CT) and Magnetic Resonance Imaging (MRI) have been investigated as potential screening and diagnostic tools.

Ultrasonography

Ultrasonography (US), in particular, transvaginal sonography (TVS) in conjunction with color Doppler remains the first line as well as the most commonly used imaging modality for examining patients with adnexal lesions because of being relatively inexpensive, noninvasive, and widely available.[7,9]

Color Doppler with spectral analysis using indices such as *PI* (pulsatility indices) and *RI* (resistance indices) has been found to be helpful in yielding better characterization of ovarian neoplasms. Neovascularization in tumors results in a lower resistance to blood flow in malignant neoplasms because the newly formed tumoral vessels are devoid of muscular layer. Low impedance to blood flow with high peak systolic velocity is suggestive of malignancy, whereas moderate-to-high impedance to blood flow is seen in benign tumors.[10] Addition of color Doppler to conventional sonography has been found to be more predictive as well as specific for predicting malignancy than with conventional sonography alone.[11]

Certain simple and clinically useful ultrasound based rules for discriminating between benign and malignant adnexal masses have been agreed upon.

Five simple rules to predict malignancy (M-rules):

(1) irregular solid tumor

(2) ascites

(3) at least four papillary structures

(4) irregular multilocular–solid tumor with a largest diameter of at least 100 mm

(5) very high color content on color Doppler examination.

Five simple rules to suggest a benign tumor (B-rules):

(1) unilocular cyst

(2) presence of solid components where the largest solid component is < 7 mm in largest diameter

(3) acoustic shadows

(4) smooth multilocular tumor less than 100 mm in largest diameter

(5) no detectable blood flow on Doppler examination.[8]

US does an excellent job in helping to characterize a majority of masses as benign or malignant, but there are a substantial number of masses that remain “indeterminate”, that is, they cannot be confidently classified as either benign or malignant based on their morphology, or when their site of origin (whether from the ovary, uterus, or other pelvic structures) is not clearly established on US.[12] It has also been studied that there is an overlap of the Doppler US parameters between benign and malignant lesions.[13,14]

Computed Tomography (CT)

CT has a limited role in primary evaluation and characterization of sonographically indeterminate ovarian lesions [15], however, CT is the imaging modality of choice to evaluate the extent of the disease in pretreatment planning of ovarian malignancies, for predicting correct tumor staging as well as optimal cytoreduction.[16] CT is useful for the assessment of tumour burden, mapping of the distribution of metastatic disease and diagnosis of possible complications, such as bowel obstruction, hydronephrosis or venous thrombosis.[17]

PET-CT

The use of [18] F-FDG PET imaging, with reported sensitivity of 52–58% and specificity of 76–78%, is not recommended for primary detection of ovarian cancer.[18] However, the addition of PET to contrast-enhanced CT

has been shown to improve accuracy in preoperative staging.[19] Also, FDG PET, combined with CT, has a relatively high sensitivity and specificity in detecting recurrent ovarian carcinoma, and is thus the most accurate technique to evaluate for suspected recurrent ovarian cancer.[20]

Magnetic Resonance Imaging (MRI)

Magnetic resonance imaging (MRI) is an excellent modality for accurate tissue characterization. There is a powerful evidence base to support the use of MRI to investigate sonographically indeterminate adnexal masses for their better characterisation.[12]

US is limited by its low specificity for the diagnosis of benignity, which can vary from 60% to 95% and can result in as many as 20% of adnexal masses being classified as indeterminate because of poor tissue characterization. Many benign and malignant adnexal masses appear solid on US, and benign masses sometimes appear complex on sonography, thereby mimicking a malignancy.[21]

Majority of sonographically indeterminate masses are not rare and exotic, but common benign adnexal conditions. A few such indeterminate masses are mature teratomas with atypical features, hemorrhagic cysts in which adherent mural blood clots may mimic mural vegetations of malignancy, and fibrous masses (ovarian fibroma/ thecoma and subserosal uterine leiomyomas) whose solid nature raises concerns for malignancy.[3,12,13]

MR imaging has the ability to confidently differentiate fat, blood products, and fibrous content within adnexal masses, features that may have a complex appearance at US.[22] Conventional MR imaging sequences include T1-weighted, T2-weighted, and fat-suppressed T1-weighted images.

At MR imaging performed with conventional protocols, morphologic features that are indicative of benignity include:

1. High signal intensity on T1-weighted images (indicative of fat or blood) with subsequent loss of signal intensity on fat-suppressed images (indicative of fat in a mature cystic teratoma).[23,24]

2. High signal intensity on T1-weighted fat-suppressed images (indicative of blood in an endometrioma), and low signal intensity on T2-weighted images (indicative of either fibrous tissue in ovarian fibroma, fibrothecoma and Brenner's tumour or blood degradation products from repeated cyclical bleeding in endometrioma). In particular, solid adnexal tissue that demonstrates low signal intensity on T2-weighted images has been shown to be highly indicative of a benign or noninvasive lesion.[23]

MR morphologic features that are indicative of a malignant adnexal mass include:[22,25,26]

1. Presence of both solid and cystic areas within a lesion
2. Necrosis within a solid lesion
3. Papillary projections from the wall or septum of a cystic lesion
4. An irregular septum or wall
5. Multiple thickened (>3 mm) septations
6. Large size (>6 cm)
7. Bilateral lesions
8. Ascites, peritoneal disease, or lymphadenopathy

Among these morphologic features, papillary projections in a cystic adnexal lesion and the presence of ascites are considered most indicative of malignancy.[25,26]

Papillary projections have been found to be the single best predictors of an epithelial malignant neoplasm.[27]

Classification of ovarian tumours

On the basis of tumor origin, ovarian tumors are classified as[28]

1. Epithelial tumors
2. Germ cell tumors
3. Sex cord–stromal cell tumors
4. Metastatic tumors

1. Epithelial Tumors

Epithelial tumors represent 60% of all ovarian neoplasms and 85% of malignant ovarian neoplasms. These are rare before puberty; their prevalence increases with age and peaks in the sixth and seventh decades of life.

Subtypes include serous, mucinous, endometrioid, clear cell, and Brenner tumors.[28,29]

Epithelial ovarian tumors can be classified as benign (60%), malignant (35%), or borderline (low-malignant potential) (5%).[29]

Serous versus Mucinous Tumors

The two most common types of epithelial neoplasms are serous and mucinous tumors.

Benign serous cystadenoma: Manifests as a unilocular or multilocular cystic mass with homogeneous signal intensity of the locules, a thin regular wall or septum, and no endocystic or exocystic vegetation. Bilaterality is more common in serous than in mucinous tumours.[30]

Benign mucinous cystadenoma: Manifests as a multilocular cystic mass that has a thin regular wall and septa and has locules with their contents having different signal intensities, but has no endocystic or exocystic vegetation. Mucinous cystadenomas are usually larger than serous cystadenomas.[31]

Calcifications, representing psammoma bodies are seen more often in malignant serous tumors. Peritoneal carcinomatosis is more commonly seen in serous than in mucinous cystadenocarcinomas. Mucinous adenocarcinoma can rupture and is associated with pseudomyxoma peritonei.[32]

Benign serous and mucinous tumors are common, but benign endometrioid tumors are very rare, and all clear cell carcinomas are malignant.[29]

Endometrioid Carcinoma

They are almost always malignant. About 15%–30% are associated with synchronous endometrial carcinoma or endometrial hyperplasia [33] Endometrioid carcinoma is the most common malignant neoplasm arising from endometriosis, followed by clear cell carcinoma.[34] They have non-specific imaging findings and may be seen as a large, complex cystic mass with solid components. Thickened endometrium may also be seen on imaging.[29]

Clear Cell Carcinoma

They represent approximately 5% of ovarian carcinomas and are always malignant [35] Common imaging findings in clear cell carcinoma include a unilocular large cyst with solid papillary projections. The cyst margin is smooth, and signal intensity of its cystic component on T1-weighted images varies from low to very high. Marked T1 hyperintensity, if present, suggests the presence of background endometriosis.[36]

Brenner Tumor

They represent about 2%–3% of ovarian tumors and are rarely malignant. Brenner tumors are usually small (<2 cm) and discovered incidentally. They manifest as a multilocular cystic mass with a solid component or as a small, predominantly solid mass. On T2-weighted images, the dense fibrous stroma demonstrates low signal intensity. Extensive amorphous calcification may be present within the solid component.[37]

2. Germ Cell Tumors

They are the second most common group of ovarian neoplasms, representing 15%–20% of all ovarian tumors and are most frequently seen in children and adolescents. Subtypes include mature and immature teratomas, dysgerminoma and endodermal sinus (yolk sac) tumour. Of these, only mature teratoma is benign; however, it is by far the most common lesion in this group. All the other tumors are malignant.[38]

Mature Teratoma

They are unilocular, contain sebaceous material and are lined by squamous epithelium. A raised protuberance projecting into the cyst cavity is known as the Rokitansky nodule. Most of the hair, bone or teeth, when present, arise from this protuberance.[39] At MRI, the sebaceous component of dermoid cysts has very high signal intensity on T1-weighted images, with suppression on T1 fat-saturated images. Signal intensity of the sebaceous component on T2-weighted images is variable, while calcifications have low signal intensity.[40]

Immature Teratoma

Represent less than 1% of all teratomas, are most commonly seen in the first two decades of life. They have prominent solid components and may demonstrate internal necrosis or hemorrhage. On imaging, they are seen as a large, complex mass with cystic and solid components, small foci of fat and scattered calcifications; in contrast, calcification in mature teratomas is localized to mural nodules. These tumors grow rapidly and frequently demonstrate perforation of their capsule, with the tumor capsule not always well defined.[40]

Dysgerminoma

Dysgerminomas are rare ovarian tumors that occur predominantly in young women. In 5% cases, serum HCG levels may be elevated. Calcifications may be present in a speckled pattern. Characteristic imaging findings include a multilobulated solid mass with prominent fibrovascular septa.[41]

Endodermal Sinus Tumor

Endodermal sinus tumor, also known as yolk sac tumor, is a rare malignant ovarian tumor that usually occurs in the second decade of life. The tumor manifests as a large, complex abdomino-pelvic mass that contains both solid and cystic components. They grow rapidly and portend a poor prognosis. Most patients have an elevated serum α-fetoprotein level.[42]

3. Sex Cord–Stromal Tumors

These tumors represent approximately 8% of ovarian neoplasms and affect all age groups. The vast majority of sex cord stromal tumors are either benign (eg, fibrothecoma, sclerosing stromal tumor) or largely confined to the ovary at diagnosis (eg, granulosa cell tumor, Sertoli-Leydig cell tumor).[43]

Granulosa Cell Tumor

It is the most common malignant sex cord–stromal tumor as well as the most common estrogen-producing ovarian tumor. They occur predominantly in peri- and postmenopausal women. Imaging findings vary from solid masses, to tumors with varying degrees of hemorrhagic or fibrotic changes, to multilocular cystic lesions, to completely cystic tumors.[44] Unlike epithelial tumours, these are mostly confined to the ovary, do not have intracystic papillary projections, have less propensity for peritoneal seeding. Estrogenic effects on the uterus may manifest as uterine enlargement or as endometrial thickening or hemorrhage.[43]

Fibrothecoma

Fibroma and thecoma are forms of a spectrum of benign stromal tumors. Thecoma demonstrates estrogenic activity and few fibroblasts. In contrast, fibroma has no thecal cells and demonstrates no estrogenic activity and is associated with ascites or Meigs syndrome. Because of their abundant collagen contents, these tumors have very low signal intensity on T2-weighted images. Dense calcifications are often seen.[45] Ovarian fibromas show late and weak contrast enhancement on dynamic contrast enhanced MR, relative to myometrium and most fibroids.[46]

Ovarian masses with fibrous components include fibroma, fibrothecoma, cystadenofibroma, and Brenner tumor. Pedunculated uterine leiomyomas and broad-ligament leiomyomas frequently appear as adnexal or ovarian masses, Subserosal myomas are supplied by the vessels from the uterine arteries that course through the adjacent myometrium and may appear as the vessels that intervene between a myoma and the adjacent uterus.

Observation of these interface vessels seems to be useful in differentiating leiomyoma from ovarian fibroma.[47]

Sclerosing Stromal Tumor

These are rare benign ovarian tumors that occur predominantly in young women. MRI reveals a large mass with hyperintense cystic components and a heterogeneous solid component. On dynamic contrast-enhanced images, the tumor demonstrates early peripheral enhancement with centripetal progression.[48]

Sertoli-Leydig Cell Tumor

These occur in young women (<30 years of age) and are considered to be a low-grade malignancy. It is the most common virilizing tumor. However, only 30% of these tumors are hormonally active. On MR imaging, it is seen as a well-defined, enhancing solid mass with intratumoral cysts. Low T2 signal intensity at MR imaging reflects the extent of fibrous stroma.[49]

Collision Tumors

Collision tumor represents the coexistence of two adjacent but histologically distinct tumors with no histologic admixture at the interface. They are most commonly composed of teratoma and cystadenoma or cystadenocarcinoma. When an ovarian tumor demonstrates imaging findings that cannot be subsumed under one histologic type, especially in cases of ovarian teratoma, a collision tumor should be considered.[50]

4. Metastatic Ovarian Tumors

The colon and stomach are the most common primary tumor sites in ovarian metastasis, followed by the breast, lung, and contralateral ovary. Krukenberg tumors are metastatic tumors to the ovary that contain mucin-secreting “signet ring” cells and usually originate in the gastrointestinal tract. MR imaging reveals bilateral complex masses with hypointense solid components (dense stromal reaction) and internal hyperintensity (mucin) on T1- and T2-weighted MR images, respectively.[51]

Miscellaneous benign entities

Endometriosis

Endometriosis is defined as ectopic endometrial glandular tissue located outside of the uterus. It is estimated that up to 10% of premenopausal women are affected by endometriosis.[52] The most important MR sequence for its diagnosis is the fat-suppressed T1-weighted sequence; marked hyperintensity on this sequence is highly specific.[53]

Hemorrhagic cysts can also demonstrate T1-weighted hyperintensity and are the primary differential consideration in the diagnosis of endometriomas. However, hemorrhagic cysts tend to be inhomogeneous in internal signal and their T1-weighted hyperintense and T2-weighted hypointense signal are less marked.[54] High concentrations of extracellular methemoglobin in endometriomas from repeated cycles of hemorrhage produce the pronounced T2-weighted hypointensity, known as “shading,” that is not seen in hemorrhagic cysts.[55]

The presence of a hematosalpinx is near-diagnostic of endometriosis.[56] Nonenhancing fluid portions of endometriomas can frequently demonstrate diffusion restriction, and this feature should not raise concern for malignancy in the absence of enhancing soft tissue components.[57]

Apart from ovarian endometriomas, endometriotic implants (peritoneal and extraperitoneal) and adhesions are an important constituent of the disease process. Deep pelvic endometriosis, also known as deep infiltrating endometriosis, is defined as subperitoneal invasion by endometriotic lesions. It frequently affects fibromuscular pelvic structures, such as the rectovaginal septum and uterosacral ligaments (69.2% of cases), as well as vagina (14.5%), alimentary tract (predominantly rectosigmoid) (9.9%) and urinary tract (urinary bladder and distal ureters) (6.4%). Certain extraperitoneal pelvic sites such as the retrocervical area, along sciatic nerve and ischioanal fossa may also be involved.[58]

On T2-weighted images, solid endometriotic implants appear as hypointense masses with irregular margins due to the presence of

abundant fibrous tissue and smooth muscle proliferation. Intermingled hyperintense foci corresponding to dilated ectopic endometrial glands may be observed with T2-weighted images. On fat-suppressed T1-weighted images, these foci may have either high or low signal intensity, depending on the presence or absence of hemorrhagic contents, respectively.[59]

Cystadenofibromas

These are benign tumors that are commonly confused for malignancy at imaging. They are solid-cystic lesions; the solid portions comprise of fibrous tissue and appear hypointense on T2-weighted images, exhibit mild delayed homogeneous enhancement, and do not show restricted diffusion.[60]

Tubo-ovarian abscesses

These may present as an adnexal mass and can mimic cancer. They appear as thick walled multilocular cystic structure, their contents may show restricted diffusion. The abscess wall, septae and adjacent inflammatory changes strongly enhance after the administration of contrast material. Associated hydrosalpinx or pyosalpinx may also be present.[61,62]

Benign extraovarian lesions

Appendiceal mucoceles can present as incidental adnexal masses, communication with the cecum is diagnostic.[63]

Nerve sheath tumors may mimic adnexal lesions, however they may be confidently diagnosed based on their location along the known course of nerve roots, their high T2-weighted signal, and avid contrast enhancement.[60]

Peritoneal inclusion cysts typically arise in premenopausal women with pelvic adhesions that trap fluid released from ovarian cysts, resulting in collections of fluid around an ovary. Common causes include pelvic inflammatory disease, endometriosis, or prior pelvic surgery. They typically contain thin uniform septations, are located lateral to the broad

ligament, conform to the surrounding pelvic structures and can envelop the ovary.[64]

Paratubal cysts also appear as fluid collections adjacent to the ovary but are typically unilocular. They represent inclusion cysts originating from the fallopian tube fimbria.[60]

Hydrosalpinx most often occurs in the setting of pelvic adhesions arising from prior infection, bowel inflammation, endometriosis, or pelvic surgery. At MR, it is seen as a tubular cystic structure, located medial to the ovary. Identification of longitudinal folds (plicae) increases the specificity for the diagnosis.[61]

Role of advanced MRI sequences:

Magnetic resonance (MR) imaging is more specific and accurate than the other imaging modalities for characterizing complex masses with accuracies ranging from 83 to 89%, compared with 63% with US.[65] However, in a population excluding endometriomas and dermoid cysts which are well diagnosed with a high accuracy in more than 90% cases by conventional MR sequences, the accuracy of conventional MR sequences remains lower than 70%.[66]

Dynamic contrast-enhanced and diffusion weighted sequences have been demonstrated to improve diagnostic confidence by about 25% and 15%, respectively, allowing an accuracy of up to 94.6%.[67]

1. Diffusion Weighted Imaging

Diffusion weighted (DW) MR imaging is based on the analysis of the movement of water molecules in a tissue. In a highly cellular tissue, there is restriction of the movement of water molecules between cells and thus, the tissue shows high signal intensity on high b-value DW images and low signal on ADC (apparent diffusion coefficient) images. On the contrary, a less cellular environment provides a larger extracellular space for free diffusion of water molecules. Thus, ADC is high and the tissue typically shows no high signal intensity on the high b-value DW images.[68]

Complex adnexal masses with their solid component exhibiting low intensity both on DWI and T2-weighted images are nearly always benign, thereby allowing a confident exclusion of malignancy, whereas high b-value signal intensity within the solid component is predictive of malignancy. However, certain benign lesions reveal decreased mean ADC values owing to abundant collagen in benign fibrous tumors such as fibromas, Brenner tumors, and cystadenofibromas. Endometriomas and cystic teratomas also exhibit a low ADC value, due to hemorrhagic and keratinoid contents, respectively. Thus, ADC measurements in the solid component are not useful to differentiate benign from malignant adnexal masses.[67,69]

As the DW signal is the combination of water diffusivity and T2 signal intensity, the typically very low T2 weighted signal intensity of fibrous tissue in these benign adnexal tumors decreases the theoretical high DW signal intensity due to the high cellularity of these tumors (T2 dark through effect).

Since DW signal is very useful for adnexal mass characterization, sequence optimization is needed to obtain a diffusion sequence with the lowest T2 signal effect and maximum contrast to noise ratio. T2 signal effect decreases with the increase of b-values. The optimal b-value is considered to be between b1000 and b1200.[67]

2. Dynamic contrast-enhanced MR Imaging

Dynamic contrast-enhanced MRI (DCE-MRI) is a technique that evaluates the leakage of contrast agent from capillaries into the extravascular extracellular space. Malignant tumors are generally hypervascular with immature and fragile tumor vessels, which could increase the vascular permeability, whereas hypovascularity is characteristic of benign tumors. These vessels are characterized by a lack of coverage by pericytes and the higher expression of the receptors of Vascular Endothelial Growth Factor (VEGF). DCE-MRI can make qualitative, semi-quantitative, and

quantitative evaluation of blood perfusion in ovarian tumors based on the different enhancement patterns.[70]

In semi-quantitative evaluation, evolution of relative signal intensity with respect to time is assessed using time intensity curves. Two regions of interest (ROIs) are placed on both external myometrium and solid component of the adnexal mass on DCE MR sequence. For characterization of adnexal masses, time intensity curve of solid tissue in an adnexal mass is compared to that of external myometrium, which acts as the internal reference. Thus, when solid tissue is enhanced with a weak and progressive curve in comparison to the myometrium, the curve is named “type 1.” When solid tissue is enhanced with a moderate enhancement in comparison to myometrium with a plateau, the curve is named “type 2.” Finally, when solid tissue is enhanced with a curve steeper than that of myometrium, whatever the intensity of enhancement, the curve is named “type 3”. This allows for a more comprehensive discrimination of ovarian tumors according to the time-intensity curves.

The addition of DCE imaging has been found to increase the diagnostic confidence of conventional MR imaging in up to 25% of tumors. Obtaining a type 1 curve has a high sensitivity and specificity for benign tumors, whereas a rapid and high level of enhancement typical of a type 3 curve is only found in invasive malignant tumors. Type 2 curve is mostly found in borderline tumors but with a lower specificity.[67]

Time intensity curve analysis has also been useful in differentiating pedunculated subserosal uterine leiomyomas and ovarian fibromas because uterine leiomyomas typically enhance with virtually the same time intensity curve as the myometrium whereas ovarian fibromas display a weak and progressive enhancement pattern (type 1 curve).[46]

In conclusion, a combination of DCE and DW imaging has added new criteria to conventional MR imaging to improve the characterization of complex adnexal masses, resulting in a decision tree giving 95%

accuracy, thus enabling young women wishing to preserve childbearing potential avoid unnecessary surgery.

AIMS & OBJECTIVES

To assess the role of advanced MRI sequences (Diffusion Weighted Imaging and Dynamic Contrast Enhanced) in characterisation of adnexal masses, into benign and malignant, with reference to histopathological examination wherever possible.

Kurjak A. et al assessed adnexal tumour neovascularisation with transvaginal color and pulsed Doppler. Sonography, vessel location, its arrangement, and pulsed Doppler waveform characteristics were used to distinguish benign from malignant vascularity. Results of this retrospective study showed that peripheral and pericystical location and resistance index above 0.40 were highly associated with benign ovarian lesions. Blood vessels located in the center, septum, and papillary projection of the tumor with diffuse dispersed vascular arrangement and resistance index below 0.41 were highly correlated with malignancy. There were no statistically significant differences in blood flow velocities observed at different vascular locations and vessel arrangement between benign and malignant ovarian masses. [71]

U M Hamper et al studied the blood flow characteristics of adnexal masses to determine whether color flow Doppler sonography is useful for distinguishing benign from malignant masses. Benign tumors and cysts were found to have a significantly higher pulsatility index (mean, 1.93 ± 1.02; range, 0.23-3.99) and resistive index (mean, 0.77 ± 0.22; range, 0.2-1.0) than did malignant tumors (pulsatility index: mean, 0.77 ± 0.33; range, 0.31-1.09; resistive index: mean, 0.5 ± 0.17; range, 0.27-0.67). It was concluded that high pulsatility and resistive indexes indicate benign adnexal processes; however, considerable overlap in pulsatility and resistive indexes between benign and malignant lesions was noted. [72]

Buy JN et al evaluated the importance of color Doppler combined with conventional sonography in characterizing adnexal masses. Using conventional sonography alone, accuracy was 83%, sensitivity was 88%, and specificity was 82%. Using conventional sonography and color Doppler, accuracy was 95%, sensitivity was 88%, and specificity was 97%. Using spectral Doppler analysis and an RI less than or equal to 0.4, accuracy was 77%, sensitivity was 18%, and specificity was 98%. For a PI less than or equal to 1, accuracy was 68%, sensitivity was 71%, and

specificity was 67%. For a PSV greater than or equal to 15 cm/sec, accuracy was 72%, sensitivity was 47%, and and specificity was 81%. They came to a conclusion that adding color Doppler to conventional sonography produced a specificity and positive predictive value higher than those of conventional sonography alone.[11]

Van Holsbeke C et al conducted a study to determine the sensitivity and specificity of the 'ovarian crescent sign' (OCS)—a rim of normal ovarian tissue seen adjacent to an ipsilateral adnexal mass—as a sonographic feature to discriminate between benign and malignant adnexal masses. The ability of the OCS to discriminate between borderline or invasively malignant vs. benign adnexal masses, as well as between invasively malignant vs. other (benign and borderline) tumors, was determined. Sensitivity and specificity for absent OCS to identify a malignancy was 92% and 42%, respectively, and the positive and negative likelihood ratios (LR+ and LR−, respectively) were 1.60 and 0.18. For discrimination between invasive vs. benign or borderline tumors, the sensitivity for absent OCS was 94%, the specificity was 40%, the LR+ was 1.58 and the LR− was 0.14. This study confirms that the presence of the OCS decreases the likelihood of invasive malignancy in adnexal masses. However it is a poor discriminator between benign and malignant adnexal masses.[73]

To determine the accuracy of transvaginal ultrasound (TVS) and of precontrast and contrast material-enhanced magnetic resonance (MR) imaging in the differentiation of adnexal masses, Yamashita Y et al analyzed MR and TVS images of 80 masses in 72 patients, and the findings were confirmed at surgery or laparoscopy. Higher diagnostic accuracy was attained with MR imaging in mature cystic teratomas and endometriomas. However, better accuracy was achieved with contrast-enhanced MR imaging and TVS in simple cysts, cystadenomas, and malignant tumors because internal details could be better visualized. Observer confidence was significantly higher with contrast-enhanced MR

imaging than with precontrast MR imaging *(P* = .011) or TVS *(P* = .002) in the differentiation of benign and malignant masses. They reached a conclusion that contrast-enhanced MR imaging is superior to precontrast MR and TVS imaging in the characterization of adnexal masses. [7]

Suidan RS et al conducted a prospective, non-randomized, multicenter trial to assess the ability of preoperative computed tomography (CT) scan of the abdomen/pelvis and serum CA-125 to predict suboptimal (>1cm residual disease) primary cytoreduction in advanced ovarian, fallopian tube, and peritoneal cancer. On multivariate analysis, three clinical and six radiologic criteria were significantly associated with suboptimal debulking: age ≥ 60 years (p=0.01); CA-125 ≥ 500 U/mL (p<0.001); ASA 3-4 (p<0.001); suprarenal retroperitoneal lymph nodes >1cm (p<0.001); diffuse small bowel adhesions/thickening (p<0.001); and lesions >1cm in the small bowel mesentery (p=0.03), root of the superior mesenteric artery (p=0.003), perisplenic area (p<0.001), and lesser sac (p<0.001). A 'predictive value score' was assigned for each criterion, and the suboptimal debulking rates of patients who had a total score of 0, 1-2, 3-4, 5-6, 7-8, and ≥ 9 were 5%, 10%, 17%, 34%, 52%, and 74%, respectively. A prognostic model combining these nine factors had a predictive accuracy of 0.758. [74]

Gatreh-Samani F et al studied the accuracy of multidetector computed tomography in diagnosis of adnexal tumors. Results of MDCT were compared with surgical and histopathological findings. The sensitivity and specificity of MDCT in determining local extension came out to be 72.2% and 93.4% respectively. And the sensitivity and specificity of MDCT in determining peritoneal seeding and liver extension was 81.8% and 93% respectively. Estimated stage was significantly agreed with the surgical (Cohen's Kappa (κ) = 0.891) and histopathological findings (κ = 0.858). MDCT was thus concluded to be a highly sensitive and specific diagnostic method in successfully staging adnexal malignancies.[75]

Sohaib SA et al prospectively studied 72 women with clinically suspected adnexal masses to evaluate the accuracy of ultrasonography (US) and magnetic resonance imaging (MRI) in characterizing adnexal masses, and to determine which patients may benefit from MRI. For characterizing lesions as malignant, the sensitivity, specificity and accuracy of MRI were 96.6%, 83.7% and 88.9%, respectively, and of US were 100%, 39.5% and 63.9%, respectively. MRI was more specific ($p<0.05$) than US. Both MRI and US correctly diagnosed 17 (24%) cases with benign and 28 (39%) cases with malignant masses. MRI correctly diagnosed 19 (26%) cases with benign lesion(s), which on US were thought to be malignant. It was concluded that MRI is more specific and accurate than US and Doppler assessment for characterizing adnexal masses.[13]

Kurtz AB et al conducted a study to determine the optimal imaging modality for diagnosis and staging of ovarian cancer. Two hundred eighty women suspected to have ovarian cancer were enrolled in a prospective study before surgery. All three modalities had high accuracy (0.91) for the overall diagnosis of malignancy. In the ovaries, the accuracy of MR imaging (0.91) was higher than that of CT and significantly higher than that of Doppler US (0.78). MR imaging was found to be superior to Doppler US and CT in diagnosis of malignant ovarian masses.[14]

Hricak H et al evaluated the accuracy of magnetic resonance (MR) imaging in the detection and characterization of complex adnexal masses, with particular reference to the findings predictive of malignancy, role of gadolinium-enhanced contrast material, and observer variability. Preoperative MR imaging of the pelvis was performed in 128 patients with ultrasonographically detected complex adnexal masses. Gadolinium-enhanced MR imaging depicted an overall accuracy for the diagnosis of malignancy of 93%. The MR imaging findings that were most predictive of malignancy were necrosis in a solid lesion (odds ratio, 107) and vegetations in a cystic lesion (odds ratio, 40). They concluded that gadolinium-enhanced MR imaging is highly accurate in the detection and

characterization of complex adnexal masses, with excellent inter- and intraobserver agreement.[25]

Sohaib SA et al, in a prospective study on 104 patients, evaluated the accuracy of MR imaging in the detection and characterization of adnexal mass lesions and to determine which imaging features are predictive of malignancy. On univariate analysis, the imaging features associated with malignancy were a solid–cystic lesion, irregularity, and vegetation on the wall and septum in a cystic lesion, the large size of the lesion, an early enhancement on dynamic contrast-enhanced MR images, and the presence of ascites, peritoneal disease, or adenopathy. On multiple logistic regression analysis, ascites and vegetation in a cystic lesion were the factors most significantly indicative of malignancy. MR imaging was proven to be highly accurate in the characterization of adnexal mass lesions.[26]

Kinkel K et al conducted a study to compare value of various diagnostic strategies in assessment of changes in posttest probability of ovarian cancer. In women with an indeterminate initial US result, posttest probability decreased after secondary testing with benign results for all imaging modalities to 2% in premenopausal women and to 8%–10% in postmenopausal women. After secondary testing for suspicious lesions, posttest probability increased more after nonenhanced (premenopausal women, 70%; postmenopausal women, 92%) or contrast-enhanced MR imaging (premenopausal women, 80%; postmenopausal women, 95%) than it did after combined gray-scale and Doppler US (premenopausal women, 30%; postmenopausal women, 69%) or CT (premenopausal women, 38%; postmenopausal women, 76%) ($P < .001$). Thus in women with an indeterminate ovarian mass at gray-scale US, MR imaging results contributed to change in probability of ovarian cancer in both pre- and postmenopausal women more than did CT or combined gray-scale and Doppler US results.[76]

Bazot M et al conducted a study with the aim to compare the accuracy of magnetic resonance imaging (MRI) and intraoperative consultation (IC) for the diagnosis of adnexal masses, with reference to final histology. Macroscopic examination and MRI determined size, nature, and presence of vegetations or solid portions within masses. Among the 151 adnexal masses studied by both MRI and IC, respective sensitivities, specificities, positive and predictive values of both methods for the diagnosis of malignancy were 89.7% and 84.5%, 91.4% and 100%, 86.7% and 100%, and 93.4% and 91.3%. Sensitivities of MR imaging and frozen section for the diagnosis of serous versus mucinous borderline tumors were 33.3% and 93.3%, and 62.5% and 12.5%, respectively. MRI is less accurate than IC for characterizing adnexal masses. However, use of MRI may increase the accuracy of IC for borderline mucinous tumors. Frozen section remains the “gold standard” for surgical management of adnexal tumors.[66]

Dias JL et al conducted a study to investigate if the shading sign is an exclusive MRI feature of endometriomas or endometrioid tumors, and to analyze its different patterns. The final sample included 51 women. The type of tumor and the pattern of shading were recorded. Thirty endometriomas and five endometrioid carcinomas were found. The remaining 16 cases corresponded to other benign and malignant tumors. Five shading patterns were identified: layering (15.7%), liquid–liquid level (11.8%), homogenous (45.1%), heterogeneous (11.8%), and focal/multifocal shading within a complex mass (19.6%). No significant correlation was found between these patterns and the type of tumor. It was concluded that the shading sign is not exclusive of endometriomas or endometrioid tumors. Homogenous shading was the most prevalent pattern in endometriomas and half of the cases with focal/multifocal shading within a complex mass were endometrioid carcinomas.[55]

Bazot M et al conducted a study aimed to analyse the morphological magnetic resonance imaging (MRI) features of borderline ovarian tumours

(BOT) and to evaluate whether MRI can be used to distinguish serous from mucinous subtypes. Predictive MRI criteria for SBOT were bilaterality, predominantly solid tumour, and the presence of vegetations, especially exophytic or with a high T2 signal ($p < 0.01$), whereas predictive MRI criteria for MBOT were multilocularity, number of septa, loculi of different signal intensity, and grouped and irregular thickened septa ($p < 0.01$). Using multivariate analysis, vegetations were independently associated with SBOT [odds ratio (OR) = 29.5] and multilocularity with MBOT (OR = 3.9). Vegetations and multilocularity were found to be the two independent MRI features that can help to distinguish between SBOT and MBOT. [77]

Chen M et al conducted a study to determine which magnetic resonance (MR) imaging findings of an ovarian mass are most predictive of malignancy and to assess the value of intravenous gadolinium administration in the characterization of an ovarian mass. The most predictive MR imaging findings for malignancy were presence of vegetations in a cystic lesion and presence of necrosis in a solid lesion. The odds ratio was even higher when the ancillary finding of peritoneal metastasis or ascites was present. Contrast media contributed significantly to lesion characterization. There were significant differences in accuracy ($P < 0.01$), sensitivity ($P < 0.01$), specificity ($P < 0.01$) between contrast-enhanced and unenhanced MR imaging. They reached a conclusion that contrast-enhanced MR imaging is highly accurate in detection and characterization of complex adnexal masses. [78]

Mansour S et al evaluated the diagnostic performance of diffusion weighted imaging (DWI) in characterising ovarian masses with suspicious features on magnetic resonance imaging (MRI). Analysis considered signal intensity (SI) at b1000 and the mean ADC values for the solid components of the 235 complex and solid ovarian masses with suspicious MRI features included in the study. Restricted diffusion was observed in all of the invasive malignancy (57.1%, n =105/184). Benign and borderline

tumors with high DWI SI represented 15.2% and 27.7% respectively ($P<0.05$). The mean ADC value was $1.2+0.34x10^{-3}$ mm^2/s, $1.1+ 0.06x10^{-3}$ mm^2/s, and $0.83 + 0.15x10^{-3}$ mm^2/s for benign, borderline and malignant masses respectively. The ADC values of malignant masses and benign masses with fibrous components showed no significant difference ($P =0.333$). The study concluded that DWI supported by conventional MRI data can confirm or exclude malignancy in suspicious ovarian masses. [79]

Bakir B et al in a study, investigated whether diffusion-weighted imaging (DWI) and apparent diffusion coefficient (ADC) values provide specific information that allows the diagnosis of solid or predominantly solid gynaecological adnexal lesions, especially whether they can discriminate benign and malignant lesions. On DWI, high signal intensity was observed more often in malignant than in benign lesions ($p<0.0001$). There was no significant difference between the ADC values of the malignant and benign lesions in either the adnexal (0.88 ± 0.16 vs 0.84 ± 0.42; $p=0.96$) or the ovarian (0.85 ± 0.14 vs 1.05 ± 0.2; $p=0.133$) lesions. When signal intensities on DWI were compared, however, malignant lesions had higher values than the benign lesions in both the adnexal (0.69 ± 0.21 vs 0.29 ± 0.13; $p<0.0001$) and the ovarian lesions (0.75 ± 0.14 vs 0.37 ± 0.24; $p=0.003$). They concluded that on DWI, high signal intensity was observed more frequently with the malignant lesions. [80]

Fujii S et al evaluated the usefulness of diffusion-weighted (DW) magnetic resonance (MR) imaging in detecting peritoneal dissemination in cases of gynecological malignancy. They retrospectively analyzed MR images obtained from 26 consecutive patients with gynecological malignancy. Peritoneal dissemination was histologically diagnosed in 15 of the 26 patients after surgery. Receiver-operating characteristic (ROC) curves were used to represent the presence of peritoneal dissemination. In addition, the sensitivity and specificity were calculated. DW imaging depicted the tumors in 14 of 15 patients with peritoneal dissemination as abnormal signal intensity. The mean sensitivity and specificity were 90

and 95.5%. It was concluded that DW imaging plays an important role in the diagnosis of peritoneal dissemination in patients with gynecological malignancy. [69]

To elucidate whether apparent diffusion coefficient (ADC) values calculated from diffusion-weighted MR imaging (DWI) are useful in the differential diagnosis of ovarian cystic masses, Nakayama T et al conducted a study in which DWI was performed in 131 patients with cystic ovarian masses. On qualitative and quantitative analyses, mature cystic teratomas tended to show higher signal intensity and had areas of lower ADC values than other benign and malignant neoplasms ($P < .005$). In vitro scanning of the cystic contents of mature cystic teratomas confirmed that high signal on DWI or low ADC value was attributable to the keratinoid substance within the tumors. It was concluded that the ADC value may add useful information to the differential diagnosis of ovarian cystic masses in limited populations, such as those with mature cystic teratomas with a small amount of fat.[81]

Balaban M conducted a study with the aim to determine the utility of diffusion-weighted magnetic resonance imaging (DWI MRI) and apparent diffusion coefficient (ADC) measurements in differentiation of endometrioma and hemorrhagic ovarian cyst. A total of 24 female patients who underwent pelvic MRI with an initial diagnosis of ovarian cyst were included in the study. The final diagnosis was endometrioma in 12 patients and hemorrhagic ovarian cyst in 12 patients. They observed significantly lower ADC values in endometriomas compared with hemorrhagic ovarian cysts in all b values. They concluded that DWI with quantitative ADC measurements can be used for differentiation of endometrioma from hemorrhagic ovarian cysts.[82]

Wang T et al assessed the added value of diffusion-weighted magnetic resonance imaging (DWI) with apparent diffusion coefficient (ADC) values compared to MRI, for characterizing the tubo-ovarian abscesses (TOA) mimicking ovarian malignancy. The mean ADC value of the cystic

component in TOA was significantly lower than in malignant tumors (1.04 ± 0 .41 × 10^{-3} mm^2/s vs. 2.42 ± 0.38 × 10^{-3} mm^2/s; p < 0.001). The mean ADC value of the enhanced solid component in 26 TOAs was 1.43 ± 0.16×$10^{-3}$$mm^2$/s, and 46.2% (12 TOAs; pseudotumor areas) showed significantly higher signal intensity on DW-MRI than in ovarian malignancy (mean ADC value 1.44 ± 0.20×10^{-3} mm^2/s vs.1.18 ± 0.36 × 10^{-3} mm^2/s; p = 0.043). The combination diagnosis of ADC value and dilated tubal structure achieved the best AUC of 0.996.It was concluded that DW-MRI is superior to MRI in the assessment of TOA mimicking ovarian malignancy. [83]

Takeuchi M et al evaluated the feasibility of diffusion-weighted imaging (DWI) with apparent diffusion coefficient (ADC) measurement in differentiating benign and malignant ovarian tumors. Solid portion of all 39 malignant tumors showed homogeneous or heterogeneous high intensity on DWI, whereas only 3 of the 10 benign tumors (3 thecomas) showed high intensity. The mean (SD) ADC value in the 39 malignant tumors (1.03 [0.19]) was significantly lower than that in 10 benign tumors (1.38 [0.30]). A relatively low ADC (1.08-1.20) in the 3 thecomas may reflect their abundant cellular nature, and the presence of low intensity on T2-weighted images was suggestive for benign fibrous tumor. They concluded that low intensity on DWI with high ADC may suggest benign lesions; however, it may be occasionally difficult to differentiate benign and malignant lesions only on the basis of DWI.[84]

Thomassin-Naggara I et al prospectively assessed the contribution of diffusion-weighted MRI (DWI) for characterizing complex adnexal masses. 77 women with complex adnexal masses underwent MR imaging including DWI before surgery. The most significant criteria for predicting benignity were low b1,000 signal intensity within the solid component (PLR= 10.9), low T2 signal intensity within the solid component (PLR=5.7), absence of solid portion (PLR=3.1), absence of ascites or peritoneal implants (PLR=2.3) and absence of papillary projections (PLR=2.3). ADC

measurements did not contribute to differentiating benign from malignant adnexal masses. All masses that displayed simultaneously low signal intensity within the solid component on T2-weighted and on b1,000 diffusion-weighted images were benign. Alternatively, the presence of a solid component with intermediate T2 signal and high b1,000 signal intensity was associated with a PLR of 4.5 for a malignant adnexal tumour. They came to the conclusion that DWI signal intensity is an accurate tool for predicting benignity of complex adnexal masses. [85]

Nasr E et al did a study aimed at reviewing and emphasizing the role of dynamic contrast enhanced MRI and diffusion-weighted MR in characterization of ovarian lesions. It was found that the specificity was higher for DWI (75%) compared to conventional MRI (58.3%), as well as the accuracy which was 73.9% for MRI while that of DWI was 86.9%. The mean ADC values for malignant lesions were ($0.84 \times 10^{-3} \pm 0.1$ SD mm^2/s), while that for benign lesions were ($1.8 \times 10^{-3} \pm 0.5$ SD mm^2/s), with cut off 1.2×10^{-3} and p value = 0.005. The specificity was higher for DCE (91%) compared to conventional MRI sequences (58.3%), as well as the accuracy which was 73.9% for MRI while that of DCE was 77%. Thus, the combination of DWI and DCE to conventional MRI was found to improve the specificity of MRI. [86]

Thomassin-Naggara I et al in a retrospective study determined the value of adding perfusion weighted (PW) and diffusion-weighted (DW) sequences to a conventional magnetic resonance (MR) imaging protocol to differentiate benign from malignant tumors. the accuracy of conventional, PW, and DW imaging combined was higher than that of conventional MR imaging alone for benign masses ($P < .01$) but not for malignant masses ($P = .24$).The addition of both PW and DW images led to a correct change in the diagnosis in 19% (11 of 57 patients), 23% (13 of 57 patients), and 24% (14 of 57 patients) of cases, with no incorrect changes. Conventional, PW, and DW MR imaging criteria were combined to generate a decision tree giving an accuracy of 95%. The addition of PW

and DW sequences to a conventional MR imaging protocol improved the diagnostic accuracy in the characterization of complex adnexal masses.[87]

Li HM et al conducted a study aimed to investigate the utility of dynamic contrast enhanced MRI (DCE-MRI) in the differentiation of malignant, borderline, and benign complex ovarian tumors DCE-MRI data of 102 consecutive complex ovarian tumors, confirmed by surgery and histopathology, were analyzed retrospectively. The patterns (I, II, and III) of time-signal intensity curve (TIC) and semi-quantitative parameters were evaluated and compared among benign, borderline, and malignant ovarian tumors. Fifty-nine of 71 (83%) malignant tumors showed a type-III TIC; 9 of 16 (56%) borderline tumors showed a type-II TIC, and 10 of 15 (67%) benign tumors showed a type-II TIC, with a statistically significant difference between malignant and benign tumors ($P < 0.001$) and between malignant and borderline tumors ($P < 0.001$). DCE-MRI was found to be helpful for characterizing complex ovarian tumors; however, semi-quantitative parameters perform poorly when distinguishing malignant from borderline tumors.[70]

Thomassin-Naggara I et al assessed the accuracy of magnetic resonance imaging (MRI), particularly, dynamic MRI, in distinguishing ovarian fibromas from subserous uterine leiomyomas. No significant difference in morphological criteria was noted between the 2 types of masses. Visualization of arterial vessels was more frequent in uterine leiomyomas than in ovarian fibromas ($P = 0.002$). The DCE MR enhancement rate was higher for uterine leiomyomas than for ovarian fibromas in terms of both maximal enhancement ($P < 0.001$) and enhancement rate at 30 ($P = 0.009$), 60 ($P = 0.007$), and 90 seconds ($P = 0.0009$). On delayed T1 postcontrast sequence, no statistical difference exists between signal intensity of ovarian fibromas and uterine leiomyomas. Their findings suggested that DCE MRI can distinguish ovarian fibromas from uterine leiomyomas and should be used if sonography fails to show the origin of a pelvic mass.[46]

Thomassin-Naggara I et al evaluated the utility of dynamic contrast enhancement (DCE) MRI for distinguishing among benign, borderline and invasive epithelial ovarian tumors. They analyzed preoperative MRI studies of 37 patients with ovarian epithelial tumors (10 benign, 11 borderline, and 16 invasive). A DCE-MRI sequence was acquired and regions of interest (ROIs) were drawn in the ovarian tumors and adjacent myometrium. A total of three patterns of enhancement were defined. Morphological criteria such as septa, papillary projection, solid portion, and T2-weighted MR signal intensity of solid tissue were useful for discriminating invasive from noninvasive ovarian tumors (P = 0.01, P = 0.02, P = 0.002, and P < 0.0001 respectively) but not for discriminating benign from borderline tumors. Curve type 3 was specific for invasive ovarian tumors. They concluded that DCE-MRI is a useful tool for characterizing epithelial ovarian tumors. [88]

Shan J et al evaluated the value of early phase dynamic enhanced MRI in the differential diagnosis of ovarian tumors. Dynamic enhanced MRI findings in 68 patients with histopathologically proved ovarian tumors were analyzed. There were 19 cases of benign tumors, 5 cases of low malignant tumors, and 44 cases of malignant tumors. Peak and the slope value of enhancement were determined from time-signal intensity curve (TIC). The difference of the enhancement index, the time to peak, and the slope value between benign and malignant ovarian tumors was statistically significant (P<0.001). The benign tumors mainly showed a curve with low and delayed enhancement, while the malignant ovarian tumors mostly a curve with high and early enhancement. The early phase dynamic enhanced MR imaging was thus proven to be helpful in the differential diagnosis of benign and malignant ovarian tumors. [89]

Malek M et al evaluated and compared the accuracy of diffusion-weighted imaging (DWI), apparent diffusion coefficient (ADC) value, and time-intensity curve (TIC) type analysis derived from dynamic contrast-enhanced MR imaging (DCE-MRI) in differentiating benign from malignant

adnexal masses. The mean ADC value was significantly lower in malignant adnexal masses ($p<0.001$). An ADC value $<1.20x10^{-3}mm^2/s$ may be the optimal cutoff for differentiating between benign and malignant tumors. The negative predictive value for low signal intensity on DWI, and type 1 TIC were 100%. The pairwise comparison among the receiver operating characteristic (ROC) curves showed that the area under the curve (AUC) of TIC was significantly larger than the AUCs of DWI and ADC ($p<0.001$ for comparison of TIC and DWI, $p<0.02$ for comparison of TIC and ADC value). DWI, ADC value and TIC type derived from DCE-MRI are all sensitive and relatively specific methods for differentiating benign from malignant adnexal masses. By comparing these functional MR techniques, TIC was found to be more accurate than DWI and ADC.[90]

Thomassin-Naggara I et al conducted a multicenter cohort study to validate the accuracy of a 5-point Ovarian-Adnexal Reporting Data System Magnetic Resonance Imaging Resonance Imaging (O-RADS MRI) score for risk stratification of adnexal masses. The end point was the analysis of true-negative and false-negative rates according to the MRI score compared with the reference standard (i.e., histology or 2-year follow-up). No invasive cancer was assigned a score of 2. Positive likelihood ratios were 0.01 for score 2, 0.27 for score 3, 4.42 for score 4, and 38.81 for score 5. MRI score correctly reclassified the mass origin as nonadnexal with a sensitivity of 0.99 and a specificity of 0.78. They concluded that applying this score in clinical practice may allow a tailored, patient centered approach for adnexal masses that are sonographically indeterminate, preventing unnecessary surgery, less extensive surgery, or fertility preservation when appropriate. [91]

MATERIALS AND METHODS

Source of Data

It was a prospective study of patients undergoing MRI Pelvis for previously detected adnexal masses, in the Department of Radiodiagnosis, Dayanand Medical College & Hospital, Ludhiana, during a one-year period.

METHOD OF COLLECTION OF DATA

Inclusion criteria

- All patients found to have an adnexal mass on MRI

Exclusion criteria

- Any contraindications to MRI (patients with cardiac pacemakers, claustrophobic patients)
- Anyone who was unwilling to participate in the study

Preparation of the patients:

Consent was obtained from each patient for inclusion in the study. The relevant clinical history, imaging records and laboratory investigations were recorded on a proforma.

Before starting the scan, the procedure was explained to the patient in her vernacular language to allay anxiety and written consent was taken. During the entire examination, patient was in contact with the technologist/doctor through a two-way intercom system.

MR imaging technique:

Patients were imaged using a 3-Tesla MRI unit (Magnetom Skyra, Siemens, Germany) and the protocol included T1 weighted images with and without fat suppression in the axial plane, T2 weighted images in all 3 planes, Diffusion-weighted images in the axial plane in b-values of 50,400 and 800 s/mm^2 and Dynamic Contrast-Enhanced MR images.

Dynamic Contrast-Enhanced MRI was performed using the Gradient Echo (GRE) T1 weighted volume interpolated breath hold examination (VIBE) sequence. The acquisition plane was adjusted in order to cover both external myometrium and the solid component of the lesion in the same

plane, as both need to be analyzed simultaneously for TIC analysis. A rapid bolus of 0.1mmol/kg body weight gadopentetate dimeglumine was given through a peripheral vein followed by injection of 10 mL of normal saline. A total of 35 acquisitions were taken with a total acquisition time of 4 minutes 44 seconds.

Finally, post-contrast delayed T1-weighted fat-saturated images were acquired in all 3 planes. Subtraction images were acquired if the lesion was bright on pre-contrast T1 fat-saturated images. The sequences were obtained with the following parameters:

Table 1: MRI acquisition parameters

Sequence	Repetition time (ms)	Echo time (ms)	Flip angle (degree)	Slice thickness (mm)	Field of view (mm)	Matrix (mm)
T1 axial	680	18	150	3	220	256x320
T1 axial with fat-saturation	600	20	150	3	220	224x320
T2 sagittal	2800	87	150	3	230	269x384
T2 axial	3100	89	150	3	220	269x384
T2 coronal	2800	87	175	3	230	269x384
Diffusion-weighted images	4000	64	-	3	220	114x114
Gradient Echo T1 VIBE	5.08	1.77	15	4	260	154x192
T1 fat-sat post contrast	600	20	160	3.5	220	224x320

MR image analysis:

Adnexal lesions were assessed based upon the following parameters:

A. Conventional MRI parameters

1. Size: The largest dimension was considered for statistical analysis
2. Bilaterality: In patients with bilateral adnexal lesions, the most complex or the largest lesion was included in the statistical analysis.
3. Solid / cystic composition: By definition, the solid component shows contrast-enhancement, and can either be thickened irregular septa, or papillary projection or solid portion (including completely solid mass) [92]. Mixed solid-cystic lesions were classified as predominantly cystic (if less than half of the mass was solid) or predominantly solid (if more than half of the mass was solid). The cystic component has been defined as tissue that has long T1 and T2 characteristics and does not enhance after the injection of contrast material.
4. T2 signal intensity in the solid component: Signal intensity of solid components was evaluated on T2-weighted MR images relative to outer myometrium, and classified as “hypointense” when lower in signal, and “intermediate” when the signal was equal to or greater than the outer myometrium.
5. Presence of marked hyperintensity in the cystic component on T1WI: Lesions displaying high T1-weighted signal intensity greater or equal to subcutaneous fat, with or without shading on T2-weighted sequence and no internal enhancement were considered to be endometriotic cysts.
6. T2 shading: Shading sign on T2WI corresponds to the complete or partial loss of the signal intensity of a hyperintense adnexal cyst from T1WI to T2WI.
7. Thickened septa: i.e. thickness of greater than or equal to 3 mm.

8. Hemorrhage: Presence of hyperintensity on T1 fat-saturated images, or T2 shading, or presence of a T2 hypointense non-enhancing component within a bright cystic lesion.
9. Papillary projections: Defined as any solid projection into the cyst from its wall with size greater than or equal to 3 mm.
10. Ancillary features such as ascites, peritoneal deposits, lymphadenopathy, distant metastases.

B. Diffusion weighted Imaging (DWI): For assessment of diffusion restriction, the signal intensity within the mass at high b-value DW images and ADC maps was evaluated. Signal intensity of the cystic and solid components was separately classified on DW images with a b-value of 800 s/mm^2 as presence of diffusion restriction (high signal intensity on DWI with a corresponding low signal on ADC maps), or absence of diffusion restriction (absence of high signal intensity on DWI), compared with serous fluid (urine or cerebrospinal fluid).

On ADC maps, mean ADC values of the lesion were measured by placing ROIs in the solid as well as cystic components of the lesion. The mean ADC values of the solid components were measured by placing the largest possible circular regions of interest (ROIs) (minimum size: 0.15 cm^2) in the solid portion of the lesions on ADC maps. The ROIs were placed on regions with the highest intensity on high b-value DWI and care was taken not to include cystic areas by referring to T2WI and/or post-contrast T1 fat-saturated images. At least three measurements were obtained and average value calculated.

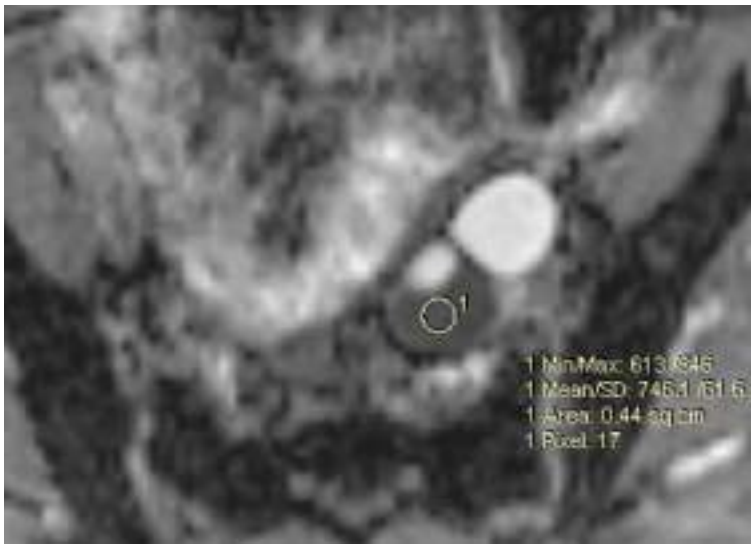

Figure 1: ROI placement on ADC maps. In a patient with granulosa cell tumor in the left adnexa, axial ADC image shows placement of ROI within the solid hypointense component of the adnexal lesion.

C. Dynamic-Contrast Enhanced MRI (DCE-MRI): Time Intensity Curve analysis was done by drawing Regions of interest (ROIs) in the dynamic sequence. One ROI was placed in the enhancing solid component of the adnexal mass or along the septa/wall in lesions in which solid component was absent, and another ROI was placed in external myometrium, which acts as an internal reference. Then, the evolution of relative enhancement of the lesion with respect to time was assessed using time intensity curves. To minimize variability, ROI size varied from 0.15 to 1.5 cm^2. Care was taken to not place the ROIs in the non-enhancing areas or vessels. When the tumour exhibited heterogeneous or numerous solid portions, at least 3 ROIs were drawn and only the maximum enhancement parameters were considered for statistical analysis.

A gradual increase in the signal intensity of enhancing component of the lesion, without a well-defined shoulder, has been defined as type I curve. A moderate initial increase in the signal intensity of solid tissue relative to that of myometrium, followed by a plateau, has been defined as type II curve. An initial increase in the signal intensity of solid tissue that was steeper than that of myometrium has been defined as type III curve.

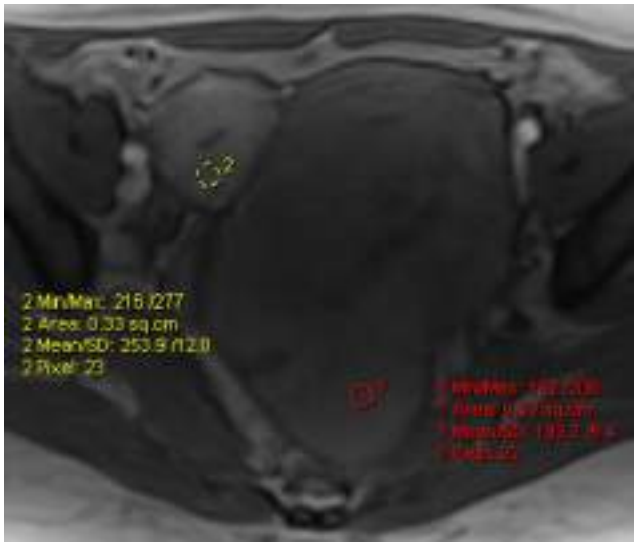

Figure 2a: ROI placement in DCE-MRI. In a patient with a large adnexal lesion, axial T1 VIBE post-contrast image shows the placement of ROIs. Red ROI (1) is placed in the solid enhancing component of the lesion, while yellow ROI (2) is placed in the external myometrium.

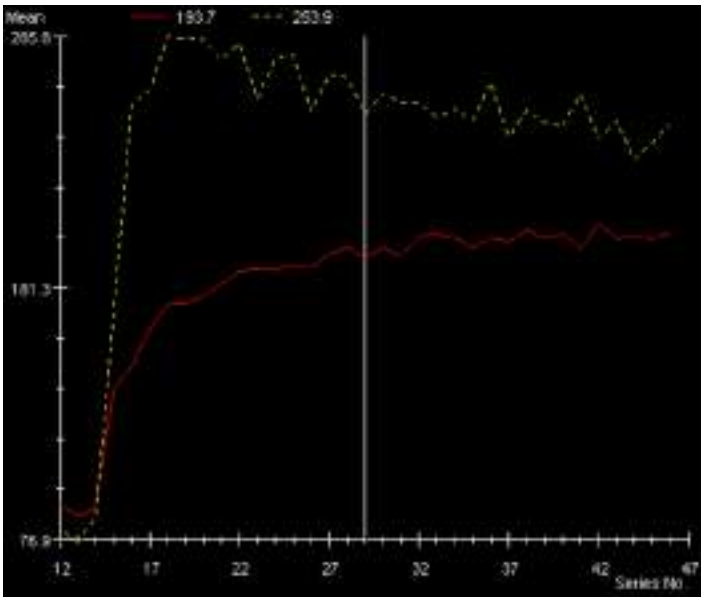

Figure 2b: Time-Intensity Curve analysis in the same patient shows moderate initial increase in the signal intensity of solid tissue of the lesion (red curve) that is less steep than that of myometrium (yellow curve), followed by a plateau, which has been defined as type II curve.

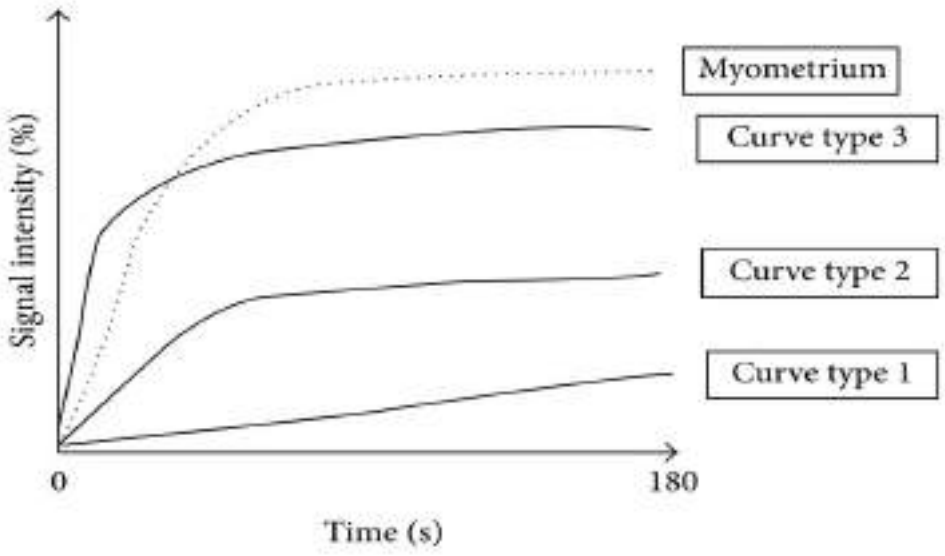

Figure 3: Types of Time-Intensity Curves [67]

Post-processing subtraction images were helpful in our study in detecting areas of true enhancement and application of ROI especially in adnexal lesions that appeared bright on unenhanced T1-weighted fat-suppressed images (hemorrhagic/proteinaceous contents).

D. Final Diagnosis

We characterized all the lesions in our study as benign or malignant, based on certain criteria that have been proven to be accurate for the prediction of benignity and malignancy in various studies.

The following criteria were considered predictive of benignity: purely cystic lesions, a homogeneous solid component with hypointense signal intensity at T2-weighted imaging, a solid component without diffusion restriction, and a solid component with a type I time-intensity curve on DCE images.[87]

The following criteria were considered predictive of malignancy: papillary projections, a heterogeneous solid component with intermediate signal intensity at T2-weighted imaging, a solid component with presence of diffusion restriction, a solid component with a type III time- intensity curve on DCE images, or associated ascites or peritoneal implants.[87]

The findings were correlated with histopathological analysis wherever possible, and with imaging follow-up findings when histopathology confirmation was not available.

Duration of Study

The study was conducted over a period of one year.

Outcome

All the lesions taken up for the study were analyzed to assess the contribution of conventional MR sequences, Diffusion-weighted images, and Dynamic contrast-enhanced MR images in classifying the adnexal masses into benign and malignant, with histopathological analysis as the reference wherever possible; and whether there is any added advantage of DWI and DCE over conventional MRI sequences alone in the characterization of adnexal masses into benign and malignant.

Statistical Analysis

Data was described in terms of range; mean ±standard deviation (±SD), median, frequencies (number of cases) and relative frequencies (percentages) as appropriate. Comparison of quantitative variables between the study groups was done using Mann Whitney U test for independent samples for non-parametric data. For comparing categorical data, Chi-square ($\chi 2$) test was performed and exact test was used when the expected frequency was less than 5. Sensitivity, specificity, positive and negative predictive values and accuracy of each pertinent parameter and their confidence interval (95% CI) were also determined. A probability value (p-value) less than 0.05 was considered statistically significant. All statistical calculations were done using SPSS (Statistical Package for the Social Science) SPSS 21 version statistical program for Microsoft Windows.

OBSERVATIONS AND RESULTS

This prospective study was conducted in the Department of Radiodiagnosis, Dayanand Medical College & Hospital, Ludhiana over a period of one year. A total of 47 patients who had an ultrasonographically detected adnexal mass and subsequently underwent MRI of the pelvis, were enrolled in this study. Of the 47 patients, 12 patients had bilateral lesions, in whom only the most complex or the largest lesion was included in the statistical analysis. Therefore, a total of 47 lesions were evaluated in our study.

A. Demographic and Clinical profile

1. Age Distribution of Patients

Age of the patients ranged from 11 to 67 years, with maximum patients (n=18; 38.3%) in the age group of 41-50 years and a mean age of 38.89 years. (Table 1, Figure 1)

Table 2: Age Distribution of Patients

AGE GROUP	No. of cases	Percentage
< 30	13	27.7%
31-40	12	25.5%
41-50	18	38.3%
> 50	4	8.5%
Total	47	100.0%

Figure 4: Age Distribution of Patients

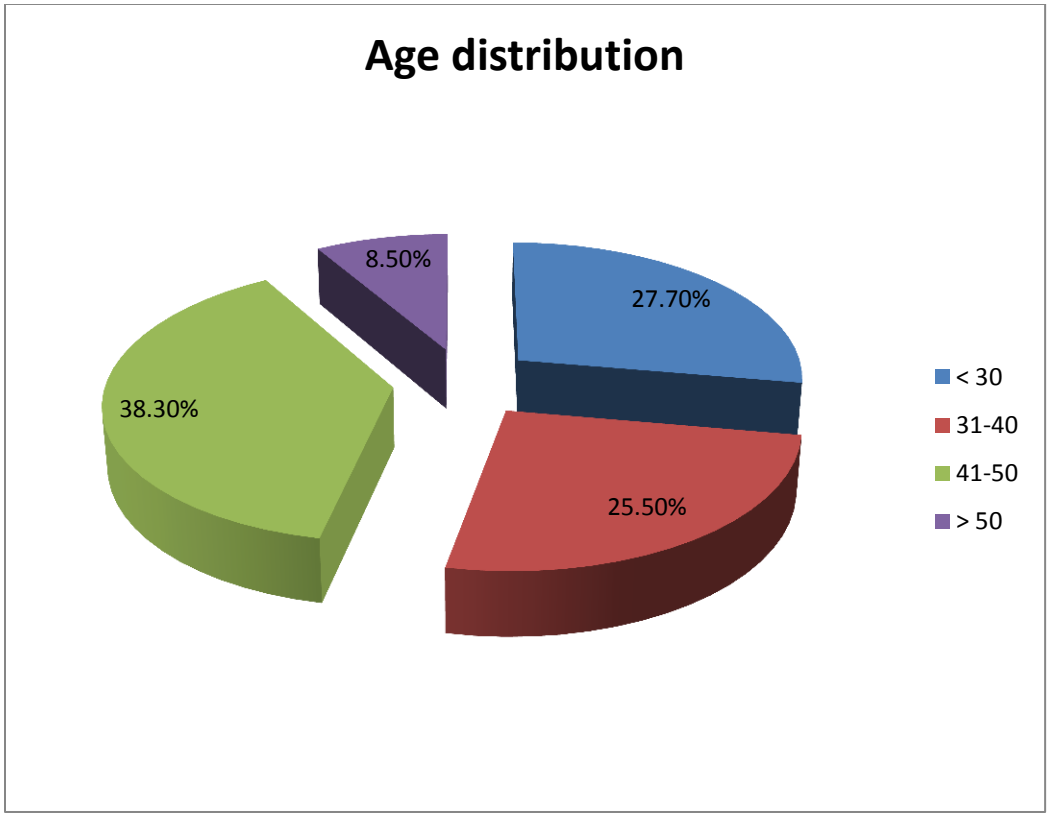

2. Final diagnosis

Table 3: Final diagnosis

FINAL DIAGNOSIS	No. of lesions	Percentage
Benign	37	78.7%
Malignant	10	21.3%
Total	47	100.0%

Out of the total 47 lesions included in our study, 37 (78.7%) were benign lesions, while 10 (21.3%) were malignant, confirmed either on histopathological analysis or on follow-up imaging.

Figure 5: Final diagnosis

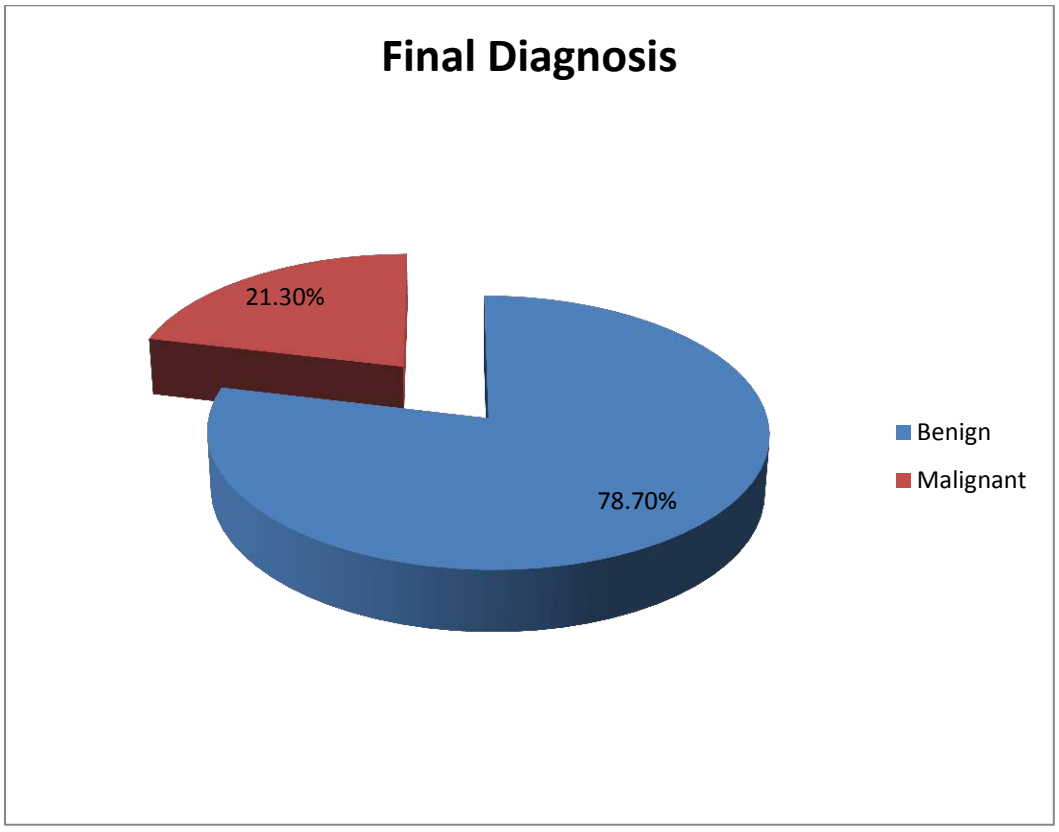

3. Age distribution of patients with benign and malignant lesions

Table 4: Age distribution of patients with benign and malignant lesions

		FINAL DIAGNOSIS				Total
		Benign		Malignant		
AGE GROUP	< 30	12	32.4%	1	10.0%	13
	31-40	10	27.0%	2	20.0%	12
	41-50	14	37.8%	4	40.0%	18
	> 50	1	2.7%	3	30.0%	4
Total		37	100%	10	100%	47

7 (70%) of the total 10 patients with malignant lesions were above the age of 40 years, while 36 (97.3%) of the 37 patients with benign lesions were below the age of 50 years. The mean age of the patients with benign lesions was 36.78 years, and 46.70 years for malignant lesions.

Figure 6: Age distribution of patients with benign and malignant lesions

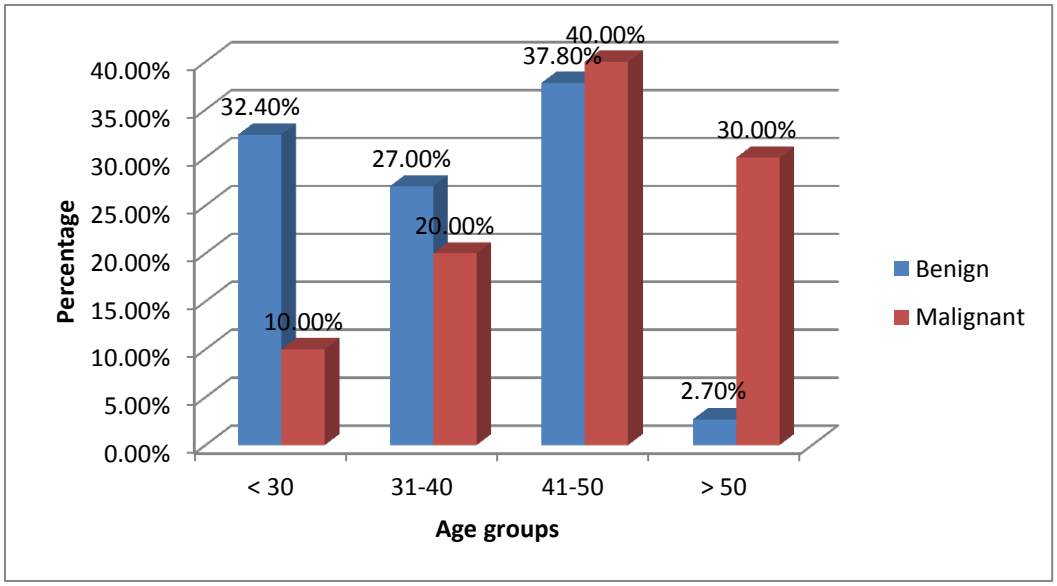

4. Presenting complaints

The most common presenting complaint was abdominal pain, which was seen in 25 (53.1%) patients. 9 (19.1%) had menorrhagia, 7 (14.9%) had dysmenorrhea, 7 (14.9%) had irregular menses, while 9 (19.1%) patients complained of abdominal heaviness. Fever (4, 8.5%), loss of appetite (4, 8.5%) and/or weight (2, 4.2%), bleeding per-vaginum (2, 4.2%), were the other presenting complaints. 2 patients were diagnosed with an adnexal mass during evaluation for infertility, another 2 while being evaluated for known carcinoma stomach. One patient had cyclical pain in the left leg with foot drop.

Table 5: Presenting complaints

PRESENTING COMPLAINTS	No. of patients	Percentage
Pain	25	53.1%
Menorrhagia	9	19.1%
Heaviness	9	19.1%
Dysmenorrhea	7	14.9%
Irregular menses	7	14.9%
Loss of appetite	4	8.5%
Fever	4	8.5%
Infertility	3	6.4%
Bleeding per-vaginum	2	4.2%
K/C/O Ca stomach, incidental adnexal mass	2	4.2%
Loss of weight	2	4.2%
Postmenopausal bleeding	2	4.2%
Cyclical pain left leg, left foot drop	1	2.1%

Figure 7: Presenting complaints

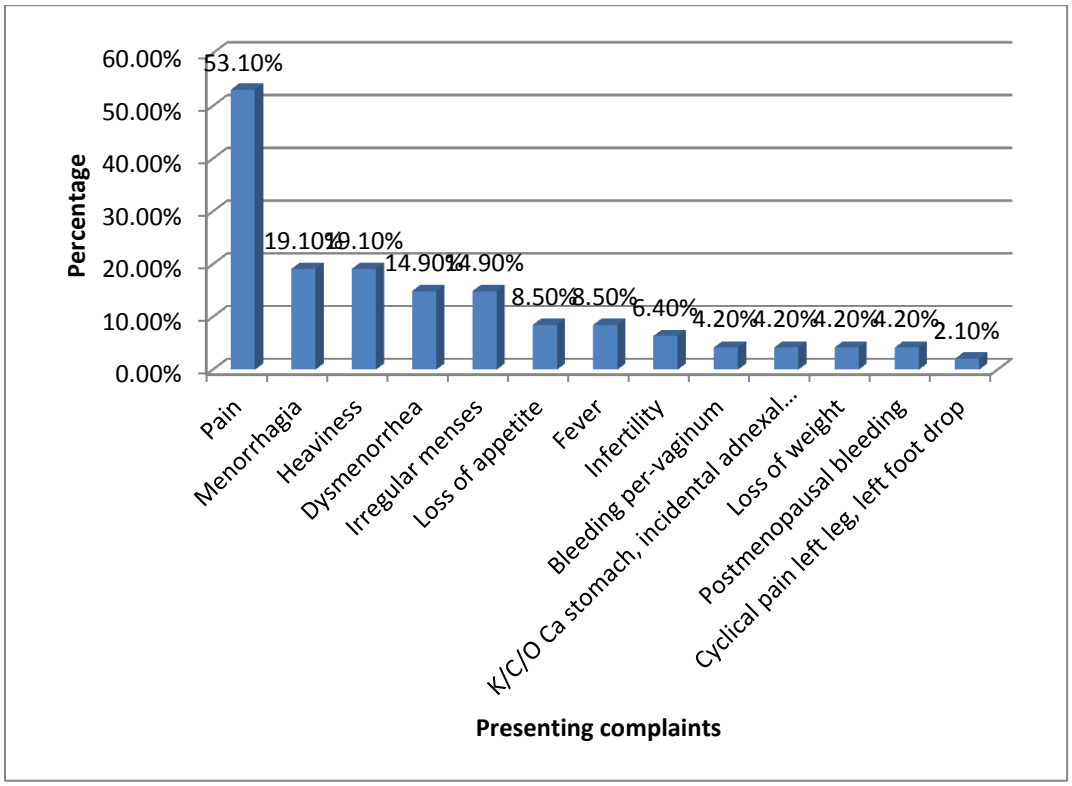

5. CA-125 levels comparison in benign and malignant lesions

Serum CA-125 levels were available for 29 patients. The mean value was 72.63 U/mL in patients with benign lesions and 102.09 U/mL in patients with malignant lesions (p=0.569).

Table 6: Mean CA-125 levels in benign and malignant lesions

	Benign		Malignant		Z	p-value
	Mean	SD	Mean	SD		
CA-125 LEVELS (U/mL)	72.63	122.69	102.09	97.69	-0.577	0.569

Figure 8: Mean CA-125 levels in benign and malignant lesions

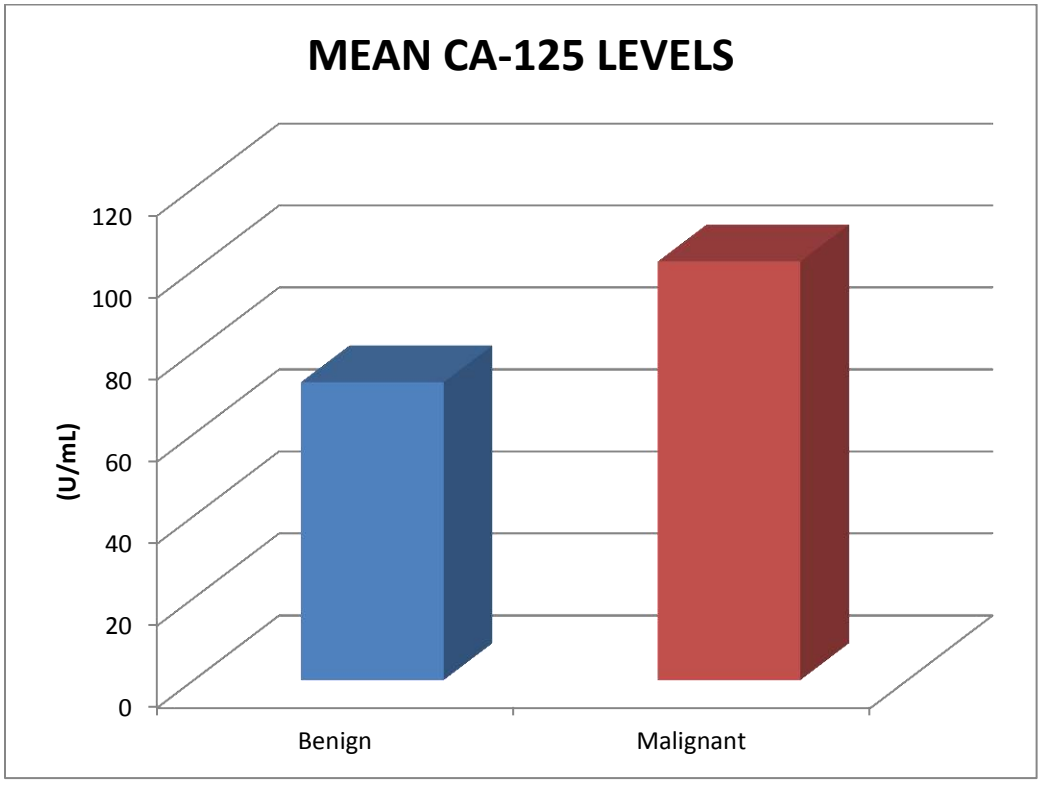

Table 7: Final diagnosis: Subtypes

Benign / Malignant	Final Diagnosis	No. of lesions	Percentage
Benign		**37**	**78.7%**
	Endometrioma	13	27.7%
	Leiomyoma (Subserosal / broad ligament)	4	8.5%
	Hemorrhagic cyst	4	8.5%
	Benign multiseptate cystic lesion (Unspecified)	4	8.5%
	Simple cyst (ovarian / para-ovarian)	3	6.4%
	Tubo-ovarian abscess	2	4.2%
	Mucinous cystadenoma	1	2.1%
	Serous cystadenoma	1	2.1%
	Serous cystadenofibroma	1	2.1%
	Dermoid cyst	1	2.1%
	Ovarian hyperstimulation	1	2.1%
	Actinomycosis	1	2.1%
	Fibrothecoma	1	2.1%
Malignant		**10**	**21.3%**
	Endometrioid carcinoma	5	10.6%
	Granulosa cell tumor	2	4.2%
	Metastases (Krukenberg tumors)	2	4.2%
	Clear cell carcinoma	1	2.1%
Total		**47**	**100%**

Among the benign lesions, 13 (27.7%) lesions were endometriomas, 4 (8.5%) were subserosal / broad ligament leiomyomas and 4 (8.5%) were hemorrhagic cysts. Among the malignant lesions, endometrioid carcinomas were the most commonly diagnosed (5, 10.6%).

Figure 9a: Final diagnosis: Benign lesions

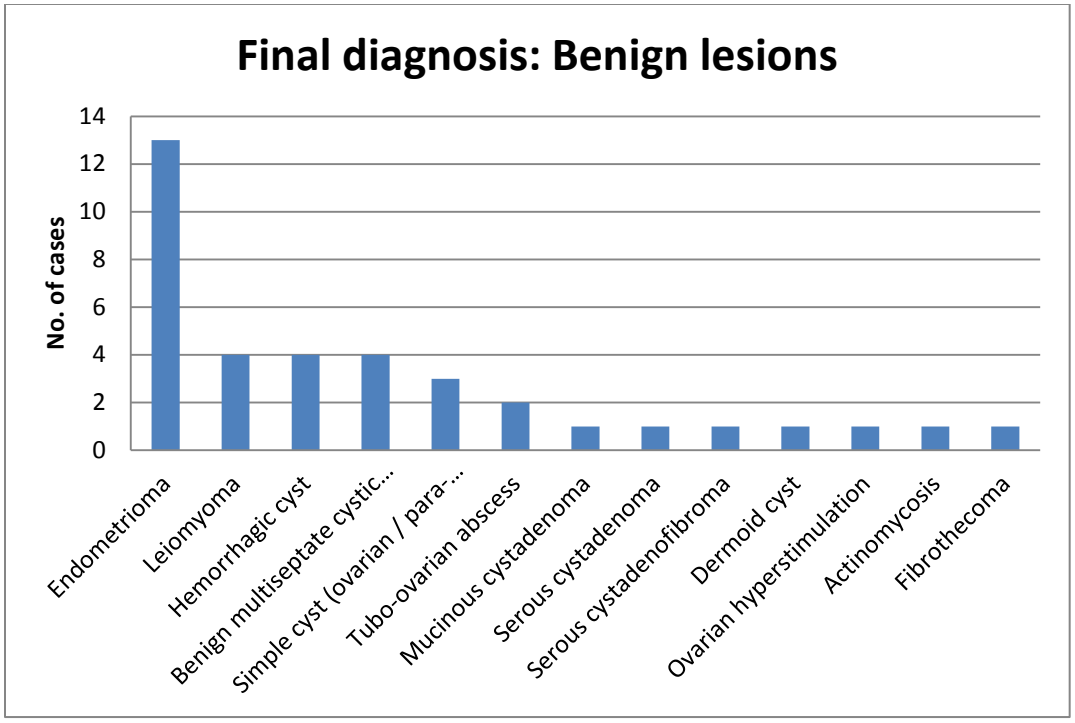

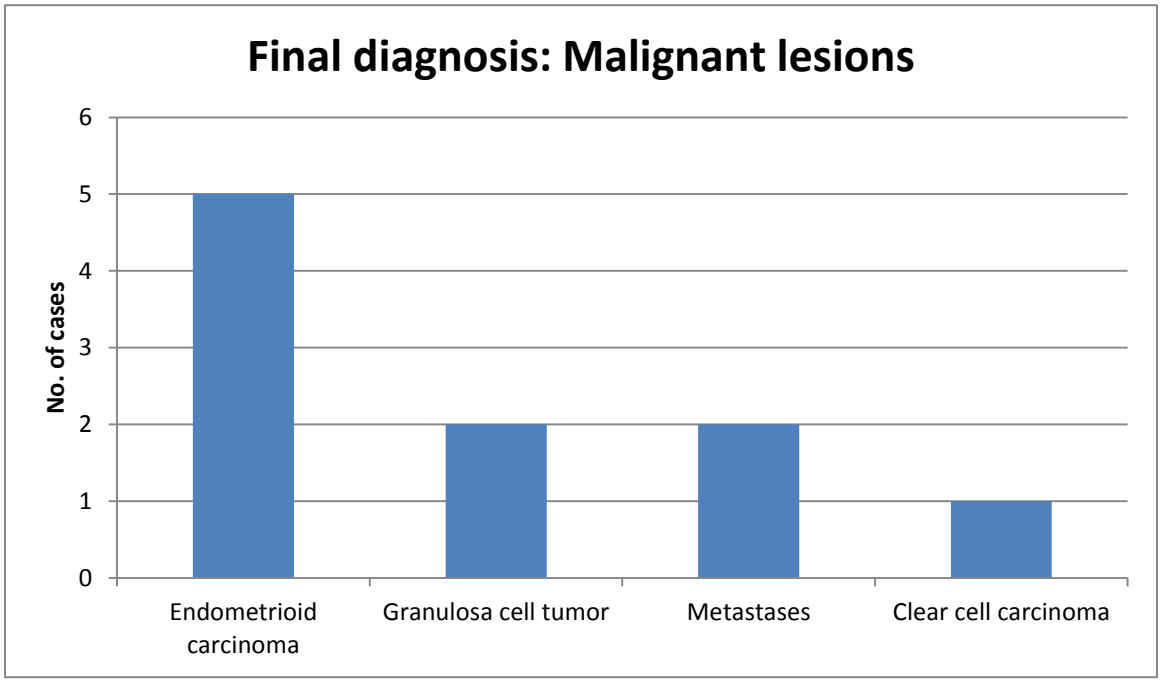

Figure 9b: Final diagnosis: Malignant lesions

B. Conventional MRI Findings:

All the adnexal masses were assessed based on the following conventional MRI parameters:

1. Size

The largest diameter of the lesions ranged from 1cm to 21cm. The mean of the largest dimension was 8.32cm.

Mean of the largest dimension was 7.65cm for benign lesions, and 10.80cm for malignant lesions (p=0.080).

Table 8: Size comparison of benign and malignant lesions

SIZE	Benign		Malignant		Z	p-value
	Mean	SD	Mean	SD		
Largest dimension (cm)	7.65	4.82	10.80	5.39	-1.789	0.080

Figure 10: Size comparison of benign and malignant lesions

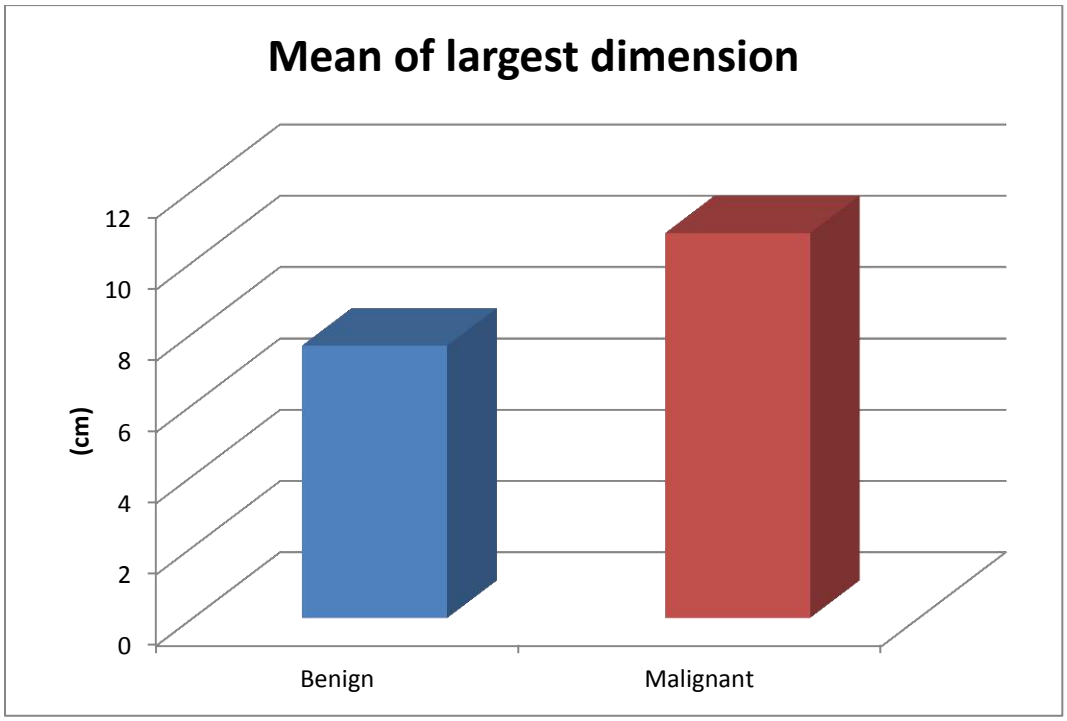

2. Bilaterality

Of the 47 patients, 12 (25.5%) patients had bilateral lesions. 8 of these patients had benign lesions, while 4 had malignant lesions (p=0.237).

Table 9: Bilaterality in benign and malignant lesions

		FINAL DIAGNOSIS				Total	Chi-square value	p-value
		Benign		Malignant				
BILATERALITY	Yes	8	21.6%	4	40.0%	12	1.399	0.237
	No	29	78.4%	6	60.0%	35		
Total		37	100.0%	10	100.0%	47		

Figure 11: Bilaterality in benign and malignant lesions

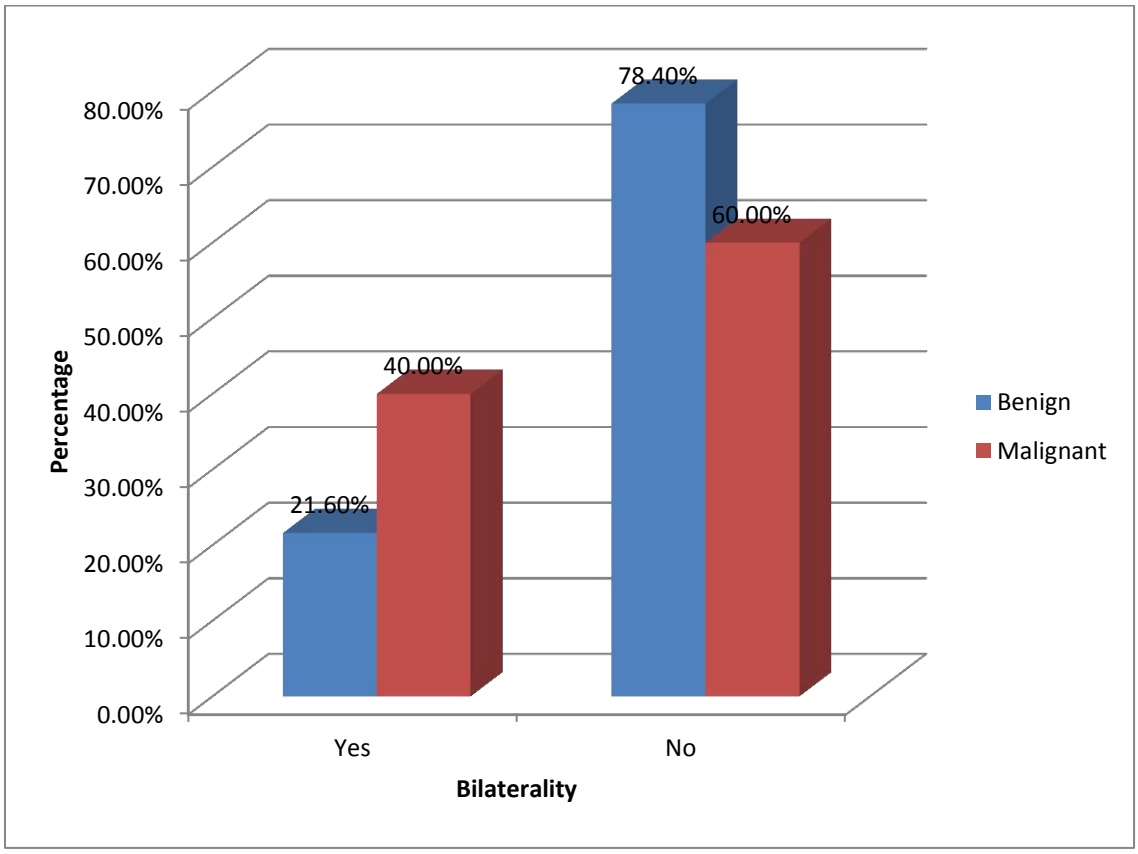

3. Solid/cystic nature of lesions

Of the 47 patients included in our study, 28 (59.6%) lesions were purely cystic, 8 (17%) were purely solid, and 11 (23.4%) were mixed solid-cystic lesions.

All 28 purely cystic lesions were benign. Out of the 8 purely solid lesions, 5 were benign and 3 were malignant. Among the 11 mixed solid-cystic lesions, 4 were benign and 7 were malignant.

Table 10a: Solid/cystic nature of lesions

SOLID/CYSTIC	No. of lesions	Percentage
Purely cystic	28	59.6%
Purely solid	8	17.0%
Predominantly cystic	9	19.1%
Predominantly solid	2	4.3%
Total	47	100.0%

Figure 12a: Solid/cystic nature of lesions

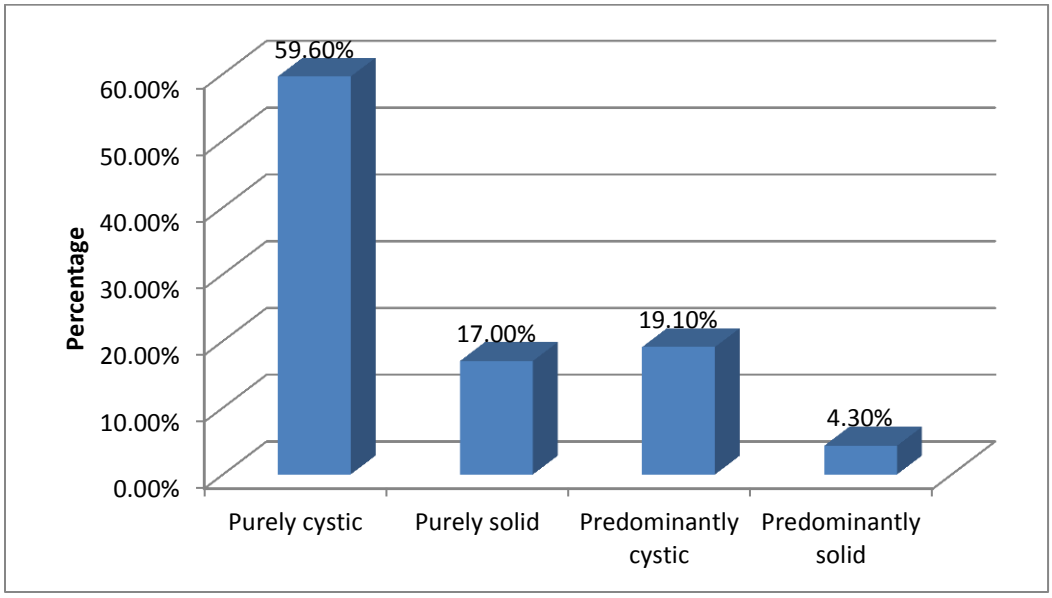

Table 10b: Comparison of solid/cystic nature in benign and malignant lesions

		FINAL DIAGNOSIS				Total	Chi-square value	p-value
		Benign		Malignant				
SOLID/ CYSTIC	Purely cystic	28	75.7%	0	0.0%	28	18.72	0.001
	Purely solid	5	13.5%	3	30.0%	8	1.515	0.218
	Predominantly cystic	4	10.8%	5	50.0%	9	7.809	0.013
	Predominantly solid	0	0.0%	2	20.0%	2	7.729	0.005
Total		37	100.0%	10	100.0%	47		

Figure 12b: Comparison of solid/cystic nature in benign and malignant lesions

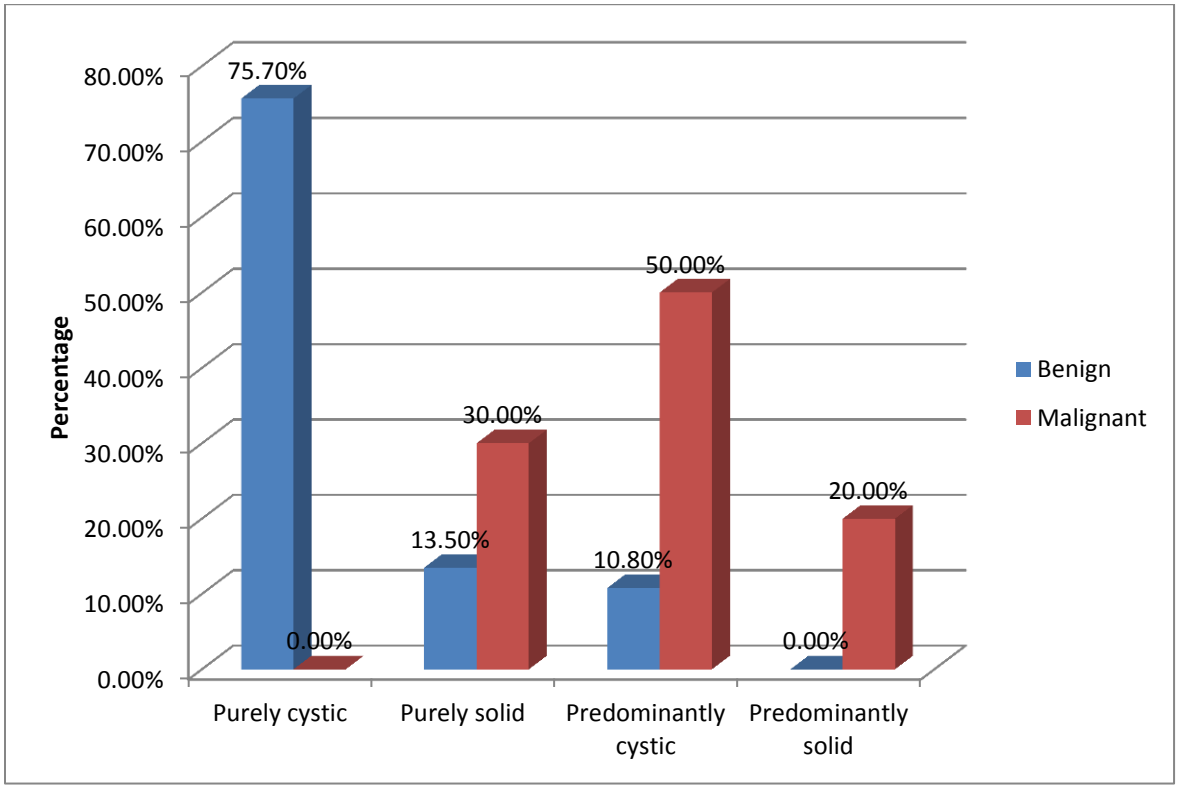

4. T2 signal intensity of solid component

In our study, 19 lesions (11 solid-cystic, 8 purely solid) had some solid component. In 14 (73.7%) of these lesions, the solid component showed intermediate signal intensity compared to the outer myometrium, while solid component of 5 (26.3%) lesions appeared hypointense on T2WI.

Intermediate T2 signal intensity within the solid component was seen in all the 10 malignant lesions, and in 4 (44.4%) out of the 9 benign lesions with some solid component. Hypointense T2 signal within the solid component was found in 5 (55.6%) of the 9 benign lesions with some solid component, and in none of the 10 malignant lesions. Presence of low T2 signal intensity in solid component had 100% PPV as well as 100% specificity for the diagnosis of a benign lesion (p=0.001).

Table 11a: T2 signal intensity of solid component

T2 SIGNAL INTENSITY OF SOLID COMPONENT	No. of lesions	Percentage
Intermediate	14	73.7%
Hypointense	5	26.3%
Total	19	100.0%

Figure 13a: T2 signal intensity of solid component

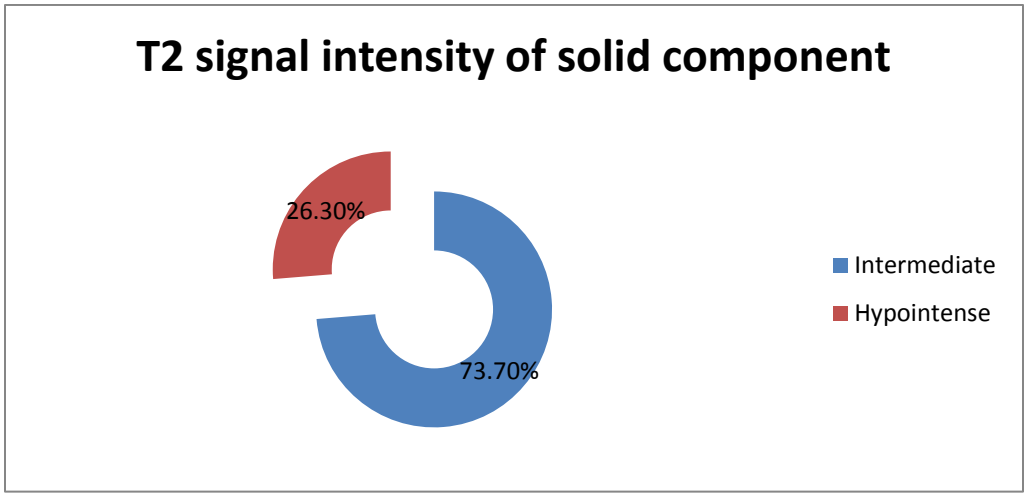

Table 11b: Comparison of T2 signal intensity of solid component in benign and malignant lesions

		FINAL DIAGNOSIS				Total	Chi-square value	p-value
		Benign		Malignant				
T2 SI SOLID COMPONENT							29.942	0.001
	Intermediate	4	44.4%	10	100.0%	14		
	Hypointense	5	55.6%	0	0.0%	5		
Total		9	100.0%	10	100.0%	19		

Figure 13b: Comparison of T2 signal intensity of solid component in benign and malignant lesions

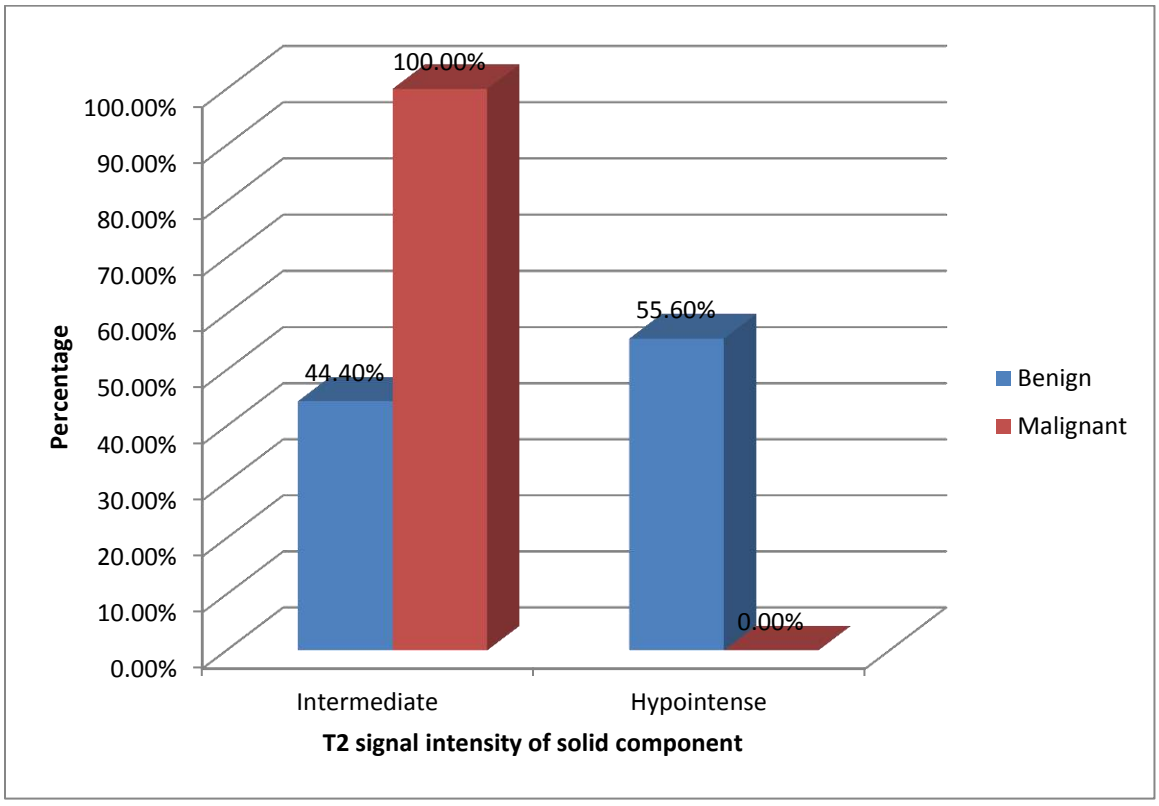

5. Marked T1 hyperintensity in cystic component

After excluding the purely solid lesions, a total of 39 lesions had some cystic component in our study, out of which 32 were benign, and 7 were malignant. Marked hyperintensity on T1WI as well as T1 fat-saturated images in the cystic component was seen in 15 (38.5%) out of 39 lesions, out of which 13 were benign, and 2 were malignant (p=0.553).

Table 12a: Marked T1 hyperintensity in cystic component

MARKED T1 HYPERINTENSITY IN CYSTIC COMPONENT	No. of lesions	Percentage
Yes	15	38.5%
No	24	61.5%
Total	39	100.0%

Figure 14a: Marked T1 hyperintensity in cystic component

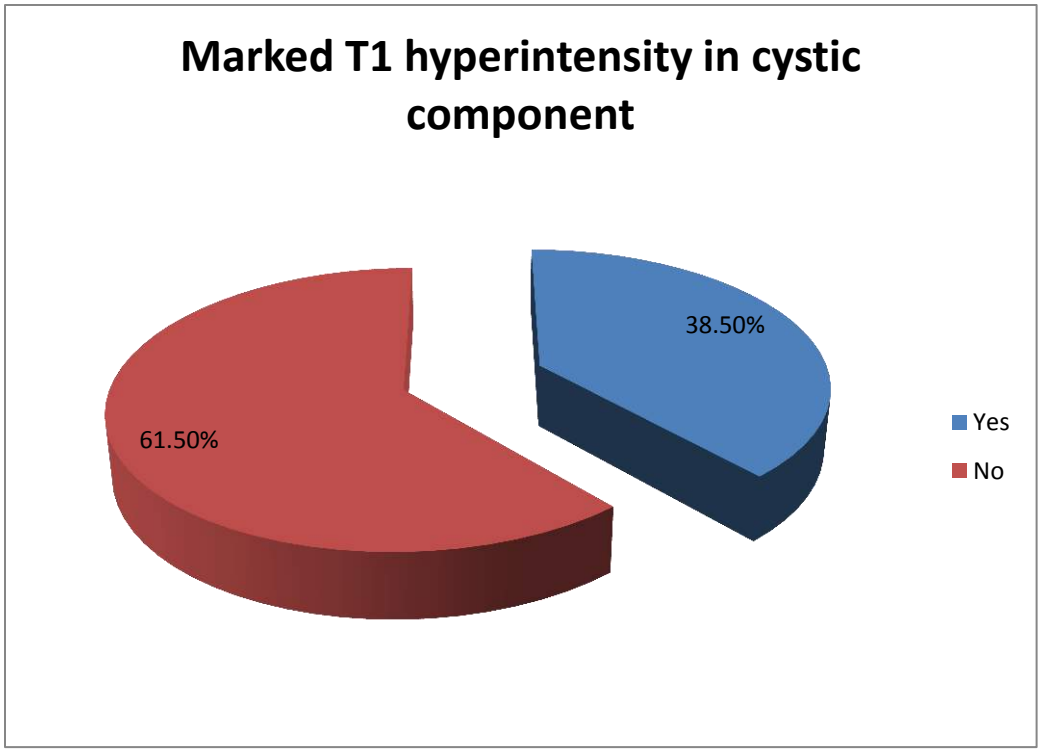

Table 12b: Marked T1 hyperintensity in cystic component in benign and malignant lesions

		FINAL DIAGNOSIS				Total	Chi-square value	p-value
		Benign		Malignant				
MARKED T1 HYPERINTENSITY IN CYSTIC COMPONENT	Yes	13	40.6%	2	28.6%	15	0.353	0.553
	No	19	59.4%	5	71.4%	24		
Total		32	100.0%	7	100.0%	39		

Figure 14b: Marked T1 hyperintensity in cystic component in benign and malignant lesions

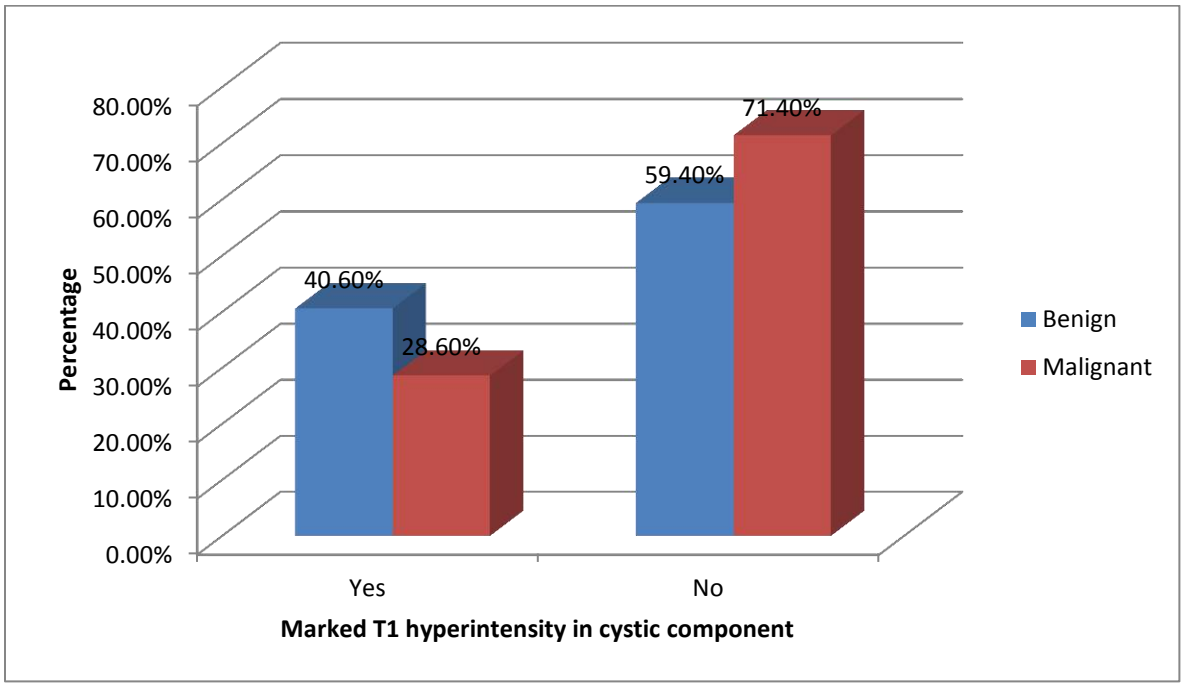

6. T2 shading

Shading sign on T2WI was present in 14/39 (35.9%) lesions. 12/32 (37.5%) of the benign and 2/7 (33.3%) of the malignant lesions showed T2 shading (p=0.655).

Table 13a: T2 shading

T2 SHADING	No. of lesions	Percentage
Yes	14	35.9%
No	25	64.1%
Total	39	100.0%

Figure 15a: T2 shading

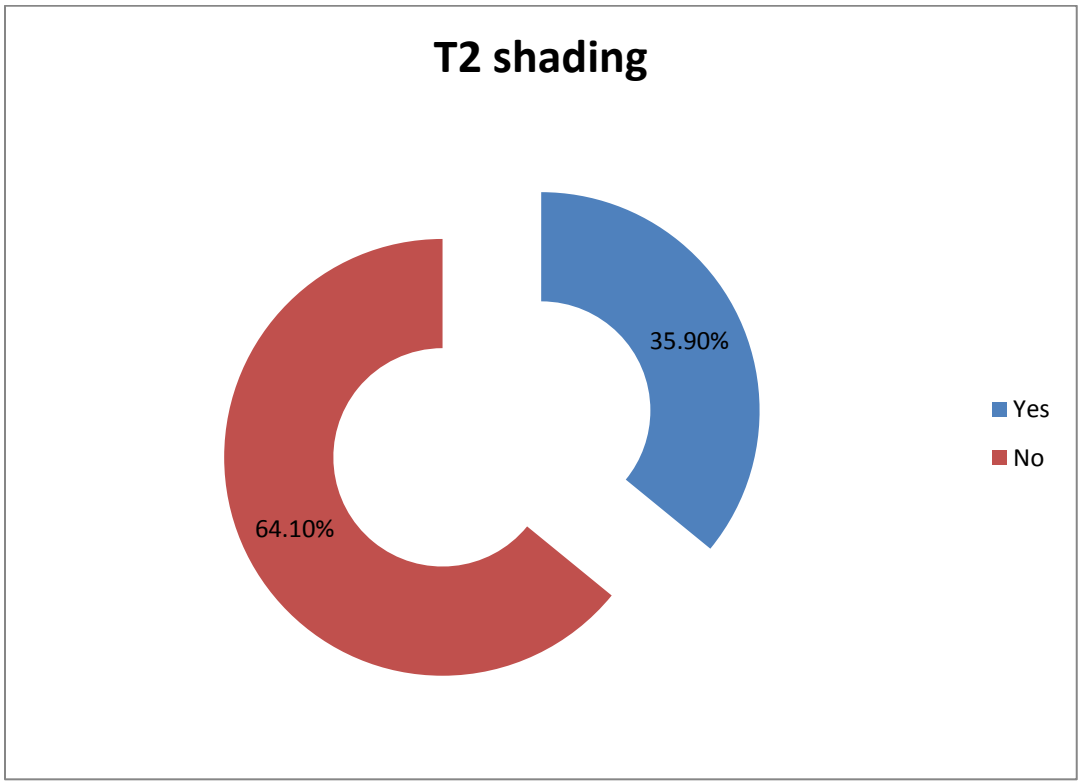

Table 13b: T2 shading in benign and malignant lesions

		FINAL DIAGNOSIS				Total	Chi-square value	p-value
		Benign		Malignant				
T2 SHADING	Yes	12	37.5%	2	28.6%	14	0.199	0.655
	No	20	62.5%	5	71.4%	25		
Total		32	100.0%	7	100.0%	39		

Figure 15b: T2 shading in benign and malignant lesions

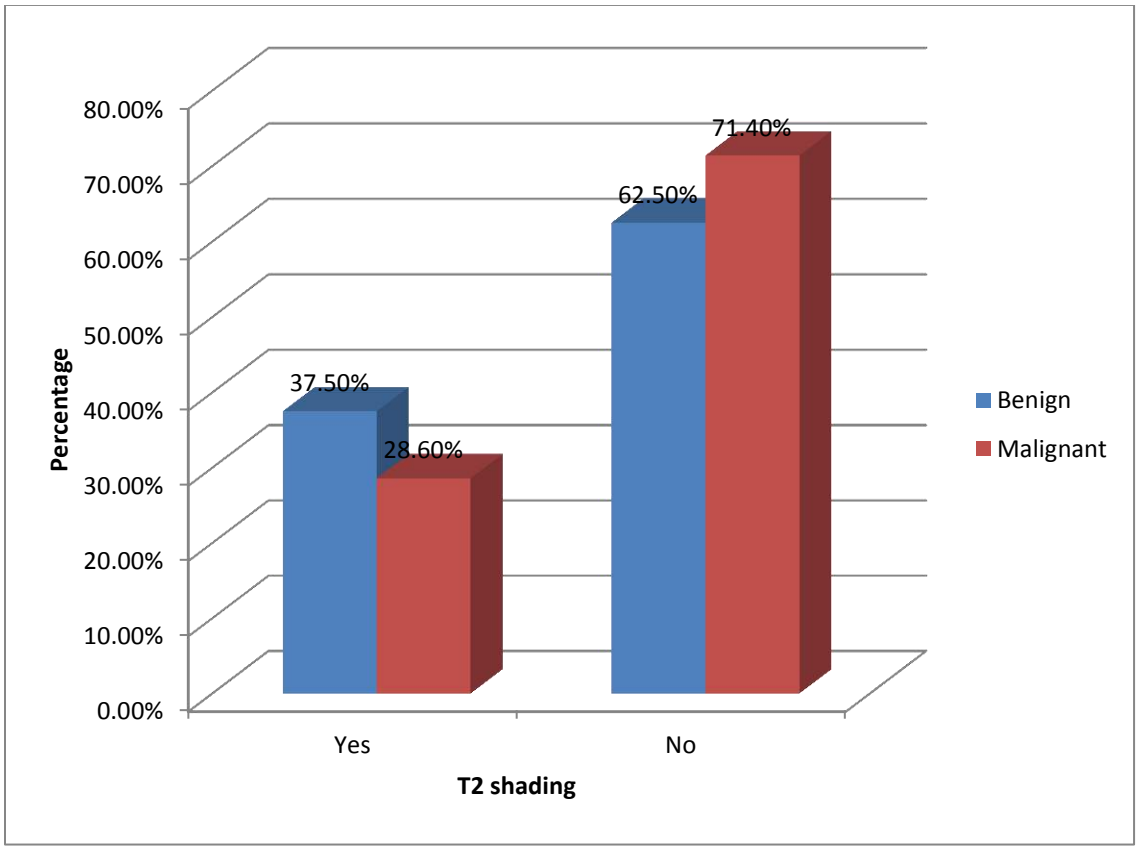

7. Thickened septa

In the 39 lesions with some cystic component, thickened septa (greater than or equal to 3 mm thickness) were present in 9/39 (23.1%) lesions, out of which, 7 were benign and 2 were malignant. Thickened septa were seen in 7/32 (21.9%) benign and 2/7 (28.6%) malignant lesions (p=0.703).

Table 14a: Thickened septa

THICKENED SEPTA	No. of lesions	Percentage
Yes	9	23.1%
No	30	76.9%
Total	39	100.0%

Figure 16a: Thickened septa

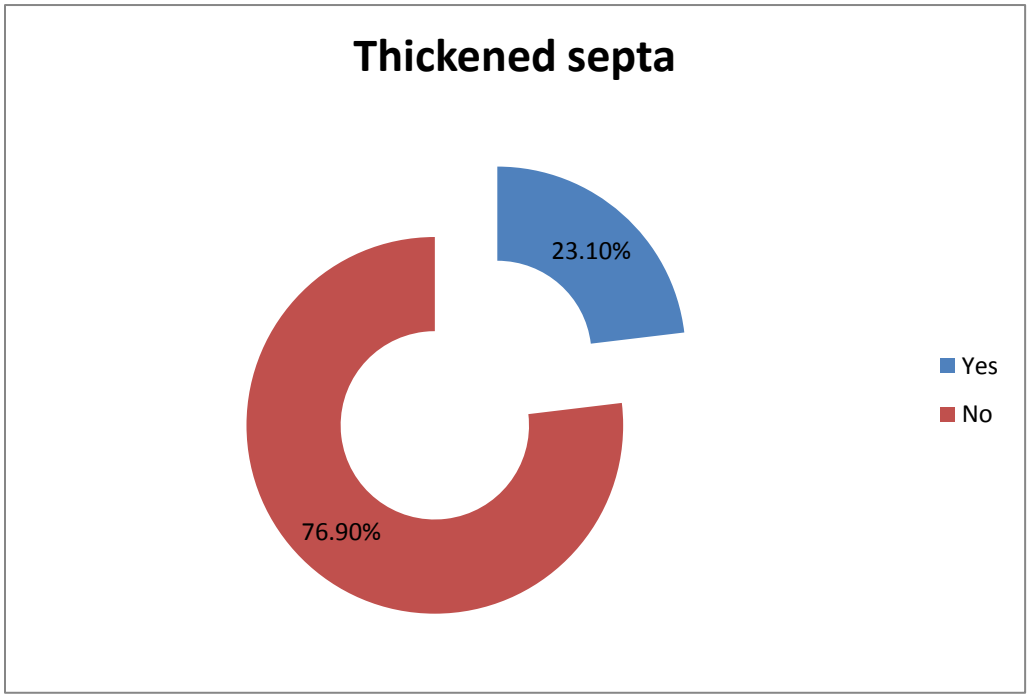

Table 14b: Thickened septa in benign and malignant lesions

		FINAL DIAGNOSIS				Total	Chi-square value	p-value
		Benign		Malignant				
THICKENED SEPTA	Yes	7	21.9%	2	28.6%	9	0.145	0.703
	No	25	78.1%	5	71.4%	30		
Total		32	100.0%	7	100.0%	39		

Figure 16b: Thickened septa in benign and malignant lesions

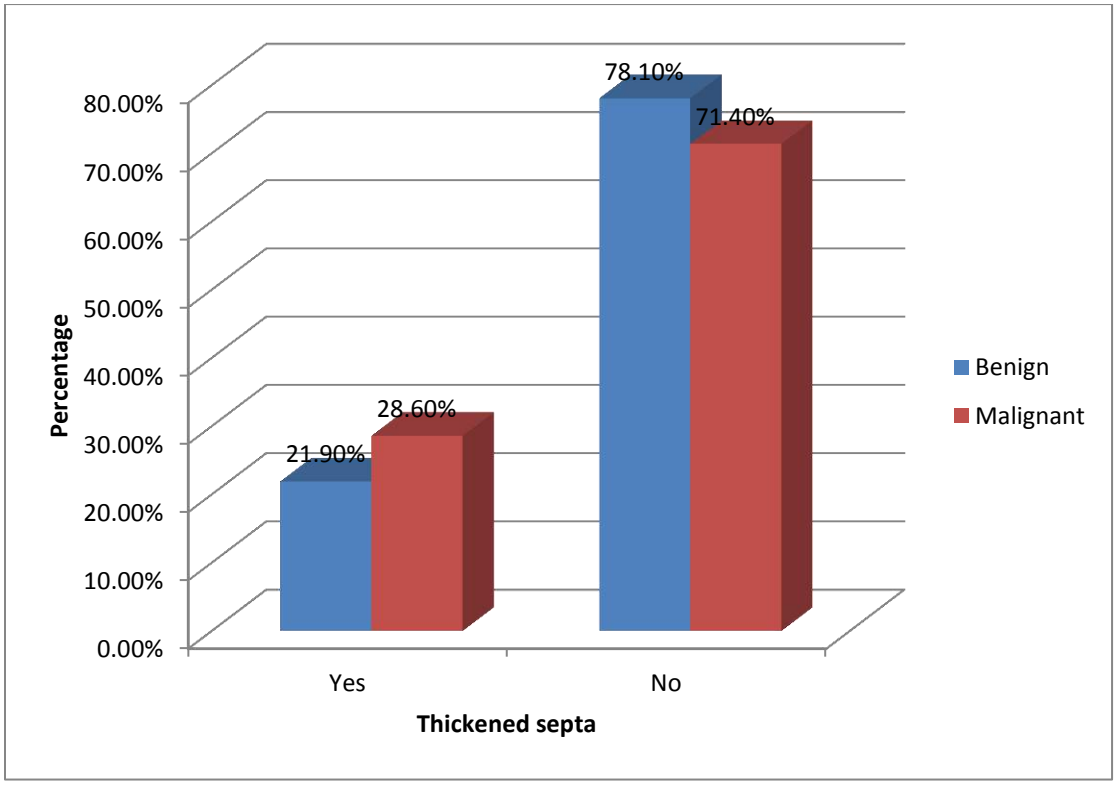

8. Hemorrhage

Out of total 47 lesions included in our study, hemorrhage was seen in 23 (48.9%) lesions, out of which, 20 lesions were benign, and 3 were malignant. (p=0.177).

Table 15a: Hemorrhage

HEMORRHAGE	No. of lesions	Percentage
Yes	23	48.9%
No	24	51.1%
Total	47	100.0%

Figure 17a: Hemorrhage

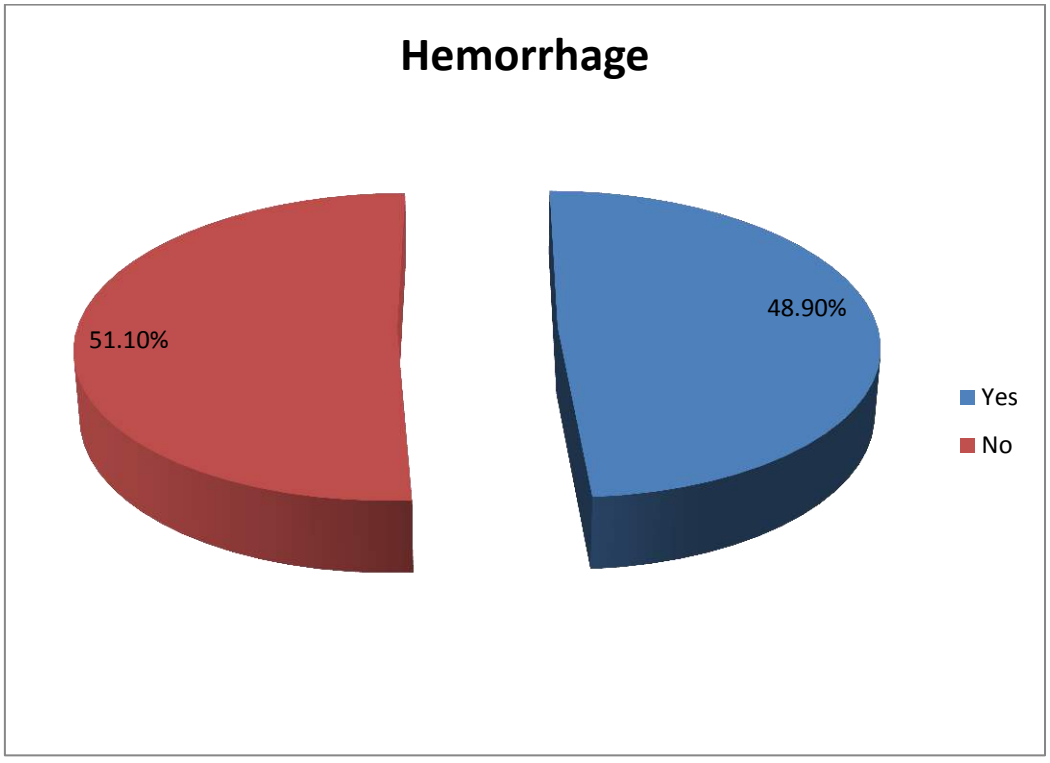

Table 15b: Hemorrhage in benign and malignant lesions

		FINAL DIAGNOSIS				Total	Chi-square value	p-value
		Benign		Malignant				
HEMORRHAGE	Yes	20	54.1%	3	30.0%	23	1.823	0.177
	No	17	45.9%	7	70.0%	24		
Total		37	100.0%	10	100.0%	47		

Figure 17b: Hemorrhage in benign and malignant lesions

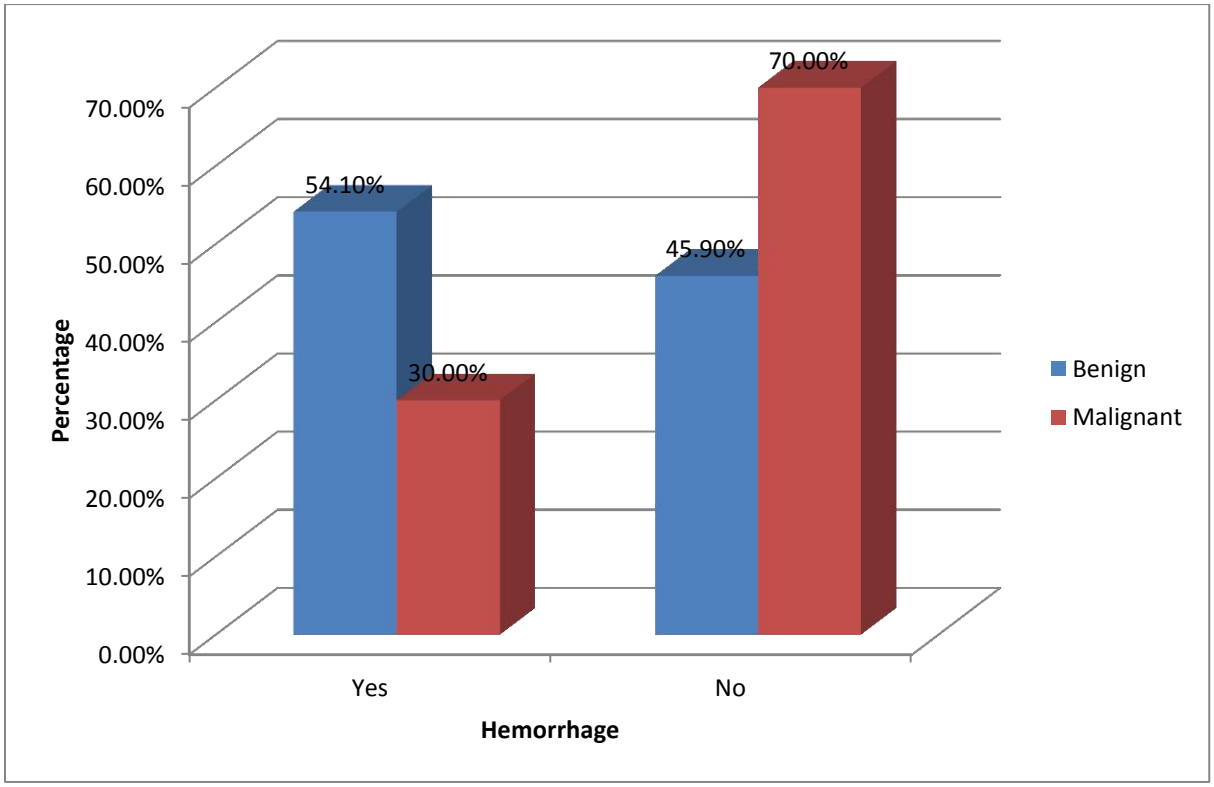

9. Papillary projections

Among the 39 lesions with some cystic component, papillary projections were seen in 4 (10.2%) lesions. 1 (3.1%) benign and 3 (42.9%) malignant lesions had papillary projections (p=0.001).

Table 16a: Papillary projections

PAPILLARY PROJECTIONS	No. of lesions	Percentage
Yes	4	10.2%
No	35	89.8%
Total	39	100.0%

Figure 18a: Papillary projections

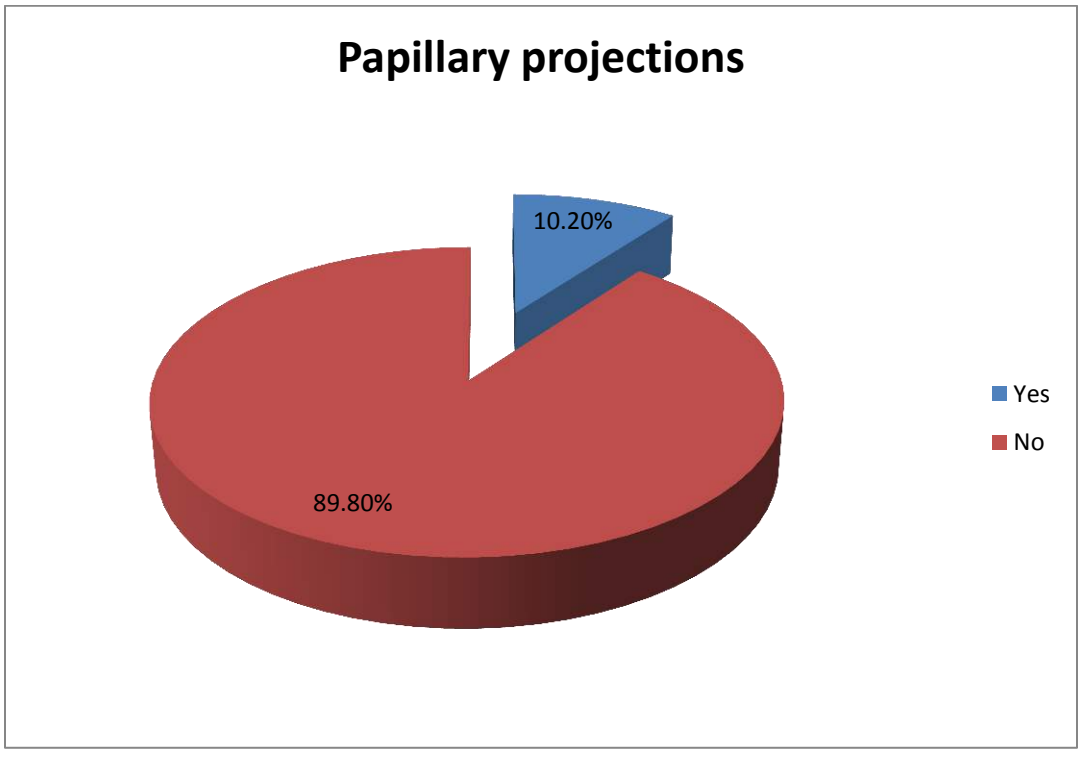

Table 16b: Papillary projections in benign and malignant lesions

		FINAL DIAGNOSIS				Total	Chi-square value	p-value
		Benign		Malignant				
PAPILLARY PROJECTIONS	Yes	1	3.1%	3	42.9%	4	9.85	0.001
	No	31	96.9%	4	57.1%	35		
Total		32	100.0%	7	100.0%	39		

Figure 18b: Papillary projections in benign and malignant lesions

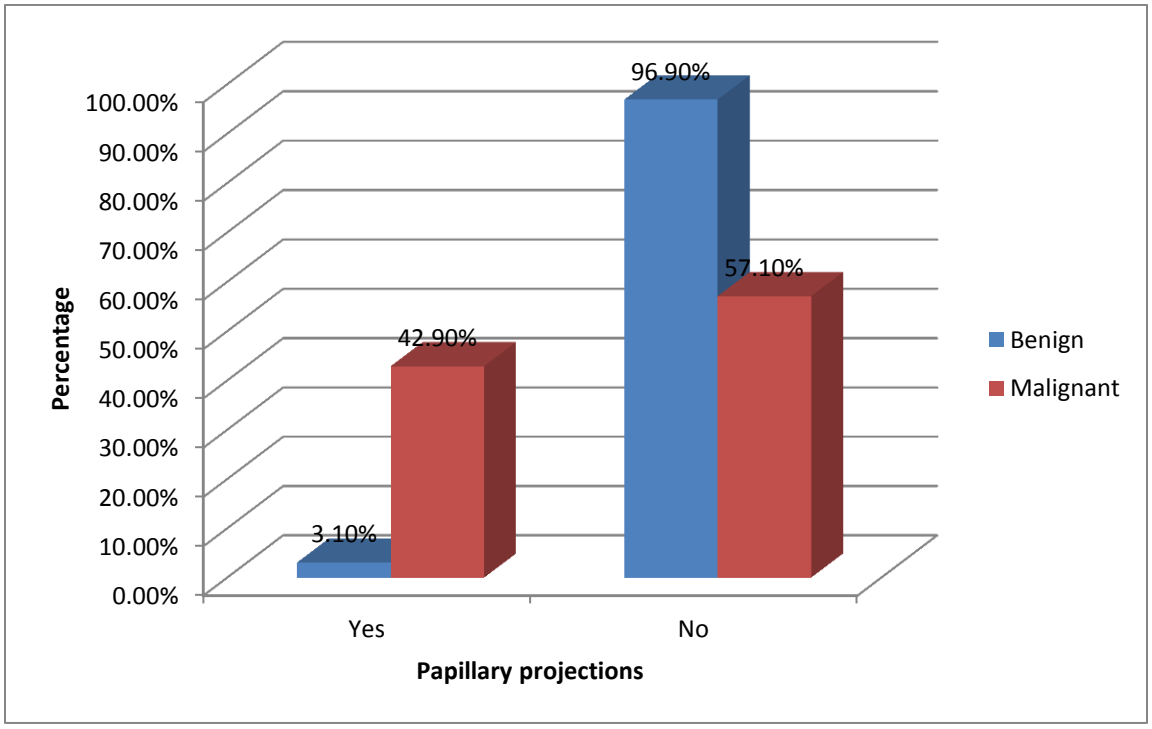

10. Ascites

Ascites was seen in 18 (38.3%) patients, and was present in 12 (32.5%) patients with benign and 6 (60.0%) patients with malignant lesions (p=0.112).

Table 17a: Ascites

ASCITES	No. of patients	Percentage
Yes	18	38.3%
No	29	61.7%
Total	47	100.0%

Figure 19a: Ascites

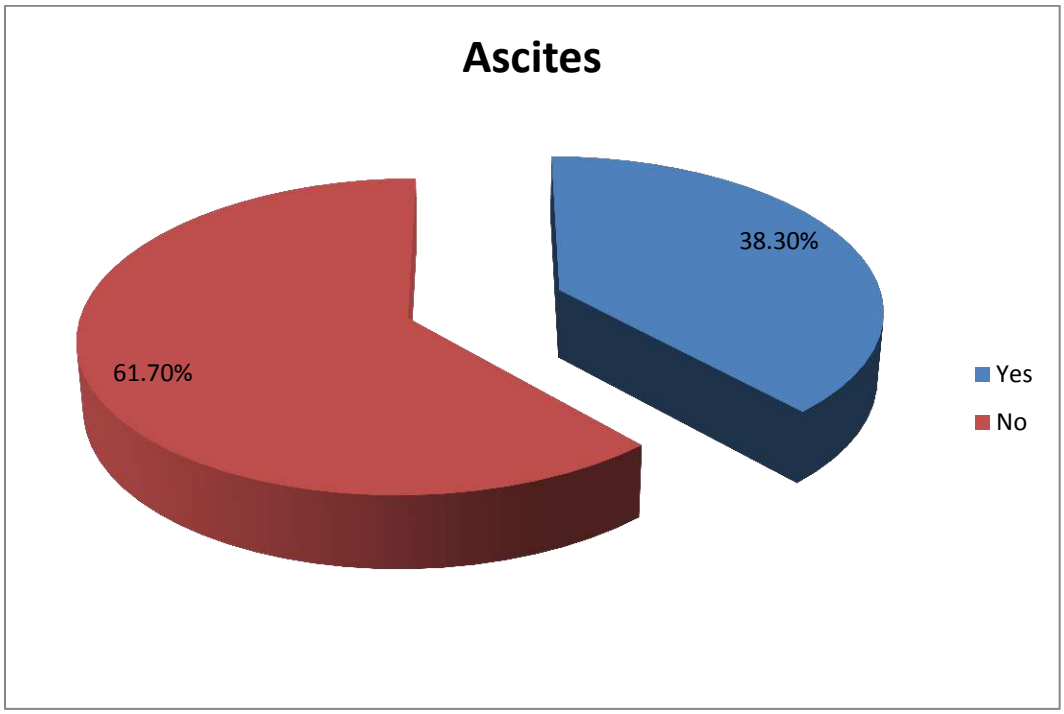

Table 17b: Ascites in benign and malignant lesions

		FINAL DIAGNOSIS				Total	Chi-square value	p-value
		Benign		Malignant				
ASCITES	Yes	12	32.4%	6	60.0%	18	2.532	0.112
	No	25	67.6%	4	40.0%	29		
Total		37	100.0%	10	100.0%	47		

Figure 19b: Ascites in benign and malignant lesions

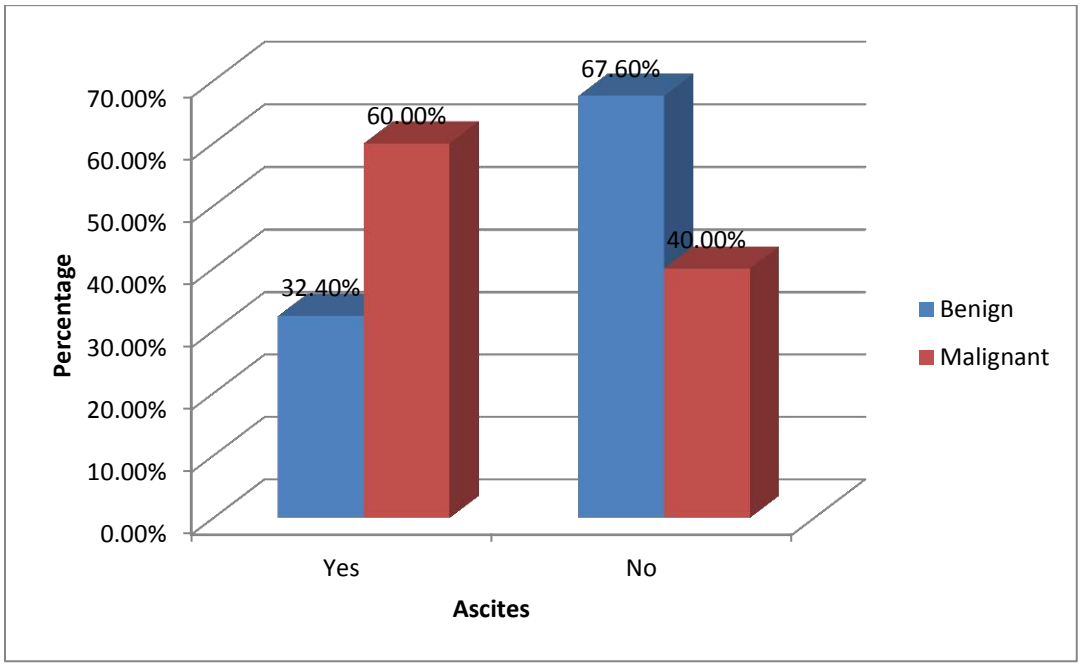

None of the patients in our study demonstrated the presence of omental/ peritoneal disease, enlarged metastatic lymph nodes or visceral metastases. This may be attributed to the fact that most of the patients with an overt ovarian malignancy with features of dissemination on US such as gross ascites, obvious omental disease, and visceral metastases were followed up with a contrast-enhanced CT of the chest and whole abdomen, which is the investigation of choice for the staging of ovarian malignancy.

C. DIFFUSION-WEIGHTED IMAGING (DWI)

Assessment of DWI and ADC parameters was done for all lesions, and the findings were recorded for solid and cystic components separately. The lesions which appeared bright on DWI and dark on ADC maps were considered positive on Diffusion weighted imaging.

1. Diffusion restriction within solid component

Out of the 19 lesions with some solid component, presence of diffusion restriction in the solid component, that is, high signal on high b-value DW images (b=800 s/mm^2), with corresponding low signal on ADC maps was present in 12 (63.2%) lesions.

Out of these 12 lesions, 2 were benign and 10 were malignant. All the malignant lesions showed restricted diffusion in their solid component. Among the 9 benign lesions with some solid component, 2 (22.2%) lesions showed restricted diffusion (p=0.0001).

Table 18a: Diffusion restriction within solid component

DIFFUSION RESTRICTION IN SOLID COMPONENT	No. of lesions	Percentage
Yes	12	63.2%
No	7	36.8%
Total	19	100.0%

Figure 20a: Diffusion restriction within solid component

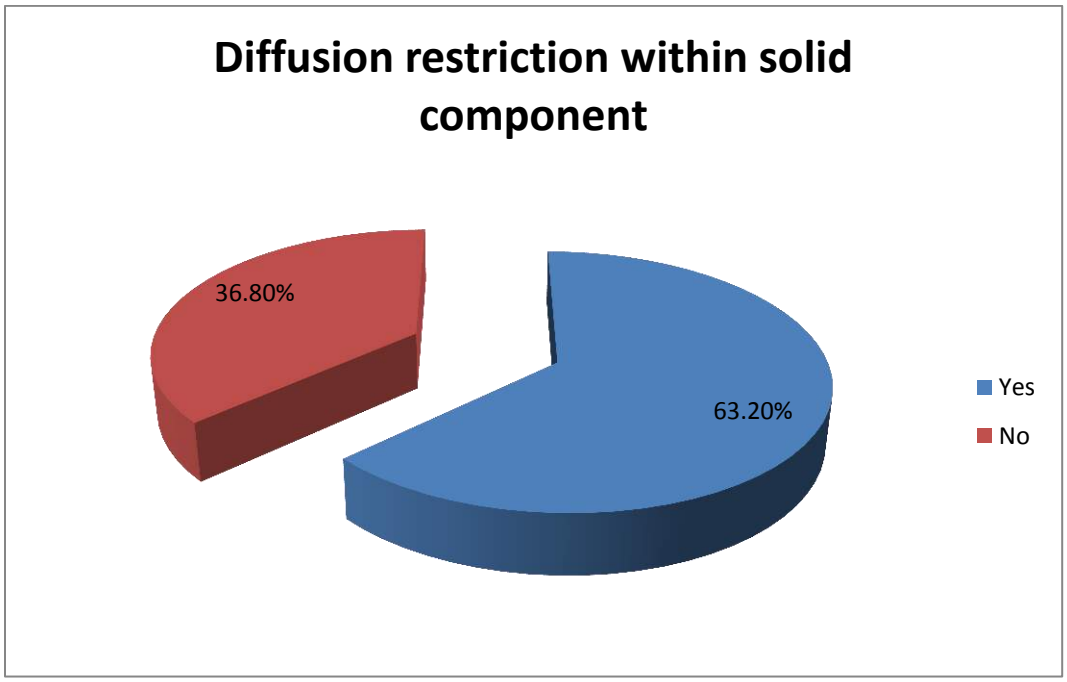

Table 18b: Comparison of Diffusion restriction within solid component in benign and malignant lesions

		FINAL DIAGNOSIS				Total	Chi-square value	p-value
		Benign		Malignant				
DIFFUSION RESTRICTION IN SOLID COMPONENT	Yes	2	22.2%	10	100.0%	12	12.315	0.0001
	No	7	77.8%	0	0.0%	7		
Total		9	100.0%	10	100.0%	19		

Figure 20b: Comparison of Diffusion restriction within solid component in benign and malignant lesions

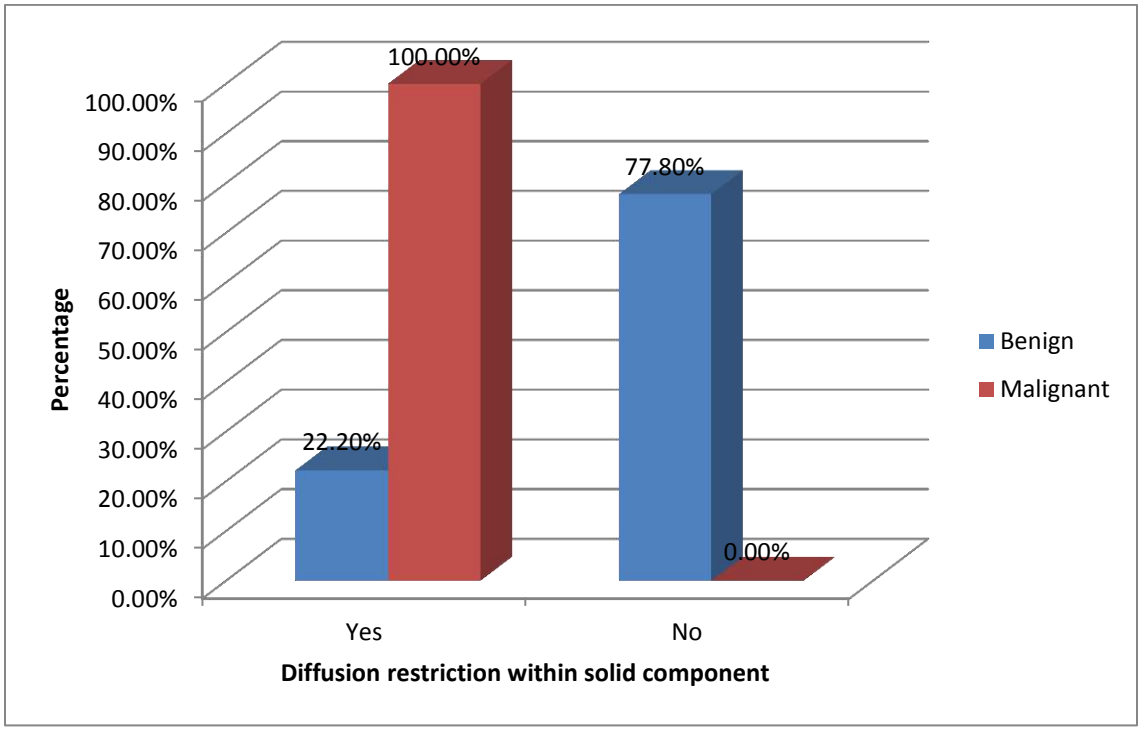

2. Diffusion restriction in cystic component

Among the 39 lesions with some cystic component, presence of diffusion restriction in the cystic component, that is, high signal on high b-value DW images (b=800 s/mm^2), with corresponding low signal on ADC maps was present in 10 (25.6%) lesions.

9 (28.1%) benign lesions and 1 (14.3%) malignant lesion showed restricted diffusion in their cystic component (p=0.447).

Table 19a: Diffusion restriction in cystic component

DIFFUSION RESTRICTION IN CYSTIC COMPONENT	No. of lesions	Percentage
Yes	10	25.6%
No	29	74.4%
Total	39	100.0%

Figure 21a: Diffusion restriction in cystic component

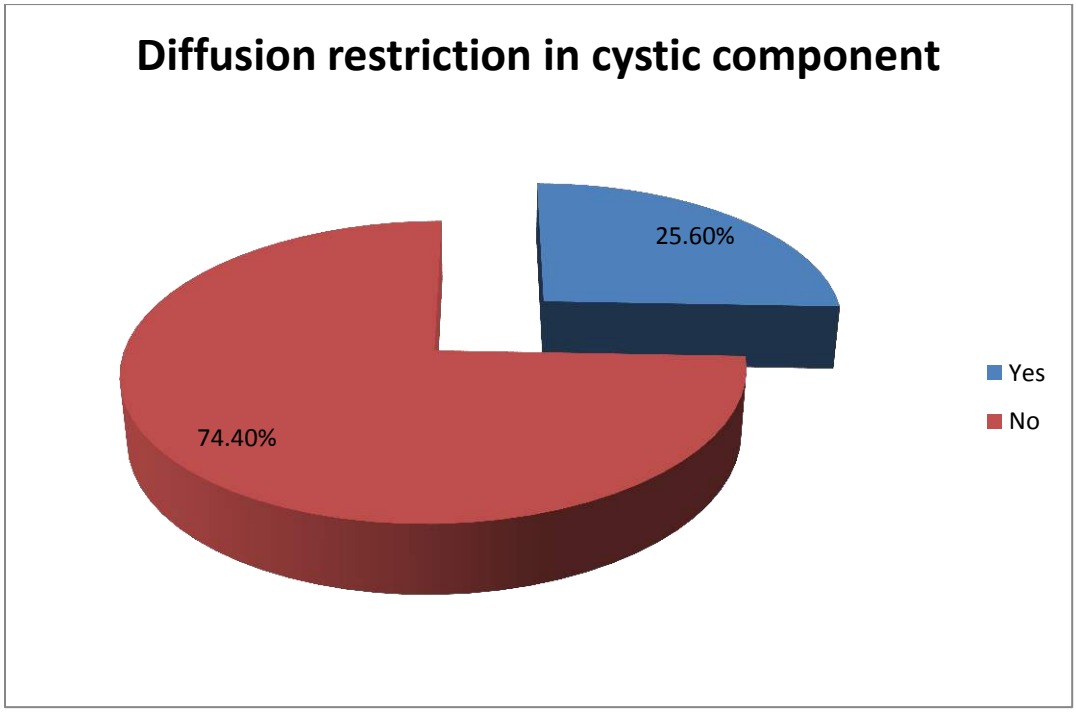

Table 19b: Comparison of Diffusion restriction in cystic component in benign and malignant lesions

		FINAL DIAGNOSIS				Total	Chi-square value	p-value
		Benign		Malignant				
DIFFUSION RESTRICTION IN CYSTIC COMPONENT	Yes	9	28.1%	1	14.3%	10	0.577	0.447
	No	23	71.9%	6	85.7%	29		
Total		32	100.0%	7	100.0%	39		

Figure 21b: Comparison of Diffusion restriction in cystic component in benign and malignant lesions

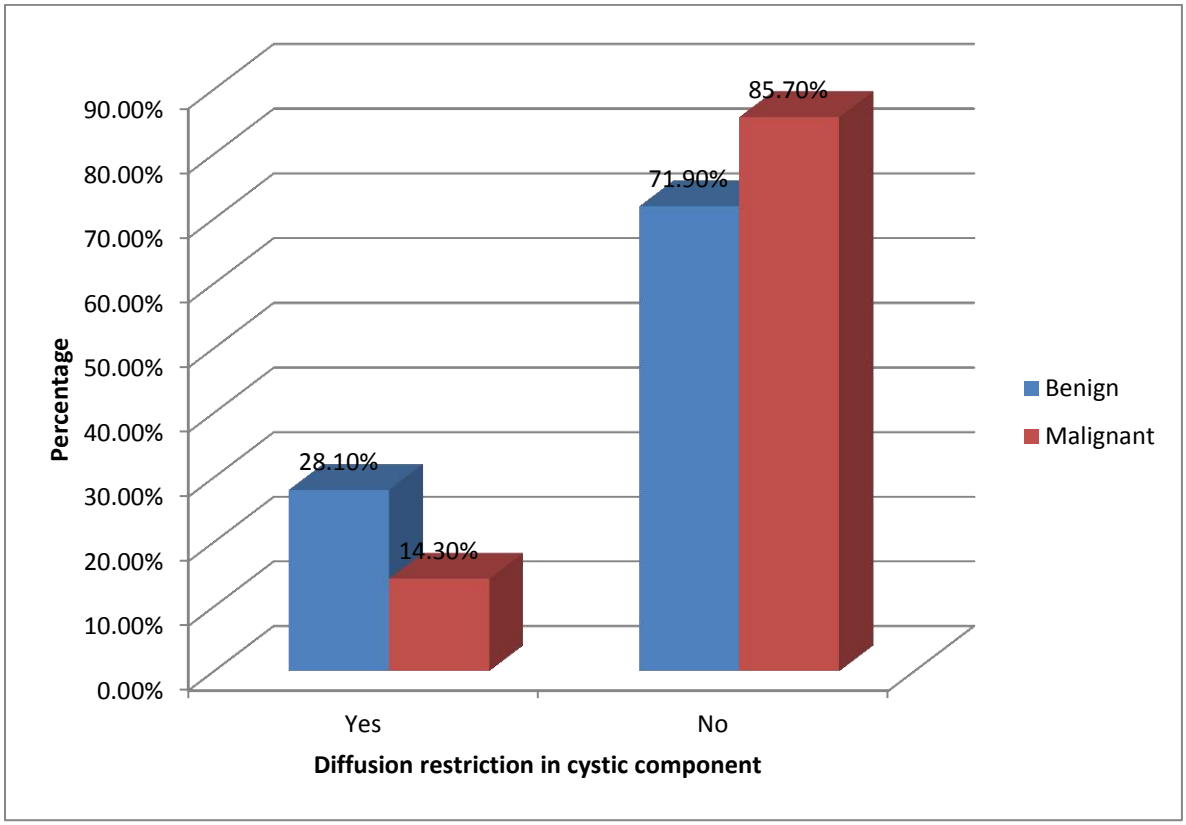

3. Low ADC signal in solid component

Out of 19 lesions with some solid component, 18 (94.7%) lesions showed hypointense signal on ADC maps.

Low signal on ADC maps was seen in the solid component of 8 (88.9%) benign and all 10 malignant lesions (p=0.279).

Table 20a: Low ADC signal in solid component

LOW ADC SIGNAL IN SOLID COMPONENT	No. of lesions	Percentage
Yes	18	94.7%
No	1	5.3%
Total	19	100.0%

Figure 22a: Low ADC signal in solid component

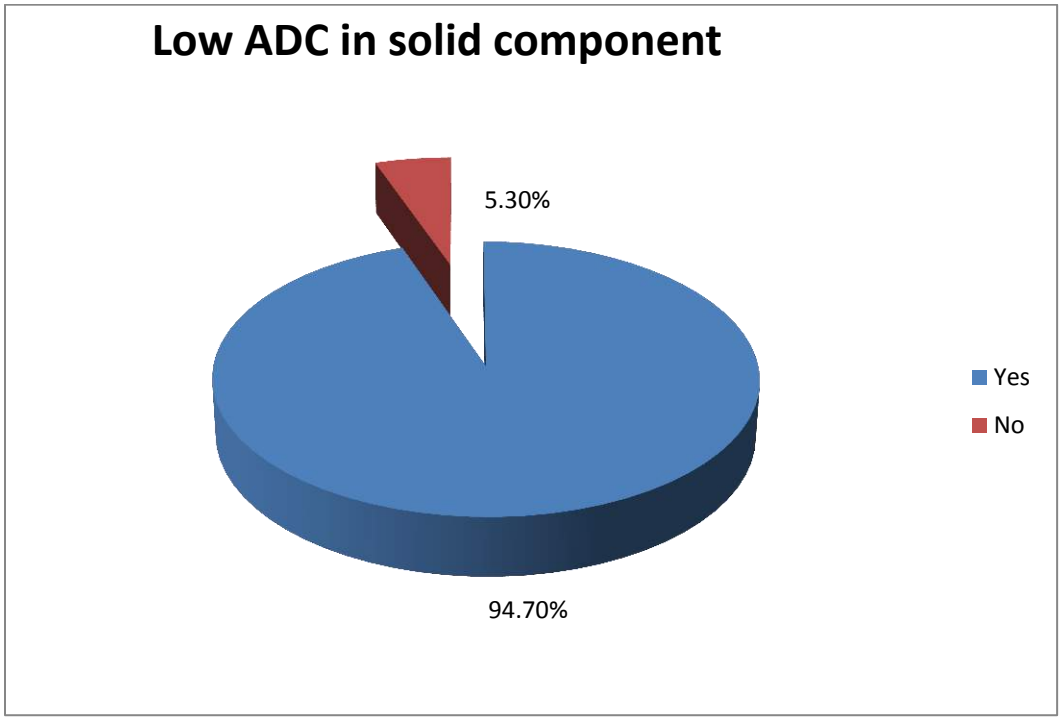

Table 20b: Comparison of low ADC signal in solid component in benign and malignant lesions

		FINAL DIAGNOSIS				Total	Chi-square value	p-value
		Benign		Malignant				
ADC HYPOINTENSE SIGNAL IN SOLID COMPONENT	Yes	8	88.9%	10	100.0%	18	1.173	0.279
	No	1	11.1%	0	0.0%	1		
Total		9	100.0%	10	100.0%	19		

Figure 22b: Comparison of low ADC signal in solid component in benign and malignant lesions

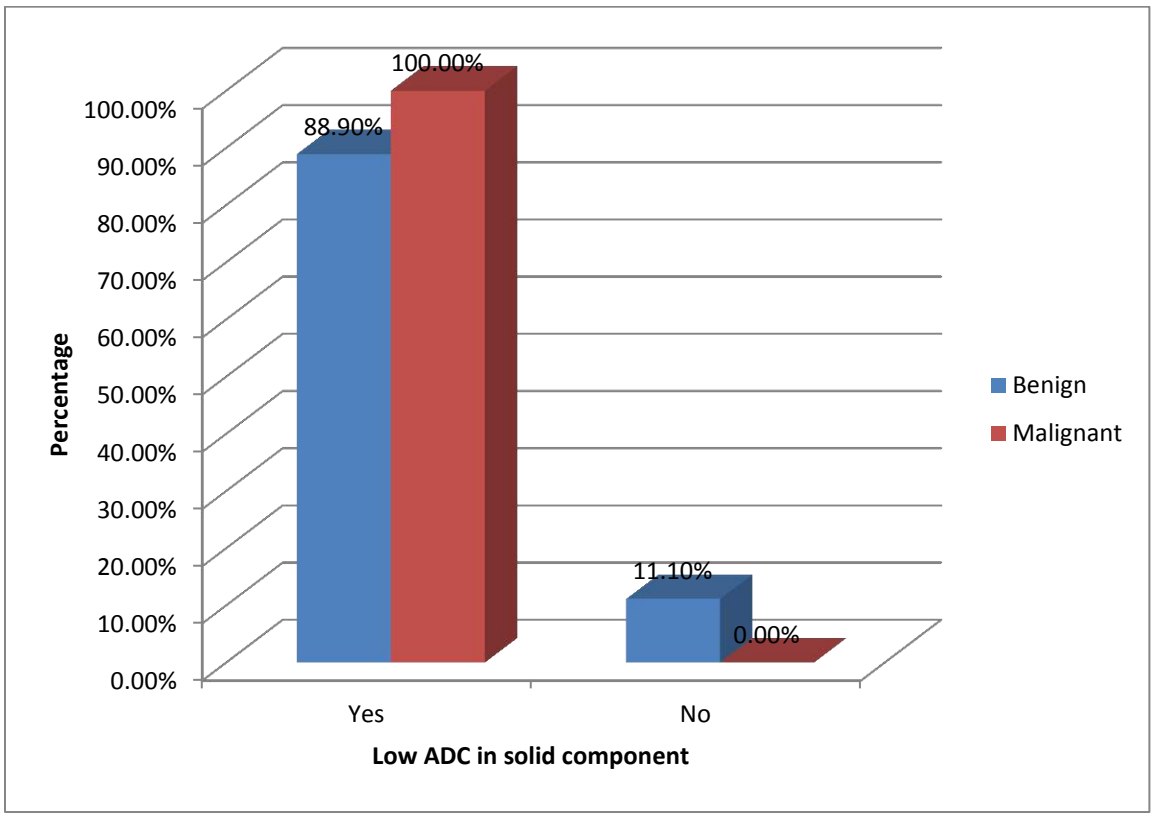

4. Mean ADC value in solid component

The mean of mean ADC values was 972.58 x 10^{-6} mm^2/s, with a range of 453 x 10^{-6} to 1532 x 10^{-6} mm^2/s. The average mean ADC value in solid component was 990.67 x 10^{-6} mm^2/s in benign lesions and 956.30 x 10^{-6} mm^2/s in malignant lesions (p=0.624).

Table 21: Mean of mean ADC values in solid component in benign and malignant lesions

	Benign		Malignant		Z	p-value
	Mean	SD	Mean	SD		
MEAN OF MEAN ADC VALUES IN SOLID COMPONENT (10^{-6} mm^2/s)	990.67	296.95	956.30	180.42	-0.490	0.624

Figure 23: Mean of mean ADC values in solid component in benign and malignant lesions

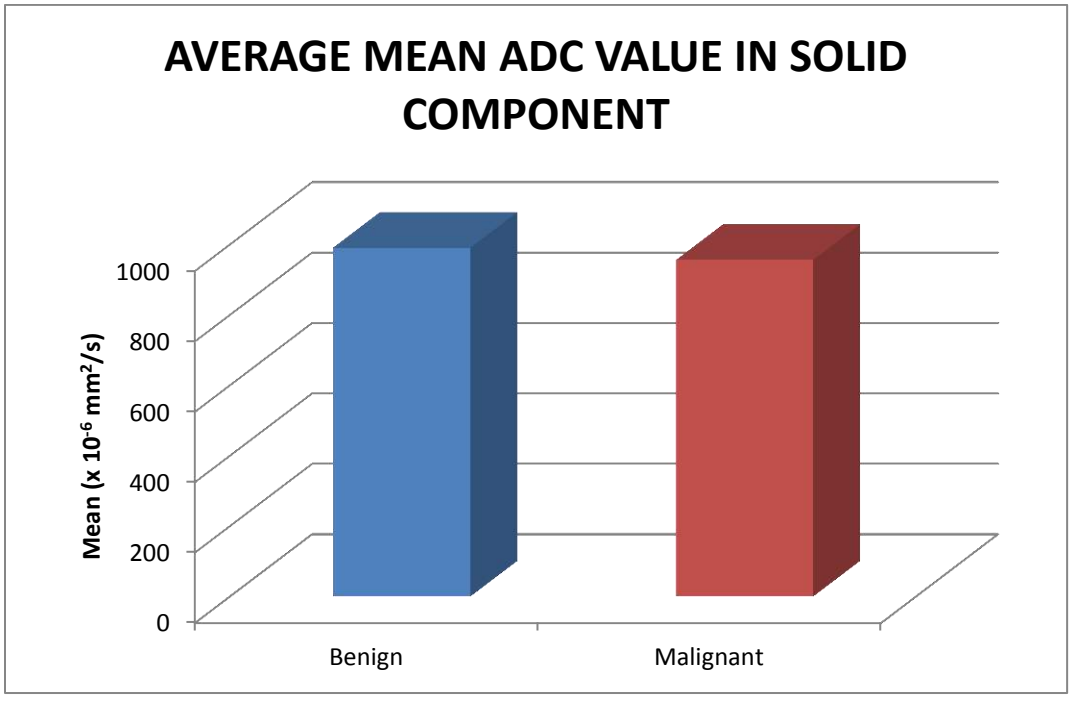

5. Low ADC signal in cystic component

Hypointense signal on ADC maps within the cystic component was seen in 19 (48.7%) lesions. The cystic component in 17 (53.1%) benign and 2 (28.6%) malignant lesions showed low ADC signal (p=0.239).

Table 22a: Low ADC signal in cystic component

LOW ADC SIGNAL IN CYSTIC COMPONENT	No. of lesions	Percentage
Yes	19	48.7%
No	20	51.3%
Total	39	100.0%

Figure 24a: Low ADC signal in cystic component

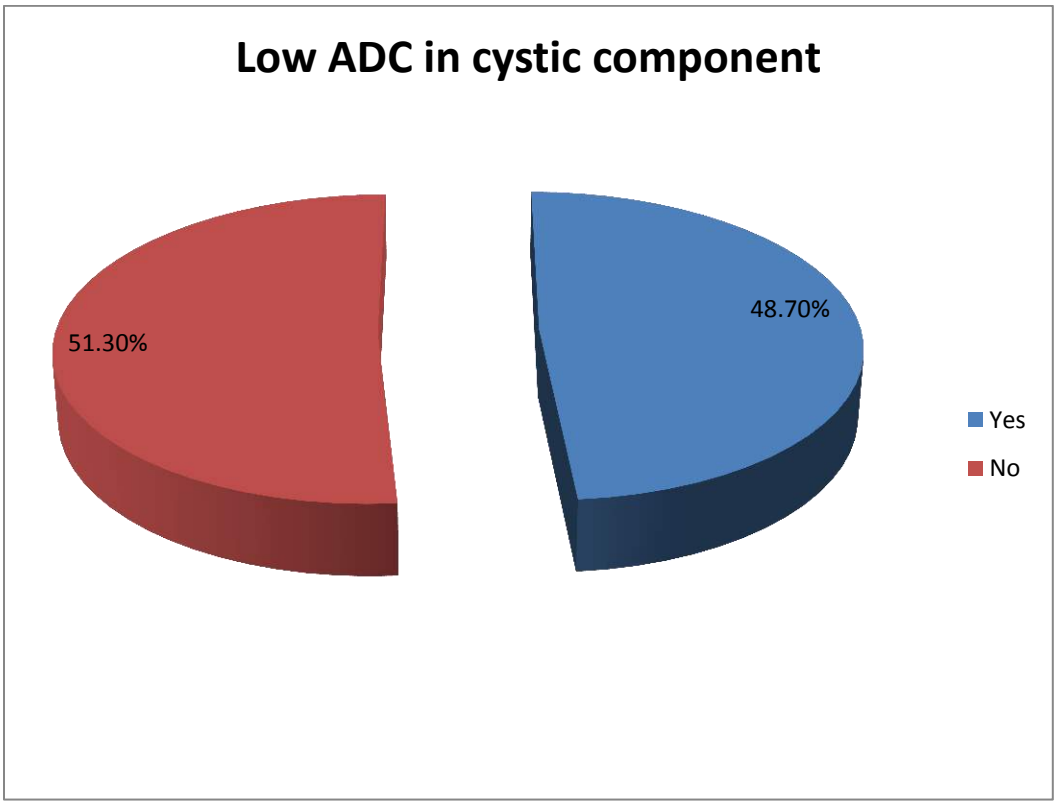

Table 22b: Low ADC signal in cystic component in benign and malignant lesions

		FINAL DIAGNOSIS				Total	Chi-square value	p-value
		Benign		Malignant				
LOW ADC SIGNAL IN CYSTIC COMPONENT	Yes	17	53.1%	2	28.6%	19	1.386	0.239
	No	15	46.9%	5	71.4%	20		
Total		32	100.0%	7	100.0%	39		

Figure 24b: Low ADC signal in cystic component in benign and malignant lesions

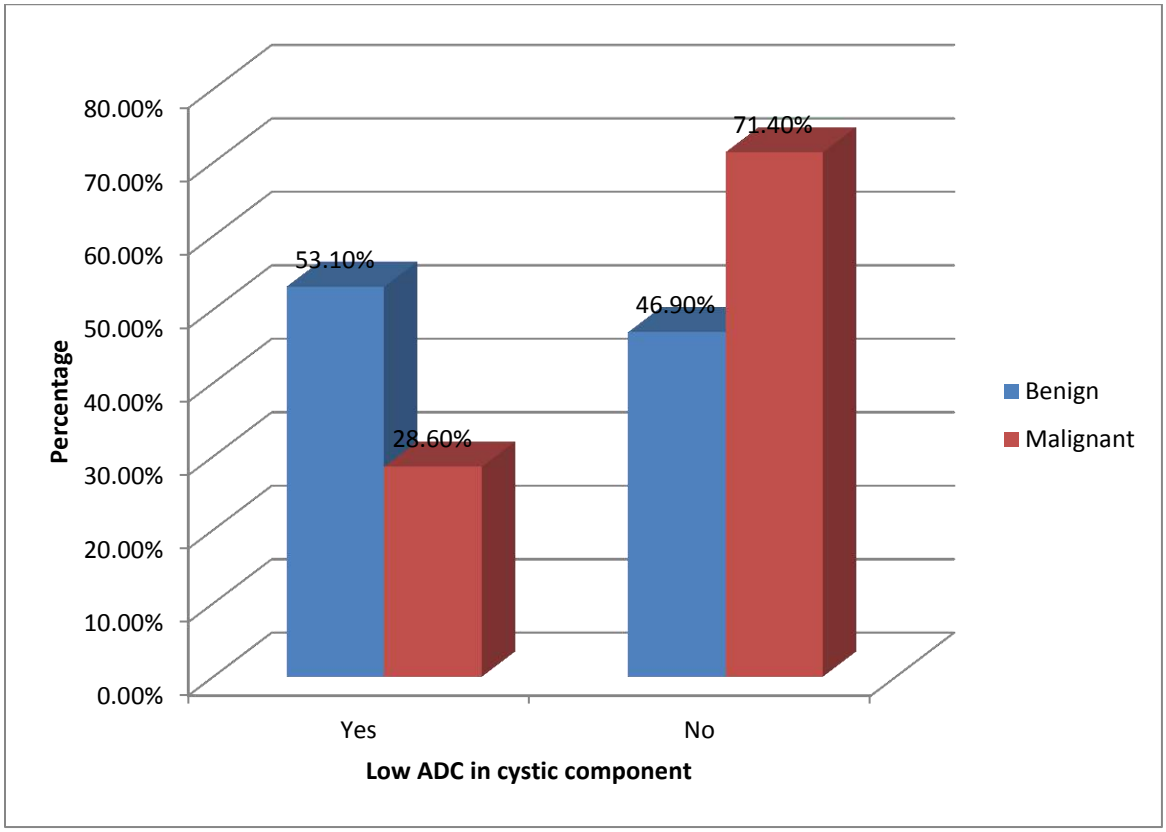

6. Mean ADC value in cystic component

Mean ADC values in cystic component ranged from 231 x 10^{-6} to 3026 x 10^{-6} mm^2/s, with a mean of 1759.98 x 10^{-6} mm^2/s. The average mean ADC value in cystic component was 1631.81 x 10^{-6} in benign lesions, and 2215.67 x 10^{-6} mm^2/s in malignant lesions (p=0.130).

Table 23: Mean of mean ADC values in cystic component in benign and malignant lesions

	Benign		Malignant		Z	p-value
	Mean	SD	Mean	SD		
MEAN OF MEAN ADC VALUES IN CYSTIC COMPONENT (10^{-6} mm^2/s)	1631.81	1067.69	2215.67	675.69	-1.548	0.130

Figure 25: Mean of mean ADC values in cystic component in benign and malignant lesions

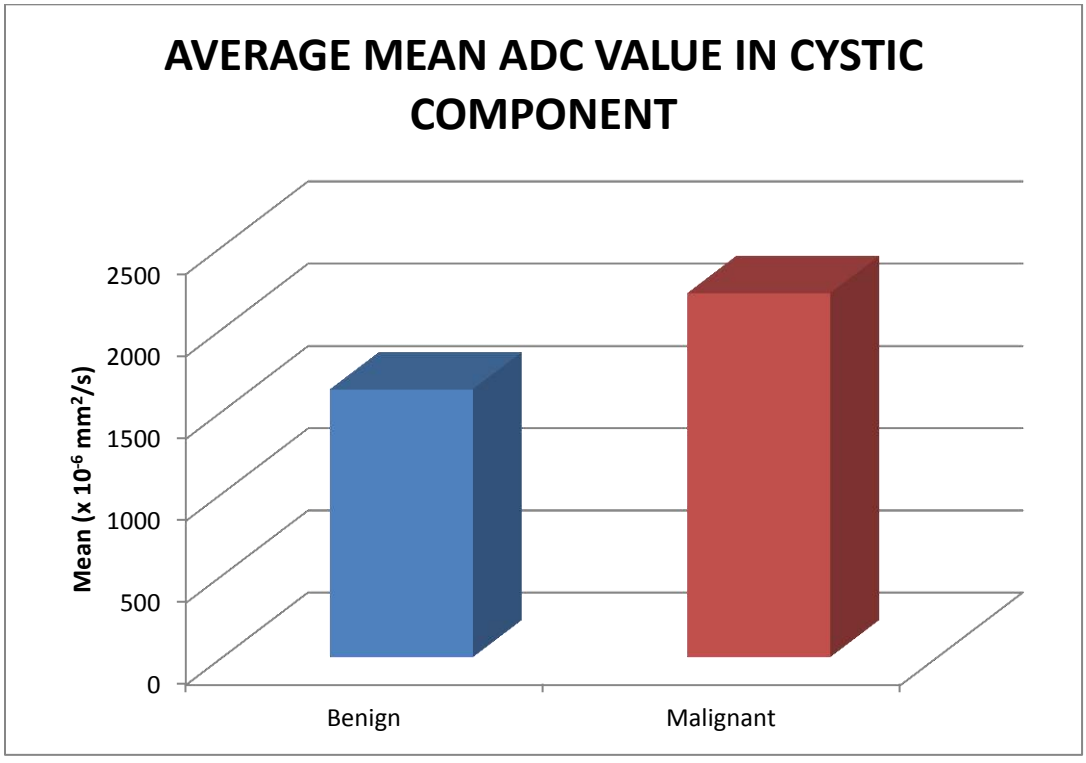

D. DYNAMIC CONTRAST-ENHANCED MRI

Of the 47 patients included in our study, Dynamic Contrast-enhanced MRI was done in 37 patients. Time Intensity Curve analysis, which requires myometrial reference for comparison, was possible in only 29 of these, as rest of the patients had a prior history of hysterectomy.

1. Type of curve (TIC)

Out of 29 patients who underwent a dynamic contrast-enhanced MRI, with Time Intensity Curve analysis, 13 (44.8%) had a Type I curve, 9 (31%) lesions had a type II curve and 7 (24.1%) lesions had a type III curve. It was observed that type I curve was seen only in benign lesions, and type III curve was seen only in malignant lesions. Type II curve was seen in both benign and malignant lesions. 7 of the lesions with a type II curve were benign and 2 were malignant.

There were 7 (77.8%) type III, 2 (22.2%) type II, and no type I of TIC in malignant ovarian lesions; and 13 (65.0%) type I, 7 (35.0%) type II, and no type III of TIC in benign lesions ($P < 0.001$).

Table 24a: Type of curve (TIC)

TYPE OF CURVE (TIC)	No. of lesions	Percentage
I	13	44.8%
II	9	31.0%
III	7	24.1%
Total	29	100.0%

Figure 26a: Type of curve (TIC)

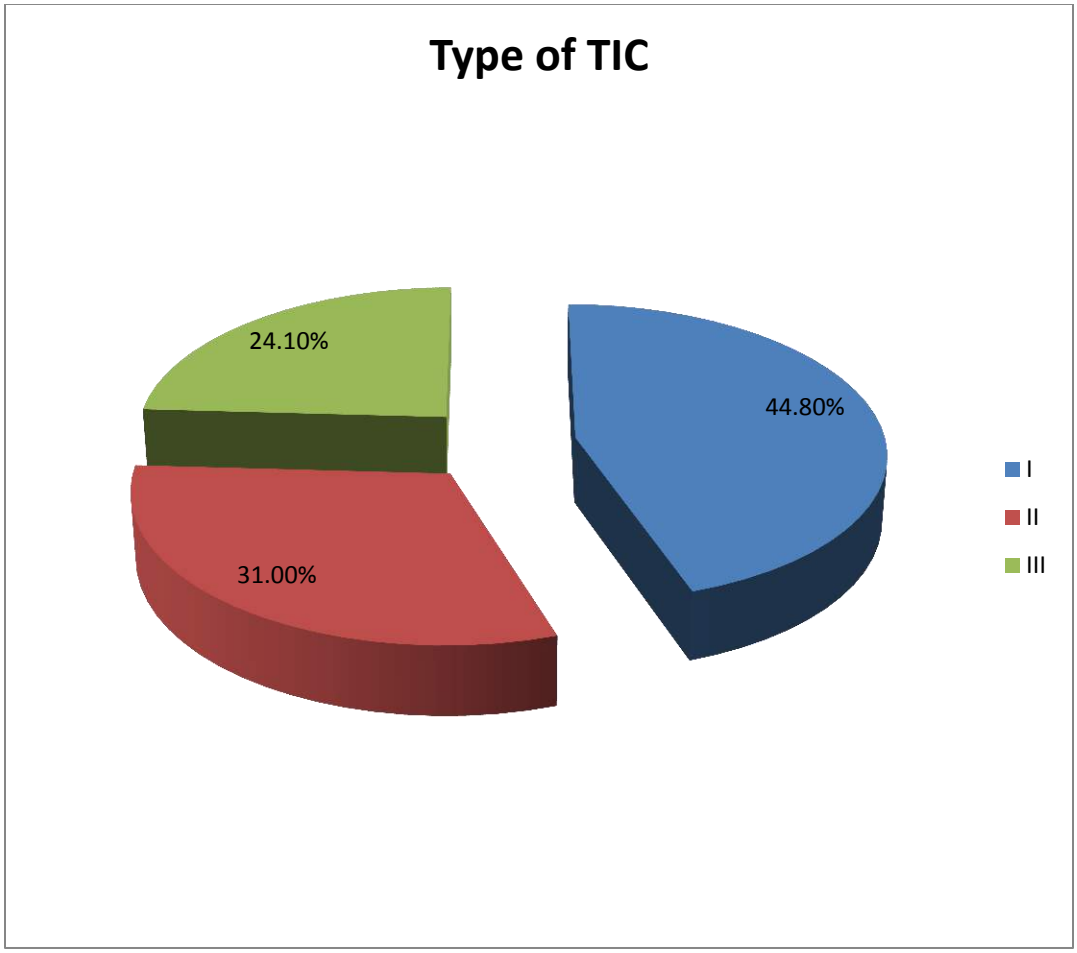

Table 24b: Type of curve (TIC) in benign and malignant lesions

		FINAL DIAGNOSIS				Total	Chi-square value	p-value
		Benign		Malignant				
TYPE OF CURVE (TIC)	I	13	65.0%	0	0.0%	13	10.603	0.001
	II	7	35.0%	2	22.2%	9	0.473	0.491
	III	0	0.0%	7	77.8%	7	20.505	0.001
Total		20	100.0%	9	100.0%	29		

Figure 26b: Type of curve (TIC) in benign and malignant lesions

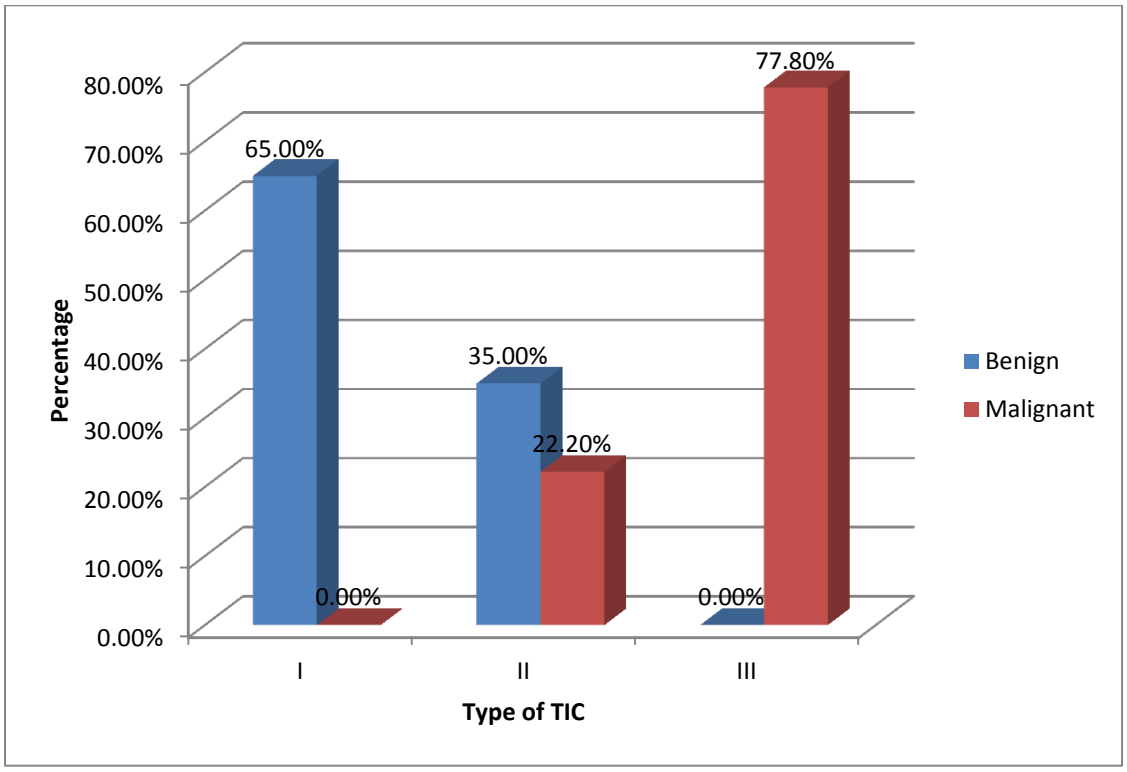

E. Final Analysis

1. Combination of intermediate T2 SI and presence of diffusion restriction in solid component

Out of 19 lesions with some solid component, the combination of intermediate signal intensity on T2WI and positive diffusion restriction was seen in 12 (63.2%) lesions. Out of these, 10 were malignant and 2 were benign.

All the malignant lesions in our study showed this combination, while only 2 (22.2%) of the benign lesions with some solid component showed this combination (p= 0.0001).

Table 25a: Combination of intermediate T2 SI and presence of diffusion restriction in solid component

INTERMEDIATE T2 + DIFFUSION RESTRICTION	No. of lesions	Percentage
Yes	12	63.2%
No	7	36.8%
Total	19	100.0%

Figure 27a: Combination of intermediate T2 SI and presence of diffusion restriction in solid component

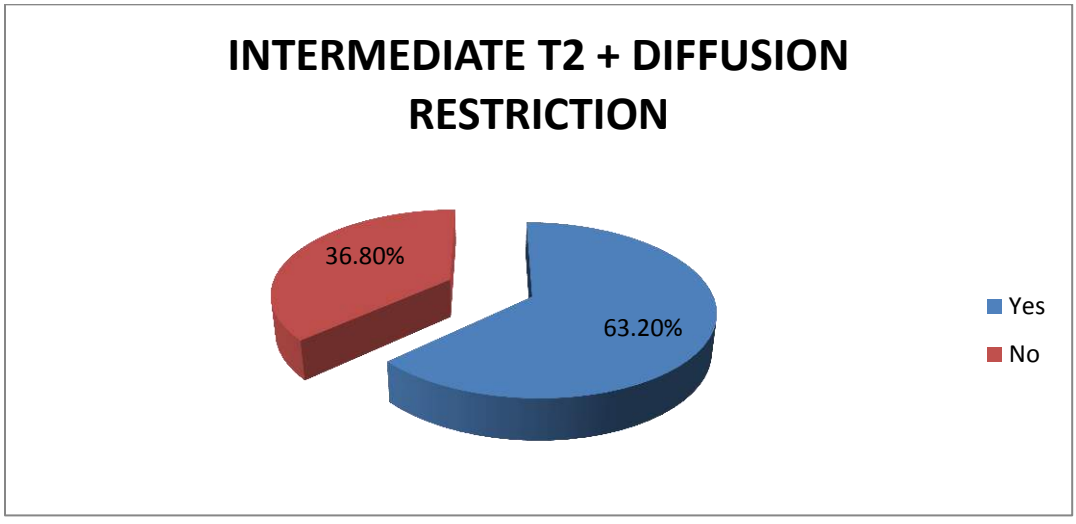

Table 25b: Combination of intermediate T2 SI and presence of diffusion restriction in solid component in benign and malignant lesions

		FINAL DIAGNOSIS				Total	Chi-square value	p-value
		Benign		Malignant				
INTERMEDIATE T2 + DIFFUSION RESTRICTION	Yes	2	22.2%	10	100.0%	12	12.315	0.0001
	No	7	77.8%	0	0.0%	7		
Total		9	100.0%	10	100.0%	19		

Figure 27b: Combination of intermediate T2 SI and presence of diffusion restriction in solid component in benign and malignant lesions

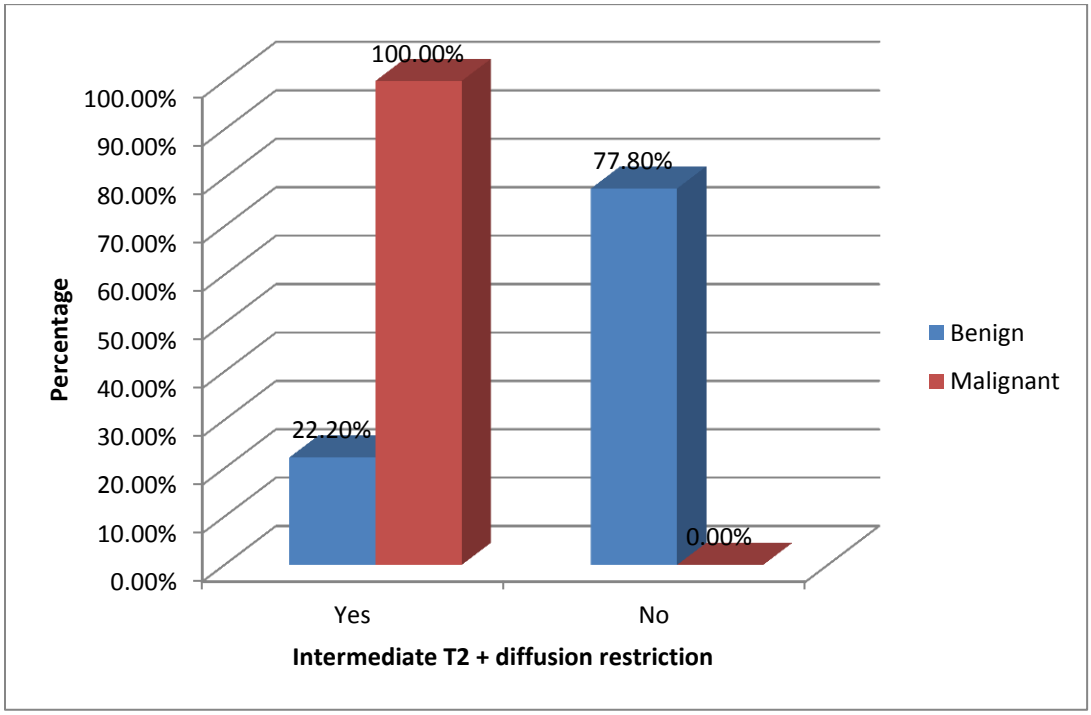

2. **Combination of intermediate T2 SI, diffusion restriction and Type III TIC in solid component**

Out of 15 lesions with some solid component and in whom DCEMR was done, the combination of intermediate signal intensity on T2WI, positive diffusion restriction and type III TIC was seen in 7 (46.7%) lesions. All these 7 lesions were malignant, while none of the benign lesions showed this combination (p=0.003).

Table 26a: Combination of intermediate T2 SI, diffusion restriction and Type III TIC in solid component

INTERMEDIATE T2 + DIFFUSION RESTRICTION + TYPE 3 TIC	No. of lesions	Percentage
Yes	7	46.7%
No	8	53.3%
Total	15	100.0%

Figure 28a: Combination of intermediate T2 SI, diffusion restriction and Type III TIC in solid component

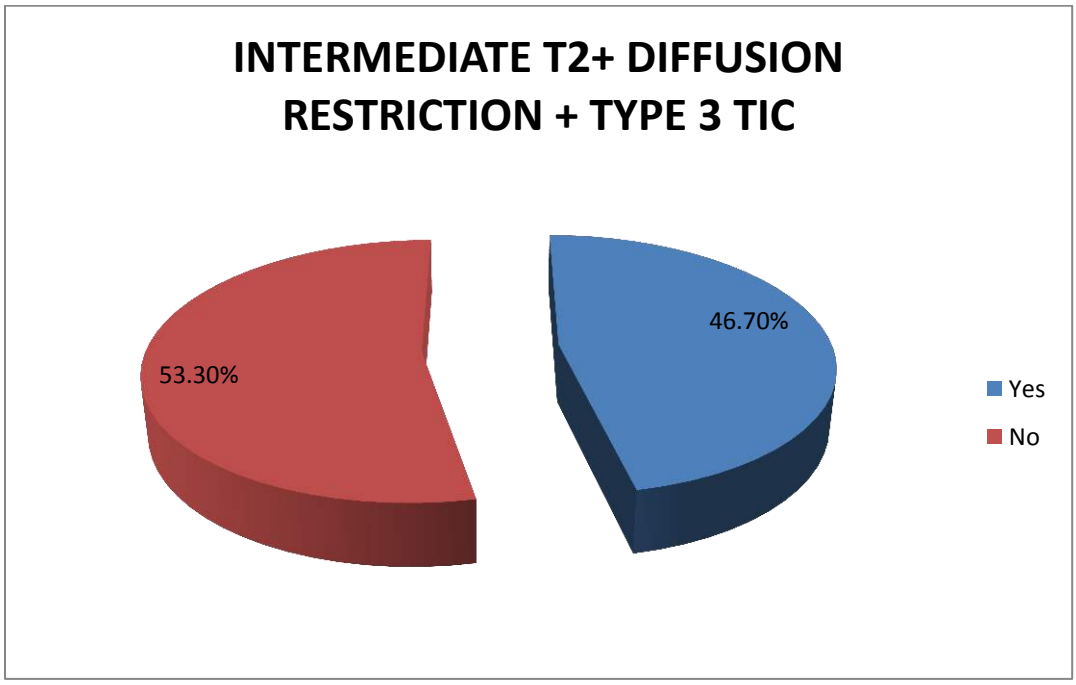

Table 26b: Combination of intermediate T2 SI, diffusion restriction and Type III TIC in solid component in benign and malignant lesions

		FINAL DIAGNOSIS				Total	Chi-square value	p-value
		Benign		Malignant				
INTERMEDIATE T2 + DIFFUSION RESTRICTION+ TYPE 3 TIC	Yes	0	0.0%	7	77.8%	7	9.752	0.003
	No	6	100.0%	2	22.2%	8		
Total		6	100.0%	9	100.0%	15		

Figure 28b: Combination of intermediate T2 SI, diffusion restriction and Type III TIC in solid component in benign and malignant lesions

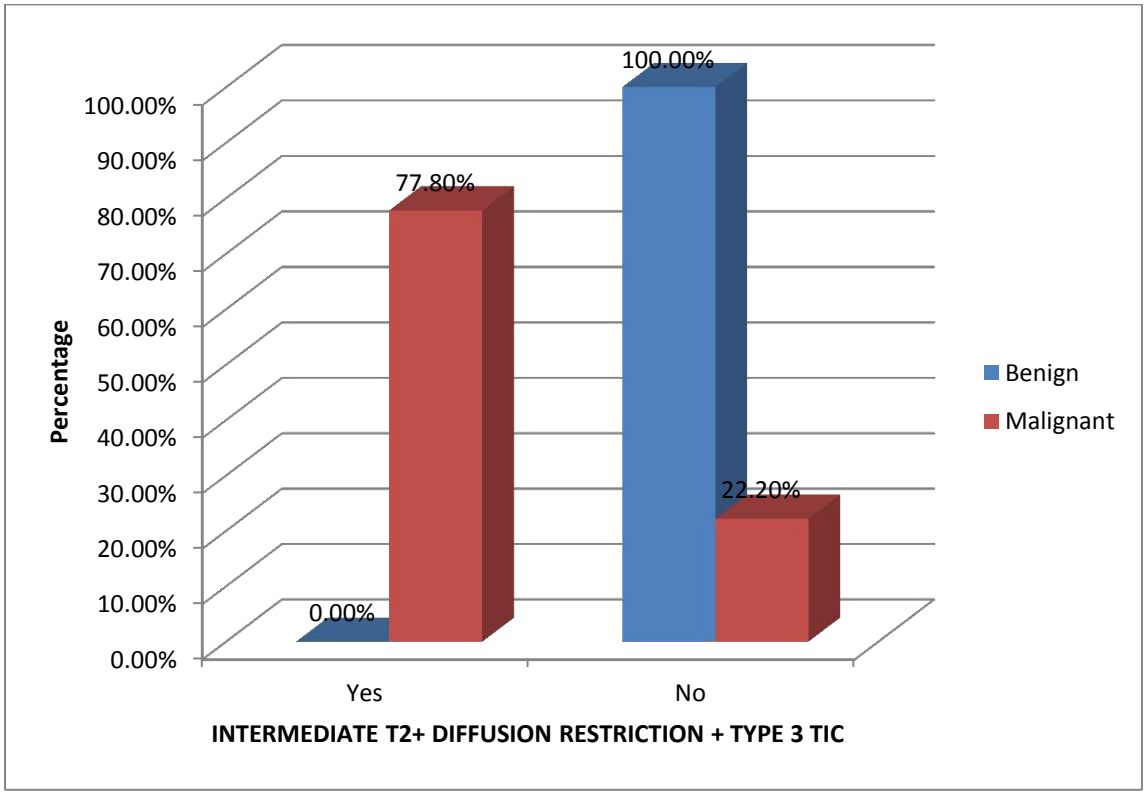

3. Statistically significant parameters for the diagnosis of benignity

For the diagnosis of benignity, conventional MRI parameters such as a purely cystic mass and hypointense signal in the solid component on T2WI had an accuracy of 80.85% and 78.95% respectively, while advanced MRI parameters such as absence of diffusion restriction and obtaining a type I or II TIC on DCEMR had accuracies reaching up to 89.47% and 93.1%, respectively.

Table 27: Statistically significant parameters for the diagnosis of benignity

PARAMETER	Sensitivity	Specificity	PPV	NPV	Accuracy
Purely cystic	75.68%	100.00%	100.00%	52.63%	80.85%
Hypointense signal in solid component on T2WI	55.56%	100.00%	100.00%	71.43%	78.95%
Absence of diffusion restriction	77.78%	100.00%	100.00%	83.33%	89.47%
Type I or II TIC on DCEMR	100.00%	77.8%	90.9%	100%	93.1%

Figure 29a: Statistically significant parameters for the diagnosis of benignity

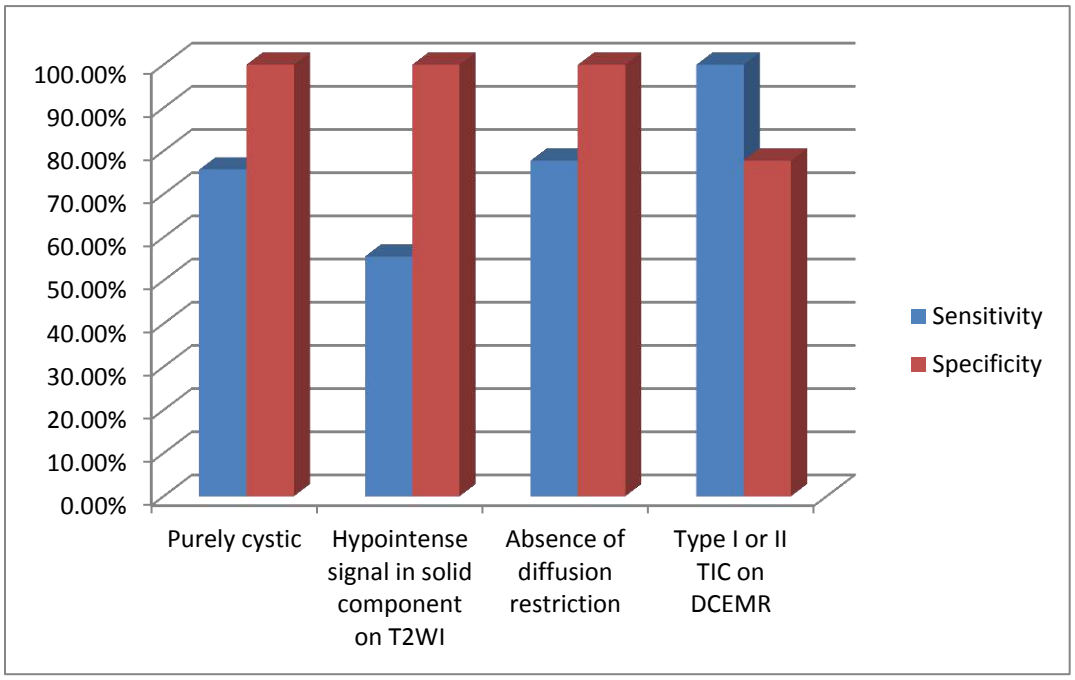

Figure 29b: Accuracy of various MRI parameters for the diagnosis of benignity

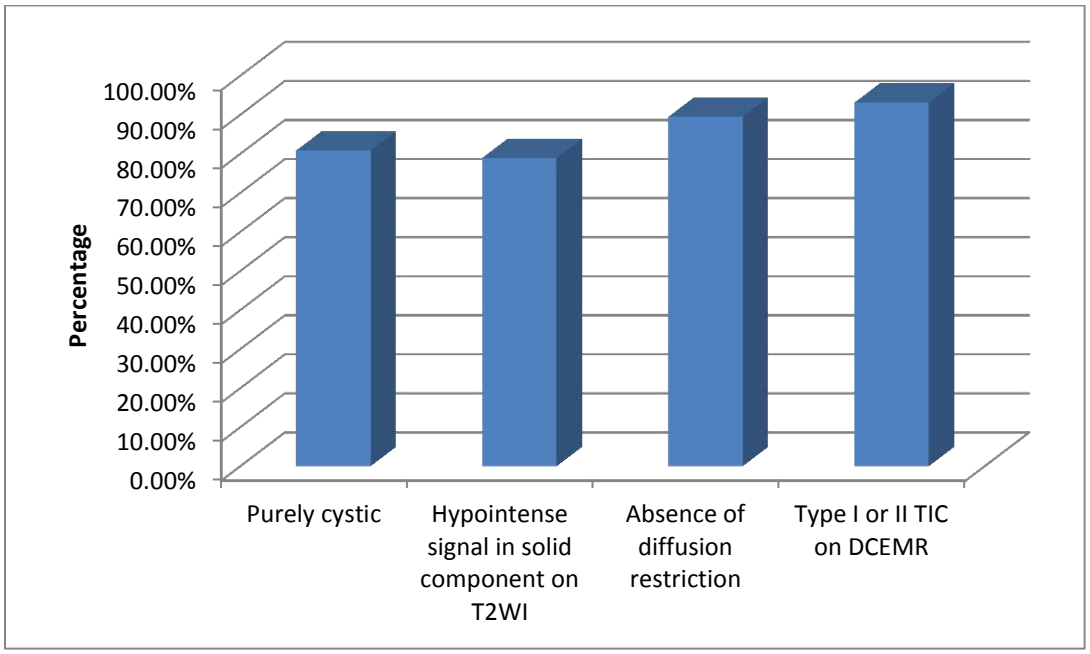

4. Statistically significant parameters for the diagnosis of malignancy

For the diagnosis of malignancy, conventional MRI parameters such as a predominantly cystic lesion with some solid component or a predominantly solid lesion, intermediate SI in the solid component on T2WI and presence of papillary projections had accuracies of 80.9%, 82.98%, 78.95% and 87.1% respectively, while advanced MRI parameters such as presence of diffusion restriction and obtaining a type III TIC on DCEMR had accuracies reaching up to 89.47% and 93.1%, respectively.

Table 28: Statistically significant parameters for the diagnosis of malignancy

PARAMETER	Sensitivity	Specificity	PPV	NPV	Accuracy
Predominantly cystic lesion with some solid component	50.0%	89.2%	55.6%	86.8%	80.9%
Predominantly solid lesion	20.0%	100.0%	100.0%	82.2%	82.98%
Intermediate SI in solid component on T2WI	100.0%	55.6%	71.4%	100.0%	78.95%
Presence of Papillary projections	42.9%	96.9%	75.0%	88.6%	87.1%
Presence of diffusion restriction	100.0%	77.8%	83.3%	100.0%	89.47%
Type III TIC on DCEMR	77.8%	100.0%	100.0%	90.9%	93.1%

Figure 30a: Statistically significant parameters for the diagnosis of malignancy

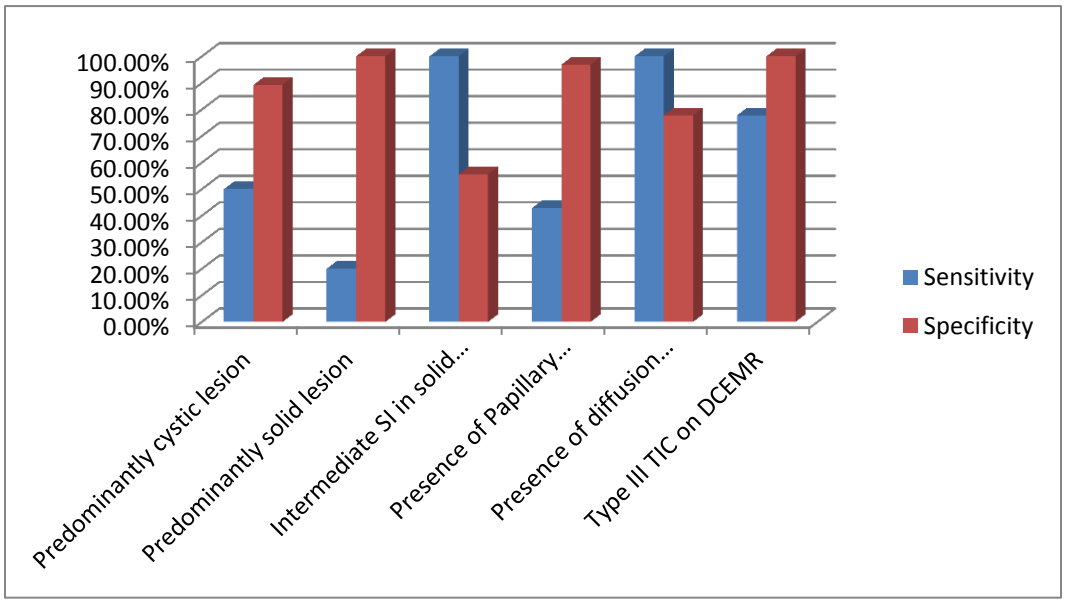

Figure 30b: Accuracy of various MRI parameters for the diagnosis of malignancy

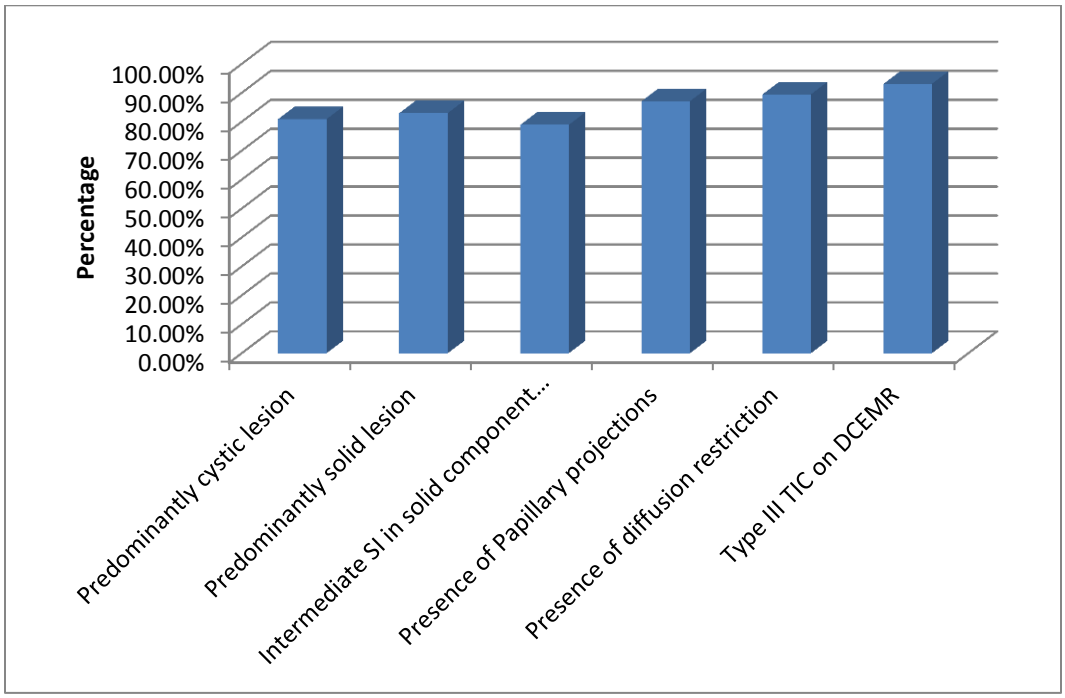

DISCUSSION

Adnexal mass lesions are a fairly common diagnosis on Ultrasonography (US) in patients presenting with gynecologic symptoms and are frequently detected incidentally in asymptomatic women as well. US is the first-line imaging modality, but there are a substantial number of lesions that are indeterminate on US, that is, they cannot be confidently characterized as benign or malignant or their site of origin is not clear.

Magnetic resonance imaging (MRI) is an excellent imaging modality for accurate tissue characterization because of its high contrast resolution. Prior to the advent of MRI, unnecessary surgery was performed in a large proportion of benign cases based on suspicious US findings. MRI is the modality of choice for characterization of a sonographically indeterminate adnexal mass lesion.

The role of advanced MRI sequences such as Dynamic contrast-enhanced and Diffusion-weighted imaging has been very promising. These sequences have been proven to significantly improve the diagnostic accuracy of MRI, in comparison to the conventional MRI sequences, and the results of our study consolidate the same.

A total of 47 patients who had an adnexal mass detected on US and subsequently underwent an MRI, were enrolled in this study. In 12 out of 47 patients who had bilateral lesions, only the most complex or the largest lesion was included in the statistical analysis. Therefore, a total of 47 lesions were evaluated in our study. Out of the 47 lesions, 37 (78.7%) were benign and 10 (21.3%) were malignant lesions; either on histopathological analysis or on follow-up imaging.

Among the benign lesions, endometriomas were the most prevalent (n=13; 27.7%), followed by subserosal / broad ligament leiomyomas (n=4; 8.5%) and hemorrhagic cysts (n=4; 8.5%). Among the malignant lesions, endometrioid carcinomas were the most commonly diagnosed (n=5; 10.6%).

Maximum (n=18; 38.3%) patients in our study were in the 41-50 years age group. The mean age of diagnosis was 38.89 years, with a range of 11 to 67 years. With increasing age, there was a higher incidence of malignancy, with 7 of the 10 patients with malignant lesions above the age of 40 years, while 36 (97.3%) of the 37 patients with benign lesions below the age of 50 years at the time of diagnosis. The mean age of the patients with benign lesions was 36.78 years, and 46.70 years for malignant lesions.

This was comparable to the study done by Malek M et al in which the mean age was 36.5 years, with a range of 14 to 76 years. The mean age of the patients with benign and malignant adnexal masses was 34.5 and 39 years, respectively. [90]

Pain was the most common presenting symptom. 25 (53.1%) patients complained of abdominal pain. Menstrual symptoms were very common in the patients included in our study, 9 (19.1%) had menorrhagia, 7 (14.9%) had dysmenorrhea, 7 (14.9%) had irregular menses, while 9 (19.1%) patients complained of abdominal heaviness. Fever, bleeding per-vaginum, loss of weight and/or appetite were the other presenting complaints. 2 patients were diagnosed with an adnexal mass during evaluation for infertility, another 2 while being evaluated for known carcinoma stomach. One patient had cyclical pain in the left leg with foot drop.

Serum CA-125 levels were available for 29 patients. The mean value was 72.63 U/mL in patients with benign lesions and 102.09 U/mL in patients with malignant lesions. The difference wasn't statistically significant (p=0.569). This could be attributed to a high preponderance of endometriotic cysts in our study, as these are often associated with high CA-125 levels. This observation was in keeping with a study done by Van Calster B et al which confirmed the limited clinical value of CA-125 for preoperative discrimination between benign and malignant ovarian pathology.[93]

For size comparison, the largest dimension of the adnexal masses was recorded, which ranged from 1 to 21cm. The mean of the largest dimension was 8.32 cm. Mean of the largest dimension was 7.65cm for benign lesions, and 10.80cm for malignant lesions. The difference wasn't statistically significant (p=0.080).

Similar findings were seen by Thomassin-Naggara I et al in their study in which the mean size of benign lesions was 7.6 cm and that of malignant lesions was 9.1 cm (p=0.35), suggesting that lesion size is not a predictor of malignancy.[87]

Of the 47 patients, 12 (25.5%) patients had bilateral lesions. 8 (21.6%) of the benign and 4 (40%) of the malignant lesions in our study were bilateral. The difference wasn't statistically significant. (p=0.237). This observation is in contrast to other studies, including those done by Thomassin-Naggara I et al and Sohaib SA et al which concluded that bilaterality is a predictor of malignancy.[87,26] This discrepancy may be explained by the high preponderance of endometriomas in our study which are very frequently bilateral.

Among the benign lesions, majority (n=28; 75.7%) were purely cystic, 4 (10.8%) were predominantly cystic and 5 (13.5%) were purely solid lesions.

Among the malignant lesions, majority (n=7; 70.0%) were mixed solid-cystic, while 3 (30.0%) were purely solid. Among the mixed solid-cystic lesions, 5 (50.0%) were predominantly cystic and 2 (20%) were predominantly solid lesions.

There were a total of 28 purely cystic lesions, and all of them were benign. A purely cystic lesion had a high PPV and specificity of 100% and sensitivity of 75.7% in predicting benignity (p=0.001). Thus, the presence of a purely cystic lesion essentially ruled out the possibility of malignancy.

Out of the 8 purely solid lesions, 5 were benign and 3 were malignant, however, the difference was not statistically significant (p=0.218). A purely

solid lesion had a specificity of 70% and sensitivity of only 13.5% in predicting benignity.

Among the 11 mixed solid-cystic lesions, 4 were benign and 7 were malignant, thus favoring malignancy, with a statistically significant difference.

Similar results were seen in a study done by Sohaib SA et al, in which 11% (10/91) of benign and 4.7% (3/64) malignant lesions were purely solid with no statistically significant difference. 72.5% (66/91) of benign and 90.6% (58/64) of malignant tumors were solid-cystic (p=0.006). 16.5% (15/91) of benign and 3% (3/64) of malignant tumors were purely cystic (p=0.024). Thus, presence of a solid-cystic or a purely cystic lesion was accurate in predicting malignancy and benignity, respectively.[26] A study done by Thomassin-Naggara I et al showed similar results. In their study, presence of a purely cystic mass was highly predictive of benignity (p<0.0001) as none of the malignancies were purely cystic. Presence of a solid portion was statistically significant in predicting malignancy (p=0.001).[85]

Hypointense T2 signal within the solid component was found in 55.6% of the benign lesions which had some solid component, and in none of the 10 malignant lesions. Intermediate signal intensity on T2WI was seen in 44.4% of the benign lesions with a solid component, and in all the 10 malignant lesions.

Presence of low T2 signal intensity in solid component was found to be 100% predictive as well as 100% specific for benignity with a low sensitivity of 55.6%.

Presence of intermediate signal intensity on T2WI was more often seen in malignant than benign lesions with a sensitivity of 100%, specificity of 55.6%, PPV of 71.4% and an accuracy of 79%, and was thus, predictive for malignancy with statistical significance (p=0.001).

Our results based on the T2 signal in solid component were compatible with multiple other studies. Low signal on T2WI within the solid component

has been proven to be statistically significant in predicting benignity, with a p-value of <0.001 in studies conducted by Thomassin-Naggara I et al.[85,88] and Sohaib SA et al [26]. In another study done by Thomassin-Naggara I et al, the presence of intermediate signal intensity within the solid component on T2WI was seen in 26% (6/23) of the benign and 88% (44/50) of the malignant lesions with some solid component (p<0.0001).[87]

Marked T1 hyperintensity within the cystic component equal to or greater than subcutaneous fat was seen in 15 (38.5%) lesions with some cystic component, out of which 13 lesions were benign and 2 were malignant. All the 13 benign lesions were endometriomas, while both the malignant tumors were endometriomas complicated with malignancy. The finding of multiple T1 hyperintense adnexal cysts is considered very specific for endometriomas.[56]

The presence of marked T1 hyperintensity in cystic component was not statistically significant in differentiating benign from malignant lesions (p=0.553).

In our study, there were 2 cases of endometriosis with malignant transformation, both of which were histopathologically confirmed endometrioid carcinomas. It has been studied that the most commonly encountered malignancies in patients with endometriosis are endometrioid and clear cell epithelial carcinomas. [56]

Shading sign on T2WI was present in 14 (35.9%) lesions in our study, out of which 12 were benign and 2 were malignant. All the 12 benign lesions were endometriomas, while both the malignant tumors were endometriomas complicated with malignancy. There was one patient with an endometrioma that did not show T2 shading, that is, there was no loss of signal on T2WI, with a markedly hyperintense signal on T1WI. Shading sign has a moderate-to-high level of sensitivity and specificity for the diagnosis of endometriomas and endometrioid tumors, but may also be found in other conditions as well. [55]

In our study, the presence of shading sign on T2WI was not statistically significant in differentiating benign from malignant lesions (p=0.655).

In the 39 lesions with some cystic component, thickened septa (greater than or equal to 3 mm thickness) were present in 9/39 (23.1%) lesions, out of which, 7 were benign and 2 were malignant. Thickened septa were seen in 7/32 (21.9%) benign and 2/7 (28.6%) malignant lesions (p=0.703). Presence of thickened septa had no statistical significance in differentiating between benign and malignant lesions (p=0.703). In a study done by Thomassin-Naggara I et al, thickened septa were present in 4/14 (28%) benign and 15/34 (44%) malignant lesions (p=0.35) [87]. The relative preponderance of thickened septa in benign lesions in our study may be explained by a higher prevalence of tubo-ovarian abscesses and endometriomas, which frequently had thickened septations. Out of the 7 benign lesions, 6 of them were either tubo-ovarian abscesses or endometriomas, and another was a multiseptated lesion with few thickened septations, which resolved on follow-up imaging, confirming its benignity.

Among benign lesions, 20 (54.1%) showed evidence of hemorrhage within them, while 3 (30%) malignant lesions had hemorrhage. Presence of hemorrhage was not statistically significant in differentiating benign and malignant lesions. (p=0.177)

These observations regarding hemorrhage correlated well with a study done by Sohaib SA et al, in which it was noted that hemorrhage was more commonly detected in the cystic component of benign lesions (36/81; 44.4%) than in malignant lesions (15/61; 24.6%). However, this feature alone did not help to differentiate benign from malignant lesions because a substantial number of malignant lesions contained hemorrhage.[26]

Papillary projections, seen as internal projections from the wall or septa in a cyst, were seen in 4 (10.2%) patients. These were seen in 1 (3.1%) benign and 3 (42.9%) malignant lesions. Presence of papillary projections had a specificity of 96.9%, sensitivity of 42.9%, PPV of 75%, NPV of

88.6%, accuracy of 87.1% for diagnosing a malignant tumor, and was thus statistically significant in differentiating benign and malignant lesions (p=0.001).

In a study conducted by Sohaib SA et al, papillary projections were present in 5/43 (11.6%) and 18/39 (46.2%) malignant lesions, and the difference was statistically significant (p=0.001) [26]. In another study by Hricak H et al, presence of papillary projections was one of the indicators predictive for malignancy, with a statistically significant difference (p=0.003).[25]

There was one benign lesion in our study which had a small papillary projection along its wall; it was a histopathologically proven dermoid cyst and the nodule was possibly a Rokitansky protuberance.

Ascites was present in 18 (38.3%) cases. Ascites was associated with 12 (32.5%) benign and 6 (60.0%) malignant lesions. Presence of ascites was not statistically significant in differentiating benign and malignant lesions (p=0.112)

Although the presence of ascites has been classically described with ovarian malignancy, in our study, ascites was more commonly found in patients with benign lesions because of the relative preponderance of tubo-ovarian abscesses, and also because certain patients with a benign lesion presented with clinical and radiological signs of torsion with associated pelvic free fluid. Pelvic ascites was seen in 4 out of the 15 cases with endometriosis in our study.

Similar results were seen in the study done by Thomassin-Naggara I et al where ascites was associated with 4/10 (40%) benign, 6/11 (54.5%) borderline and 13/16 (81.2%) malignant lesions, with no statistically significant difference [88] and in another study by Li HM et al in which ascites was present in 10/15 (66.7%) and 42/71 (59.1%) lesions (p=0.638).[70]

Diffusion-Weighted Imaging

Presence of diffusion restriction in the solid component, that is, high signal on high b-value DW images (b=800), with corresponding low signal on ADC maps was present in 12 (63.2%) out of 19 lesions with some solid component. Out of these, 2 were benign and 10 were malignant.

All the malignant lesions in our study showed restricted diffusion in their solid component. Among the 9 benign lesions with some solid component, 2 (22.2%) lesions showed restricted diffusion. Diffusion restriction in solid component was proven to be statistically significant in differentiating benign and malignant lesions (p=0.0001).

In our study, the 2 benign lesions with restricted diffusion in their solid component were a dermoid cyst, and a multiseptated cystic lesion with restricted diffusion in one of its irregularly thickened septation; this lesion resolved on serial follow-up imaging. The restricted Brownian movement of water molecules within the keratinoid substance in a dermoid cyst results in a high signal on DWI and a low ADC value.[81]

The sensitivity, specificity, positive predictive value (PPV), negative predictive value (NPV) and accuracy of restricted diffusion in our study was 100%, 77.8%, 83.3%, 100% and 89.5% respectively.

Similar results have been seen in a study by Thomassin-Naggara I et al, in which high signal intensity within the solid component at high b-value DW images was seen in 5/18 (28%) benign and 42/45 (93%) malignant tumors (p=0.0001).[87]

In another study by Thomassin-Naggara I et al, low signal intensity within solid component on high b-value DWI was seen in 6/20 (30%) benign and 44/47 (93.6%) malignant tumors (p <0.0001).[85]

In a study by Takeuchi M et al, the solid portion of all the 39 malignant/borderline malignant tumors showed high signal intensity on DWI, whereas only 3 benign tumors showed high intensity.[84]

In a study by Mansour S et al, the sensitivity, specificity, positive predictive value (PPV), negative predictive value (NPV) and accuracy of the DW

sequence in the assessment of ovarian masses yielded 93.3%, 85%, 88.5%, 94.4% and 82.3% respectively.[79]

Presence of diffusion restriction in the cystic component, that is, high signal on high b-value DW images (b=800), with corresponding low signal on ADC maps was seen in 10 (25.6%) lesions.

9 (28.1%) benign lesions and 1 (14.3%) malignant lesion showed restricted diffusion in their cystic component. This had no statistical significance in differentiating benign from malignant lesions (p=0.447). All these lesions were either tubo-ovarian abscesses or endometriomas; this may be attributed to purulent and intracystic hemorrhagic contents, respectively.

In the study by Thomassin-Naggara I et al, high signal in the cystic component on high b-value DW images was seen in 3/18 (16.7%) benign and 7/37 (18.9%) malignant tumors (p=0.83) [85]. Similar findings were seen in another study by Fujii S et al in which almost half of the endometriomas demonstrated abnormal high signal intensity on DWI.[69]

Out of 19 lesions with some solid component, 18 (94.7%) lesions showed hypointense signal on ADC maps within their solid component. Low signal on ADC maps was seen in the solid component of 8 (88.9%) benign and all 10 malignant lesions. This had no statistical significance in differentiating benign from malignant lesions (p=0.279).

The lowest recorded mean ADC value in the solid component was 453 x 10^{-6} mm^2/s, and the maximum was 1532 x 10^{-6} mm^2/s, with a mean of 972.58 x 10^{-6} mm^2/s. The average mean ADC value in solid component was 990.67 x 10^{-6} mm^2/s in benign lesions and 956.30 x 10^{-6} mm^2/s in malignant lesions. Mean ADC values had no statistical significance in differentiating benign and malignant lesions. (p= 0.624)

Although low signal on ADC maps has been classically associated with malignancy, ADC measurements in the solid component in our study could not distinguish benign and malignant adnexal masses. This is possibly due to the pathologic characteristics of some benign ovarian

lesions. A majority of such benign lesions were subserosal/ broad ligament leiomyomas and an ovarian fibrothecoma. These are known to be composed of tissue with a great number of collagen-producing fibroblastic cells and a dense network of collagen fibers within the extracellular matrix, with resultant hindrance in the free movement of water molecules. The mean ADC value of the solid component in these lesions was low. This has also been termed as the ‘‘T2 blackout effect’’, i.e. hypointensity on DWI owing to hypointensity on T2 weighted images, which causes a decrease in the ADC. Also, there was a dermoid cyst with a papillary projection showing low ADC values, which could be attributable to keratinoid contents. To avoid misinterpreting low ADC values, diffusion-weighted images and ADC maps should be interpreted together with other images, such as T2-weighted and post-contrast images.

In a meta-analysis of 21 studies by Kim HJ et al, no significant difference in ADC values was found between benign and malignant masses in their solid component. (Weighted mean difference = 0.27, 95% Confidence Interval = -0.17–0.7, p-value = 0.23).[94]

Low signal on ADC maps within the cystic component had no statistical significance in differentiating benign and malignant lesions (p=0.239).

Mean ADC values in cystic component ranged from 231 x 10^{-6} to 3026 x 10^{-6} mm^2/s, with a mean of 1759.98 x 10^{-6} mm^2/s. The average mean ADC value in cystic component was 1631.81 x 10^{-6} mm^2/s in benign lesions and 2215.67 x 10^{-6} mm^2/s in malignant lesions. Mean ADC values in cystic component had no statistical significance in differentiating benign and malignant lesions (p=0.130). All of these lesions were either tubo-ovarian abscesses or endometriomas, and the low ADC values may be attributed to purulent and hemorrhagic contents, respectively.

Thomassin-Naggara I et al came to a very similar conclusion that mean ADC value (10^{-3} mm^2/s) of the cystic component did not differ between malignant (2.34±0.47) and benign adnexal masses (2.32±0.56) (p=0.82),

nor did the mean ADC value (10^{-3} mm^2/s) of the solid component (1.14±0.28 vs. 1.15±0.55) (p=0.89).[85]

In a meta-analysis of 21 studies by Kim HJ et al, no significant difference in ADC values was found between benign and malignant masses in their cystic component. (Weighted mean difference = 0.05, 95% Confidence Interval = -0.1–0.2, p-value = 0.51).[94]

DCE-MRI

Of the 47 patients, Dynamic Contrast-enhanced MRI was done in 37 patients. Time Intensity Curve analysis, which requires myometrial reference for comparison, was possible in only 29 of these, as the rest of the patients had a prior history of hysterectomy.

Out of 29 lesions evaluated by dynamic contrast-enhanced MRI with Time Intensity Curve analysis, 13 (44.8%) had a Type I curve, 9 (31%) lesions had a type II curve and another 7 (24.1%) lesions had a type III curve.

There were 7 (77.8%) type III, 2 (22.2%) type II, and no type I TIC in malignant ovarian lesions; and 13 (65.0%) type I, 7 (35.0%) type II, and no type III TIC in benign lesions, with a statistically significant difference between malignant and benign lesions ($P < 0.001$).

It was observed that type I curve was seen only in benign lesions, and type III curve was seen only in malignant tumors. Type II curve was seen in both benign and malignant lesions. 7 of the lesions with a type II curve were benign and 2 were malignant.

A slow, low-level enhancement pattern typical of a type I curve had a sensitivity of 65% and specificity and PPV of 100% and an accuracy of 75.8% for the diagnosis of a benign lesion (p=0.001).

A rapid and high level of enhancement typical of a type III curve was only found in invasive malignant tumors with a sensitivity of 77.8%, specificity and PPV of 100% and an accuracy of 93.1% (p=0.001).

Obtaining a type II curve was neither sensitive nor specific for either of the diagnoses, with no statistically significant difference (p=0.491). The only two malignant tumors with a type II curve in our study were a granulosa

cell tumor and an endometrioid carcinoma. However, obtaining a type II curve was not specific or sensitive for either of these two tumors.

Very similar findings were seen in a study by Thomassin-Naggara I et al, in which type I curve had a sensitivity of 70% and a specificity of 88.8% for benign tumors, whereas a type III curve was only found in invasive malignant tumors (100% specificity) with a sensitivity of 67%. A type II curve was mostly found in borderline tumors (sensitivity 72.4%) but with a lower specificity.[67]

In a study by Elzayat WA, Type I curve was noted in 7 (21.8%) masses including 4 benign, 2 borderline and 1 malignant lesion. Type II curve was noted in 13 (40.6%) masses; 3 benign, 2 borderline and 8 malignant lesions. Finally, type III curve was noted in 12 (37.5%) masses; all of them being malignant tumors (100% specificity). In discrimination of benign versus borderline and malignant ovarian masses, DCE- MRI showed 80% sensitivity; 100% specificity; 96% accuracy; 100% PPV and 58% NPV, when compared to histopathology.[95]

In another study by Sohaib SA et al, malignant lesions showed greater enhancement than benign lesions during the early phase of enhancement rather than the late phase. The pattern of strong early enhancement gave a specificity of 100% in identifying malignant lesions.[26]

Combination of intermediate T2 SI and presence of diffusion restriction in solid component

Out of 19 lesions with some solid component, the combination of intermediate signal intensity on T2WI and positive diffusion restriction was seen in 12 (63.2%) lesions, out of which 10 were malignant and 2 were benign. All the malignant lesions in our study showed this combination, while only 2 (22.2%) of the benign lesions with some solid component showed this combination.

Presence of this combination had a sensitivity of 100%, specificity of 77.8%, PPV of 83.3%, NPV of 100%, and an accuracy of 89.5% for the diagnosis of malignancy, with a statistically significant p-value of 0.0001.

Combination of intermediate T2 SI, diffusion restriction and Type III TIC in solid component

Out of 15 lesions with some solid component and in whom DCEMR was done, the combination of intermediate signal intensity on T2WI, positive diffusion restriction and type III TIC was seen in 7 (46.7%) lesions. All these 7 lesions were malignant, while none of the benign lesions showed this combination.

Presence of this combination had a sensitivity of 77.8%, specificity of 100%, PPV of 100%, NPV of 75%, and an accuracy of 86.7% for the diagnosis of malignancy with a statistically significant p-value of 0.003.

The following parameters were proven to be statistically significant for the diagnosis of benignity: ($p<0.05$)

1. Purely cystic lesion
2. Hypointense signal within solid component on T2WI
3. Absence of diffusion restriction
4. Type I or II TIC on DCEMR

The presence of any of these parameters either in isolation or in combination was 100% specific and 100% predictive of the benignity of a lesion. While presence of a purely cystic lesion and hypointense signal of the solid component on T2WI had accuracies of 80.85% and 78.95%, absence of diffusion restriction had an excellent accuracy reaching up to 89.5%.

Obtaining either a type I or type II TIC on DCEMR (in other words, absence of a type III TIC) had a high combined accuracy of 93.1%.

The following parameters were proven to be statistically significant for the diagnosis of malignancy: ($p<0.05$)

1. Predominantly cystic lesion with some solid component
2. Predominantly solid lesion
3. Intermediate SI within solid component on T2WI
4. Presence of papillary projection
5. Presence of diffusion restriction

6. Type III TIC on DCEMR

Conventional MRI parameters such as a predominantly cystic lesion with some solid component or a predominantly solid lesion (Mixed solid-cystic lesions), intermediate SI within solid component on T2WI and the presence of papillary projections had accuracies of 80.9%, 82.98%, 78.95%, 87.1%, respectively.

However, Diffusion restriction and type III TIC on DCEMR yielded higher accuracies of 89.5% and 93.1%, respectively, with improved sensitivity and specificity as compared to the conventional MRI parameters.

The combination of intermediate T2 SI and presence of diffusion restriction in solid component yielded an accuracy of 89.5%, sensitivity of 100% and a relatively low specificity of 77.8%, while the combination of intermediate T2 SI, diffusion restriction and type III TIC on DCEMR in the solid component yielded an accuracy of 86.7% with much improved specificity of 100%; thereby consolidating the added advantage of DWI and DCE, when these sequences are added to the conventional MRI protocol.

Our results are in keeping with a study by Thomassin Naggara I et al, in which Dynamic contrast-enhanced and diffusion weighted sequences were demonstrated to improve diagnostic confidence by about 25% and 15%, respectively, compared to conventional MRI sequences, allowing an accuracy of up to 94.6%.[87]

In a study by Li HM et al, DCEMR generated a sensitivity of 83% (59/71), a specificity of 100%(15/15), and an accuracy of 86% (74/86) between malignant and benign tumors if type III TIC indicated a malignant tumor, type II and I TIC represented a benign or borderline tumor.[70]

In a study by Emad-Eldin S et al, the addition of the DWI improved the sensitivity, specificity and accuracy of the conventional MRI from 94.12%, 90.32%, and 92.3% respectively to 100%, 100% and 98.46%.[96]

In a study by Elzayat WA et al, DCE-MRI had higher specificity and accuracy (100% & 96% respectively) than conventional MRI (57.1% &

84.4% respectively), but the latter had higher sensitivity (92% compared to 80%).[95]

Limitations of the study:

The small sample size in the present study was one of the limitations and further studies with larger sample populations should be conducted to confirm or negate our findings.

A large number of lesions in our study were endometriomas, a confident diagnosis of which is usually possible based on conventional MRI parameters.

Moreover, in this study, we classified borderline tumors in the same group as the malignant lesions. Although these two categories may share some characteristics, it is suggested that further studies include more patients with borderline tumors so that a more comprehensive comparison could be made between their characteristics and that of malignant lesions.

In addition to TIC analysis on DCE-MR, obtaining semi-quantitative and quantitative parameters, such as Ktrans, Kep, etc, using a two-compartment pharmacokinetic model, could have allowed for a more comprehensive evaluation of the role of DCE-MR.

SUMMARY & CONCLUSION

There are a vast number of complex masses which cannot be accurately characterized on US and many of these actually turn out to be benign, thereby subjecting patients to unnecessary surgical morbidity. MRI, due to its excellent contrast resolution, allows confident characterization of indeterminate masses, and thus has a crucial role in guiding management. A total of 47 patients who had a sonographically indeterminate adnexal mass and subsequently underwent an MRI in our department, were enrolled in this study. In 12 out of 47 patients who had bilateral lesions, only the most complex or the largest lesion was included in the statistical analysis. Therefore, a total of 47 lesions were evaluated in our study. Majority of the lesions turned out to be benign (n=37; 78.7%), while 10 (21.3%) were malignant.

A purely cystic lesion had a high PPV and specificity of 100% and sensitivity of 75.7% in predicting benignity (p=0.001). Among the 11 mixed solid-cystic lesions, 7 were malignant, thus favoring malignancy, with a statistically significant difference.

Presence of low T2 signal intensity in solid component was found to be 100% predictive and specific for benign lesions with a low sensitivity of 55.6%. Presence of intermediate signal intensity on T2WI had a sensitivity of 100%, specificity of 55.6%, PPV of 71.4% and an accuracy of 79% for the diagnosis of malignancy (p=0.001).

Presence of papillary projections had a specificity of 96.9%, sensitivity of 42.9%, PPV of 75%, NPV of 88.6%, and accuracy of 87.1% for diagnosing a malignant lesion (p=0.001).

Thickened septa, hemorrhage, ascites, marked T1 hyperintensity, or T2 shading; presence of none of these parameters was statistically significant in differentiating between benign and malignant lesions.

Presence of diffusion restriction in the solid component was seen in 12 (63.2%) out of 19 cases with some solid component. All the 10 malignant

and 2/9 (22.2%) benign lesions showed restricted diffusion in their solid component (p=0.001). The sensitivity, specificity, positive predictive value (PPV), negative predictive value (NPV) and accuracy of restricted diffusion in our study was 100%, 77.8%, 83.3%, 100% and 89.5% respectively.

Out of 19 lesions with some solid component, low ADC signal was seen in 8 (88.9%) benign and all 10 malignant lesions (p=0.279). The average mean ADC value in solid component was 990.67 x 10^{-6} mm^2/s in benign and 956.30 x 10^{-6} mm^2/s in malignant lesions (p=0.624). Thereby, ADC signal alone, or mean ADC values were not statistically significant in the differentiation of benign and malignant lesions.

Out of 29 lesions evaluated by dynamic contrast-enhanced MRI with Time Intensity Curve analysis, Type I curve was seen in 13 (44.8%) lesions, type II curve was seen in 9 (31%), and type III curve was seen in 7 (24.1%) lesions. Type I curve had a sensitivity of 65% and a specificity and PPV of 100% and an accuracy of 75.8% for the diagnosis of a benign lesion (p=0.001). Type III curve was only found in malignant tumors with a sensitivity of 77.8%, specificity and PPV of 100% and an accuracy of 93.1% (p=0.001). Obtaining a type II curve was neither sensitive, nor specific for either of the diagnoses (p=0.491).

The following parameters were found to be statistically significant for the diagnosis of benignity: ($p<0.05$)

1. Purely cystic lesion
2. Hypointense signal within solid component on T2WI
3. Absence of diffusion restriction
4. Type I Time-Intensity Curve on Dynamic-Contrast enhanced MRI

The presence of any of these parameters either in isolation or in combination was 100% specific and 100% predictive of the benignity of a lesion. While presence of a purely cystic lesion and the low T2 SI of the solid component had accuracies of 80.85% and 78.95%, absence of diffusion restriction had an excellent accuracy reaching up to 89.5%.

Obtaining either a type I or type II TIC on DCEMR had a high combined accuracy of 93.1%.

The following parameters were proven to be statistically significant for the diagnosis of malignancy: ($p<0.05$)

1. Predominantly cystic lesion with some solid component
2. Predominantly solid lesion
3. Intermediate SI within solid component on T2WI
4. Presence of papillary projection
5. Presence of diffusion restriction
6. Type III TIC on DCEMR

Conventional MRI parameters such as a predominantly cystic lesion with some solid component or a predominantly solid lesion (Mixed solid-cystic lesions), intermediate SI within solid component on T2WI and the presence of papillary projections had accuracies of 80.9%, 82.98%, 78.95%, 87.1% respectively. However, Diffusion restriction and type III TIC on DCEMR yielded higher accuracies of 89.5% and 93.1%, respectively, with improved sensitivity and specificity as compared to the conventional MRI parameters.

Hence, addition of DWI and DCE to the conventional MRI parameters resulted in significant improvement in the accuracy of characterization of adnexal masses, thereby playing a crucial role in determining the surgical strategy or feasibility of conservative management.

BIBLIOGRAPHY

1. Givens V, Mitchell GE, Harraway-Smith C, Reddy A, Maness DL. Diagnosis and management of adnexal masses. Am Fam Physician. 2009;80:815-820.
2. Bhagde AD, Jani SK, Patel MS, Shah SR. An analytical study of 50 women presenting with an adnexal mass. Inter J Reprod Contracept Obstetr Gynecol. 2016;6:262-5.
3. Puri S, Chadha V, Pandey AK. Epidemiology of ovarian tumours in Northern India-A tertiary hospital based study. Indian Journal of Community and Family Medicine. 2018;4:37.
4. Munkarah A, Chatterjee M, Tainsky MA. Update on ovarian cancer screening. Curr Opin Obstet Gynecol. 2007;19:22-6.
5. Garefalakis M, Hickey M, Johnson N. Gynecological Morbidity. International Encyclopedia of Public Health. 2017;342–53.
6. Craig ME, Sudanagunta S, Billow M. Anatomy, Abdomen and Pelvis, Broad Ligaments. [Updated 2020 Aug 10]. In: StatPearls [Internet]. Treasure Island (FL): StatPearls Publishing; 2020 Jan-. Available from: https://www.ncbi.nlm.nih.gov/books/NBK499943/.
7. Yamashita Y, Torashima M, Hatanaka Y. Adnexal masses: accuracy of characterization with transvaginal US and precontrast and postcontrast MR imaging. Radiology. 1995;194:557-65.
8. Timmerman D, Testa AC, Bourne T, Ameye L, Jurkovic D, Van Holsbeke C, et al. Simple ultrasound-based rules for the diagnosis of ovarian cancer. Ultrasound in Obstetrics and Gynecology: The Official Journal of the International Society of Ultrasound in Obstetrics and Gynecology. 2008;31:681-90.
9. Timmerman D, Schwärzler P, Collins WP, Claerhout F, Coenen M, Amant F, et al. Subjective assessment of adnexal masses with the use of ultrasonography: an analysis of interobserver variability and experience. Ultrasound in Obstetrics and Gynecology: The Official

Journal of the International Society of Ultrasound in Obstetrics and Gynecology. 1999;13:11-6.

10. Shah D, Shah S, Parikh J, Bhatt CJ, Vaishnav K, Bala DV. Doppler ultrasound: a good and reliable predictor of ovarian malignancy. The Journal of Obstetrics and Gynecology of India. 2013;63:186-9.
11. Buy JN, Ghossain MA, Hugol D, Hassen K, Sciot C, Truc JB, et al. Characterization of adnexal masses: combination of color Doppler and conventional sonography compared with spectral Doppler analysis alone and conventional sonography alone. AJR. American journal of roentgenology. 1996;166:385-93.
12. Spencer JA, Ghattamaneni S. MR imaging of the sonographically indeterminate adnexal mass. Radiology. 2010;256:677-94.
13. Sohaib SA, Mills TD, Sahdev A, Webb JA, Vantrappen PO, Jacobs IJ, et al. The role of magnetic resonance imaging and ultrasound in patients with adnexal masses. Clinical radiology. 2005;60:340-8.
14. Kurtz AB, Tsimikas JV, Tempany CM, Hamper UM, Arger PH, Bree RL, et al. Diagnosis and staging of ovarian cancer: comparative values of Doppler and conventional US, CT, and MR imaging correlated with surgery and histopathologic analysis—report of the Radiology Diagnostic Oncology Group. Radiology. 1999;212:19-27.
15. Wasnik AP, Menias CO, Platt JF, Lalchandani UR, Bedi DG, Elsayes KM. Multimodality imaging of ovarian cystic lesions: Review with an imaging based algorithmic approach. World journal of radiology. 2013;5:113.
16. Iyer VR, Lee SI. MRI, CT, and PET/CT for ovarian cancer detection and adnexal lesion characterization. American Journal of Roentgenology. 2010;194:311-21.
17. Forstner R, Sala E, Kinkel K, Spencer JA. ESUR guidelines: ovarian cancer staging and follow-up. European radiology. 2010;20:2773-80.

18. Fenchel S, Grab D, Nuessle K, Kotzerke J, Rieber A, Kreienberg R, et al. Asymptomatic adnexal masses: correlation of FDG PET and histopathologic findings. Radiology. 2002;223:780-8.
19. Schwarz JK, Grigsby PW, Dehdashti F, Delbeke D. The role of 18F-FDG PET in assessing therapy response in cancer of the cervix and ovaries. J Nucl Med. 2000;50:64S-73S.
20. Hauth EA, Antoch G, Stattaus J, Kuehl H, Veit P, Bockisch A, et al. Evaluation of integrated whole-body PET/CT in the detection of recurrent ovarian cancer. European journal of radiology. 2005;56:263-8.
21. Adusumilli S, Hussain HK, Caoili EM, Weadock WJ, Murray JP, Johnson TD, et al. MRI of sonographically indeterminate adnexal masses. American journal of roentgenology. 2006;187:732-40.
22. Mohaghegh P, Rockall AG. Imaging strategy for early ovarian cancer: characterization of adnexal masses with conventional and advanced imaging techniques. Radiographics. 2012;32:1751-73.
23. Siegelman ES, Outwater EK. Tissue characterization in the female pelvis by means of MR imaging. Radiology. 1999;212:5-18.
24. Kier R, Smith RC, McCarthy SM. Value of lipid-and water-suppression MR images in distinguishing between blood and lipid within ovarian masses. AJR. American journal of roentgenology. 1992;158:321-5.
25. Hricak H, Chen M, Coakley FV, Kinkel K, Yu KK, Sica G, et al. Complex adnexal masses: detection and characterization with MR imaging—multivariate analysis. Radiology. 2000;214:39-46.
26. Sohaib SA, Sahdev A, Trappen PV, Jacobs IJ, Reznek RH. Characterization of adnexal mass lesions on MR imaging. American Journal of Roentgenology. 2003;180:1297-304.
27. Outwater EK, Huang AB, Dunton CJ, Talerman A, Capuzzi DM. Papillary projections in ovarian neoplasms: appearance on MRI. Journal of Magnetic Resonance Imaging. 1997;7:689-95.

28. Koonings PP, Campbell K, Mishell DR Jr, Grimes DA. Relative frequency of primary ovarian neoplasms: a 10-year review. Obstet Gynecol. 1989;74:921–6.
29. Kawamoto S, Urban BA, Fishman EK. CT of epithelial ovarian tumors. Radiographics. 1999;19:S85-102.
30. Ghossain MA, Buy JN, Ligneres C, Bazot M, Hassen K, Malbec L, et al. Epithelial tumors of the ovary: comparison of MR and CT findings. Radiology. 1991;181:863-70.
31. Pretorius ES, Outwater EK, Hunt JL, Siegelman ES. Magnetic resonance imaging of the ovary. Topics in Magnetic Resonance Imaging. 2001;12:131-46.
32. Occhipinti KA. Computed tomography and magnetic resonance imaging of the ovary. In: Anderson JC, ed. Gynecologic imaging. London, England: Churchill Livingstone; 1999. p. 345–59.
33. Buy JN, Ghossain MA, Sciot C, Bazot M, Guinet C, Prevot S, et al. Epithelial tumors of the ovary: CT findings and correlation with US. Radiology. 1991;178:811-8.
34. Tanaka YO, Yoshizako T, Nishida M, Yamaguchi M, Sugimura K, Itai Y. Ovarian carcinoma in patients with endometriosis: MR imaging findings. American Journal of Roentgenology. 2000;175:1423-30.
35. Wagner BJ, Buck JL, Seidman JD, McCabe KM. From the archives of the AFIP. Ovarian epithelial neoplasms: radiologic-pathologic correlation. Radiographics. 1994;14:1351-74.
36. Matsuoka Y, Ohtomo K, Araki T, Kojima K, Yoshikawa W, Fuwa S. MR imaging of clear cell carcinoma of the ovary. European radiology. 2001;11:946-51.
37. Moon WJ, Koh BH, Kim SK, Kim YS, Rhim HC, Cho OK, et al. Brenner tumor of the ovary: CT and MR findings. Journal of computer assisted tomography. 2000;24:72-6.

38. Brammer 3rd HM, Buck JL, Hayes WS, Sheth S, Tavassoli FA. From the archives of the AFIP. Malignant germ cell tumors of the ovary: radiologic-pathologic correlation. Radiographics. 1990;10:715-24.
39. COMERCI JT, Licciardi F, Bergh PA, Gregori C, Breen JL. Mature cystic teratoma: a clinicopathologic evaluation of 517 cases and review of the literature. Obstetrics & Gynecology. 1994;84:22-8.
40. Outwater EK, Siegelman ES, Hunt JL. Ovarian teratomas: tumor types and imaging characteristics. Radiographics. 2001;21:475-90.
41. Kim SH, Kang SB. Ovarian dysgerminoma: color Doppler ultrasonographic findings and comparison with CT and MR imaging findings. Journal of ultrasound in medicine. 1995;14:843-8.
42. Levitin A, Haller KD, Cohen HL, Zinn DL, O'Connor MT. Endodermal sinus tumor of the ovary: imaging evaluation. AJR. American journal of roentgenology. 1996;167:791-3.
43. Outwater EK, Wagner BJ, Mannion C, McLarney JK, Kim B. Sex cord-stromal and steroid cell tumors of the ovary. Radiographics. 1998;18:1523-46.
44. Morikawa K, Hatabu H, Togashi K, Kataoka ML, Mori T, Konishi J. Granulosa cell tumor of the ovary: MR findings. Journal of computer assisted tomography. 1997;21:1001-4.
45. Troiano RN, Lazzarini KM, Scoutt LM, Lange RC, Flynn SD, McCarthy S. Fibroma and fibrothecoma of the ovary: MR imaging findings. Radiology. 1997;204:795-8.
46. Thomassin-Naggara I, Daraï E, Nassar-Slaba J, Cortez A, Marsault C, Bazot M. Value of dynamic enhanced magnetic resonance imaging for distinguishing between ovarian fibroma and subserous uterine leiomyoma. Journal of computer assisted tomography. 2007;31:236-42.
47. Kim SH, Sim JS, Seong CK. Interface vessels on color/power Doppler US and MRI: a clue to differentiate subserosal uterine

myomas from extrauterine tumors. Journal of computer assisted tomography. 2001;25:36-42.

48. Matsubayashi R, Matsuo Y, Doi J, Kudo S, Matsuguchi K, Sugimori H. Sclerosing stromal tumor of the ovary: radiologic findings. European radiology. 1999;9:1335-8.
49. Outwater EK, Marchetto B, Wagner BJ. Virilizing tumors of the ovary: imaging features. Ultrasound in Obstetrics and Gynecology: The Official Journal of the International Society of Ultrasound in Obstetrics and Gynecology. 2000;15:365-71.
50. Kim SH, Kim YJ, Park BK, Cho JY, Kim BH, Byun JY. Collision tumors of the ovary associated with teratoma: clues to the correct preoperative diagnosis. Journal of computer assisted tomography. 1999;23:929-33.
51. Ha HK, Baek SY, Kim SH, Kim HH, Chung EC, Yeon KM. Krukenberg's tumor of the ovary: MR imaging features. AJR. American journal of roentgenology. 1995;164:1435-9.
52. Giudice LC, Kao LC. Endometriosis. Lancet 2004;364:1789–99
53. Togashi K, Nishimura K, Kimura I, Tsuda Y, Yamashita K, Shibata T, et al. Endometrial cysts: diagnosis with MR imaging. Radiology. 1991;180:73-8.
54. Outwater E, Schiebler ML, Owen RS, Schnall MD. Characterization of hemorrhagic adnexal lesions with MR imaging: blinded reader study. Radiology. 1993;186:489-94.
55. Dias JL, Gomes FV, Lucas R, Cunha TM. The shading sign: is it exclusive of endometriomas?. Abdominal imaging. 2015;40:2566-72.
56. Siegelman ES, Oliver ER. MR imaging of endometriosis: ten imaging pearls. Radiographics. 2012;32:1675-91.
57. Busard MP, Mijatovic V, Van Kuijk C, Pieters-van den Bos IC, Hompes PG, Van Waesberghe JH. Magnetic resonance imaging in the evaluation of (deep infiltrating) endometriosis: The value of diffusion-weighted imaging. Journal of Magnetic Resonance Imaging:

An Official Journal of the International Society for Magnetic Resonance in Medicine. 2010;31:1117-23.

58. Domingues MD, Marchiori E. MR Imaging in Deep Pelvic Endometriosis: A Pictorial Essay1. RadioGraphics. 2011;31:549-67.
59. Loubeyre P, Petignat P, Jacob S, Egger JF, Dubuisson JB, Wenger JM. Anatomic distribution of posterior deeply infiltrating endometriosis on MRI after vaginal and rectal gel opacification. American Journal of Roentgenology. 2009;192:1625-31.
60. Masch WR, Daye D, Lee SI. MR imaging for incidental adnexal mass characterization. Magnetic Resonance Imaging Clinics. 2017;25:521-43.
61. Kim MY, Rha SE, Oh SN, Jung SE, Lee YJ, Kim YS, et al. MR imaging findings of hydrosalpinx: a comprehensive review. Radiographics. 2009;29:495-507.
62. Ha HK, Lim GY, Cha ES, Lee HG, Ro HJ, Kim HS, et al. MR imaging of tubo-ovarian abscess. Acta Radiologica. 1995;36:510-4.
63. Pickhardt PJ, Levy AD, Rohrmann Jr CA, Kende AI. Primary neoplasms of the appendix: radiologic spectrum of disease with pathologic correlation. Radiographics. 2003;23:645-62.
64. Jain KA. Imaging of peritoneal inclusion cysts. American Journal of Roentgenology. 2000;174:1559-63.
65. Rieber A, Nüssle K, Stöhr I, Grab D, Fenchel S, Kreienberg R, et al. Preoperative diagnosis of ovarian tumors with MR imaging: comparison with transvaginal sonography, positron emission tomography, and histologic findings. American Journal of Roentgenology. 2001;177:123-9.
66. Bazot M, Nassar-Slaba J, Thomassin-Naggara I, Cortez A, Uzan S, Daraï E. MR imaging compared with intraoperative frozen-section examination for the diagnosis of adnexal tumors; correlation with final histology. European radiology. 2006;16:2687.

67. Thomassin-Naggara I, Balvay D, Rockall A, Carette MF, Ballester M, Darai E, et al. Added value of assessing adnexal masses with advanced MRI techniques. BioMed research international. 2015;2015:785206.
68. Koh DM, Collins DJ. Diffusion-weighted MRI in the body: applications and challenges in oncology. American Journal of Roentgenology. 2007;188:1622-35.
69. Fujii S, Kakite S, Nishihara K, Kanasaki Y, Harada T, Kigawa J, et al. Diagnostic accuracy of diffusion-weighted imaging in differentiating benign from malignant ovarian lesions. Journal of Magnetic Resonance Imaging: An Official Journal of the International Society for Magnetic Resonance in Medicine. 2008;28:1149-56.
70. Li HM, Qiang JW, Ma FH, Zhao SH. The value of dynamic contrast–enhanced MRI in characterizing complex ovarian tumors. Journal of ovarian research. 2017;10:4.
71. Kurjak A, Predanic M, Kupesic-Urek S, Jukic S. Transvaginal color and pulsed Doppler assessment of adnexal tumor vascularity. Gynecologic oncology. 1993;50:3-9.
72. Hamper UM, Sheth S, Abbas FM, Rosenshein NB, Aronson D, Kurman RJ. Transvaginal color Doppler sonography of adnexal masses: differences in blood flow impedance in benign and malignant lesions. AJR. American journal of roentgenology. 1993;160:1225-8.
73. Van Holsbeke C, Van Belle V, Leone FP, Guerriero S, Paladini D, Melis GB, et al. Prospective external validation of the ‘ovarian crescent sign’as a single ultrasound parameter to distinguish between benign and malignant adnexal pathology. Ultrasound in obstetrics & gynecology. 2010;36:81-7.
74. Suidan RS, Ramirez PT, Sarasohn DM, Teitcher JB, Mironov S, Iyer RB, et al. A multicenter prospective trial evaluating the ability of preoperative computed tomography scan and serum CA-125 to

predict suboptimal cytoreduction at primary debulking surgery for advanced ovarian, fallopian tube, and peritoneal cancer. Gynecologic oncology. 2014;134:455-61.

75. Gatreh-Samani F, Tarzamni MK, Olad-Sahebmadarek E, Dastranj A, Afrough A. Accuracy of 64-multidetector computed tomography in diagnosis of adnexal tumors. Journal of Ovarian Research. 2011;4:1-6.
76. Kinkel K, Lu Y, Mehdizade A, Pelte MF, Hricak H. Indeterminate ovarian mass at US: incremental value of second imaging test for characterization—meta-analysis and Bayesian analysis. Radiology. 2005;236:85-94.
77. Bazot M, Haouy D, Darai E, Cortez A, Dechoux-Vodovar S, Thomassin-Naggara I. Is MRI a useful tool to distinguish between serous and mucinous borderline ovarian tumours?. Clinical Radiology. 2013;68:e1-8.
78. Chen M, Wang WC, Zhou C, Zhou NN, Cai K, Yang ZH, et al. Differentiation between malignant and benign ovarian tumors by magnetic resonance imaging. Chinese medical sciences journal= Chung-kuo i hsueh k'o hsueh tsa chih. 2006;21:270-5.
79. Mansour S, Wessam R, Raafat M. Diffusion-weighted magnetic resonance imaging in the assessment of ovarian masses with suspicious features: strengths and challenges. The Egyptian Journal of Radiology and Nuclear Medicine. 2015;46:1279-89.
80. Bakir B, Bakan S, Tunaci M, Bakir VL, Iyibozkurt AC, Berkman S, et al. Diffusion-weighted imaging of solid or predominantly solid gynaecological adnexial masses: is it useful in the differential diagnosis?. The British journal of radiology. 2011;84:600-11.
81. Nakayama T, Yoshimitsu K, Irie H, Aibe H, Tajima T, Nishie A, et al. Diffusion-weighted echo-planar MR imaging and ADC mapping in the differential diagnosis of ovarian cystic masses: usefulness of detecting keratinoid substances in mature cystic teratomas. Journal

of Magnetic Resonance Imaging: An Official Journal of the International Society for Magnetic Resonance in Medicine. 2005;22:271-8.

82. Balaban M, Idilman IS, Toprak H, Unal O, Ipek A, Kocakoc E. The utility of diffusion-weighted magnetic resonance imaging in differentiation of endometriomas from hemorrhagic ovarian cysts. Clinical imaging. 2015;39:830-3.
83. Wang T, Li W, Wu X, Yin B, Chu C, Ding M, et al. Tubo-ovarian abscess (with/without pseudotumor area) mimicking ovarian malignancy: role of diffusion-weighted MR imaging with apparent diffusion coefficient values. PLoS One. 2016;11:e0149318.
84. Takeuchi M, Matsuzaki K, Nishitani H. Diffusion-weighted magnetic resonance imaging of ovarian tumors: differentiation of benign and malignant solid components of ovarian masses. Journal of computer assisted tomography. 2010;34:173-6.
85. Thomassin-Naggara I, Daraï E, Cuenod CA, Fournier L, Toussaint I, Marsault C, et al. Contribution of diffusion-weighted MR imaging for predicting benignity of complex adnexal masses. European radiology. 2009;19:1544-52.
86. Nasr E, Hamed I, Abbas I, Khalifa NM. Dynamic contrast enhanced MRI in correlation with diffusion weighted (DWI) MR for characterization of ovarian masses. The Egyptian Journal of Radiology and Nuclear Medicine. 2014;45:975-85.
87. Thomassin-Naggara I, Toussaint I, Perrot N, Rouzier R, Cuenod CA, Bazot M, et al. Characterization of complex adnexal masses: value of adding perfusion-and diffusion-weighted MR imaging to conventional MR imaging. Radiology. 2011;258:793-803.
88. Thomassin-Naggara I, Daraï E, Cuenod CA, Rouzier R, Callard P, Bazot M. Dynamic contrast-enhanced magnetic resonance imaging: A useful tool for characterizing ovarian epithelial tumors. Journal of

Magnetic Resonance Imaging: An Official Journal of the International Society for Magnetic Resonance in Medicine. 2008;28:111-20.

89. Shan J, Xu J, Gong J, Wang X, Xu H, Feng X. Value of dynamic enhanced MR imaging in the differential diagnosis of benign and malignant ovarian tumors. Chinese Journal of Radiology. 2003;37:1001-6.
90. Malek M, Pourashraf M, Mousavi AS, Rahmani M, Ahmadinejad N, Alipour A, et al. Differentiation of benign from malignant adnexal masses by functional 3 tesla MRI techniques: diffusion-weighted imaging and time-intensity curves of dynamic contrast-enhanced MRI. Asian Pac J Cancer Prev. 2015;16:3407-12.
91. Thomassin-Naggara I, Poncelet E, Jalaguier-Coudray A, Guerra A, Fournier LS, Stojanovic S, et al. Ovarian-Adnexal Reporting Data System Magnetic Resonance Imaging (O-RADS MRI) Score for Risk Stratification of Sonographically Indeterminate Adnexal Masses. JAMA Network Open. 2020;3:e1919896-.
92. Timmerman D, Valentin L, Bourne TH, Collins WP, Verrelst H, Vergote I. Terms, definitions and measurements to describe the sonographic features of adnexal tumors: a consensus opinion from the International Ovarian Tumor Analysis (IOTA) Group. Ultrasound Obstet Gynecol. 2000;16:500–5.
93. Van Calster B, Valentin L, Van Holsbeke C, Zhang J, Jurkovic D, Lissoni AA, et al. A novel approach to predict the likelihood of specific ovarian tumor pathology based on serum CA-125: a multicenter observational study. Cancer Epidemiology and Prevention Biomarkers. 2011;20:2420-8.
94. Kim HJ, Lee SY, Shin YR, Park CS, Kim K. The value of diffusion-weighted imaging in the differential diagnosis of ovarian lesions: a meta-analysis. PloS one. 2016;11:e0149465.
95. Elzayat WA, El-Kalioubie M, Abdel-Naby MM, Abdel-Malek RR. The role of dynamic contrast enhanced MR imaging in the assessment of

inconclusive ovarian masses. The Egyptian Journal of Radiology and Nuclear Medicine. 2017;48:1159-69.

96. Emad-Eldin S, Grace MN, Wahba MH, Abdella RM. The diagnostic potential of diffusion weighted and dynamic contrast enhanced MR imaging in the characterization of complex ovarian lesions. The Egyptian Journal of Radiology and Nuclear Medicine. 2018;49:884-91.

Case 1: Granulosa cell tumor

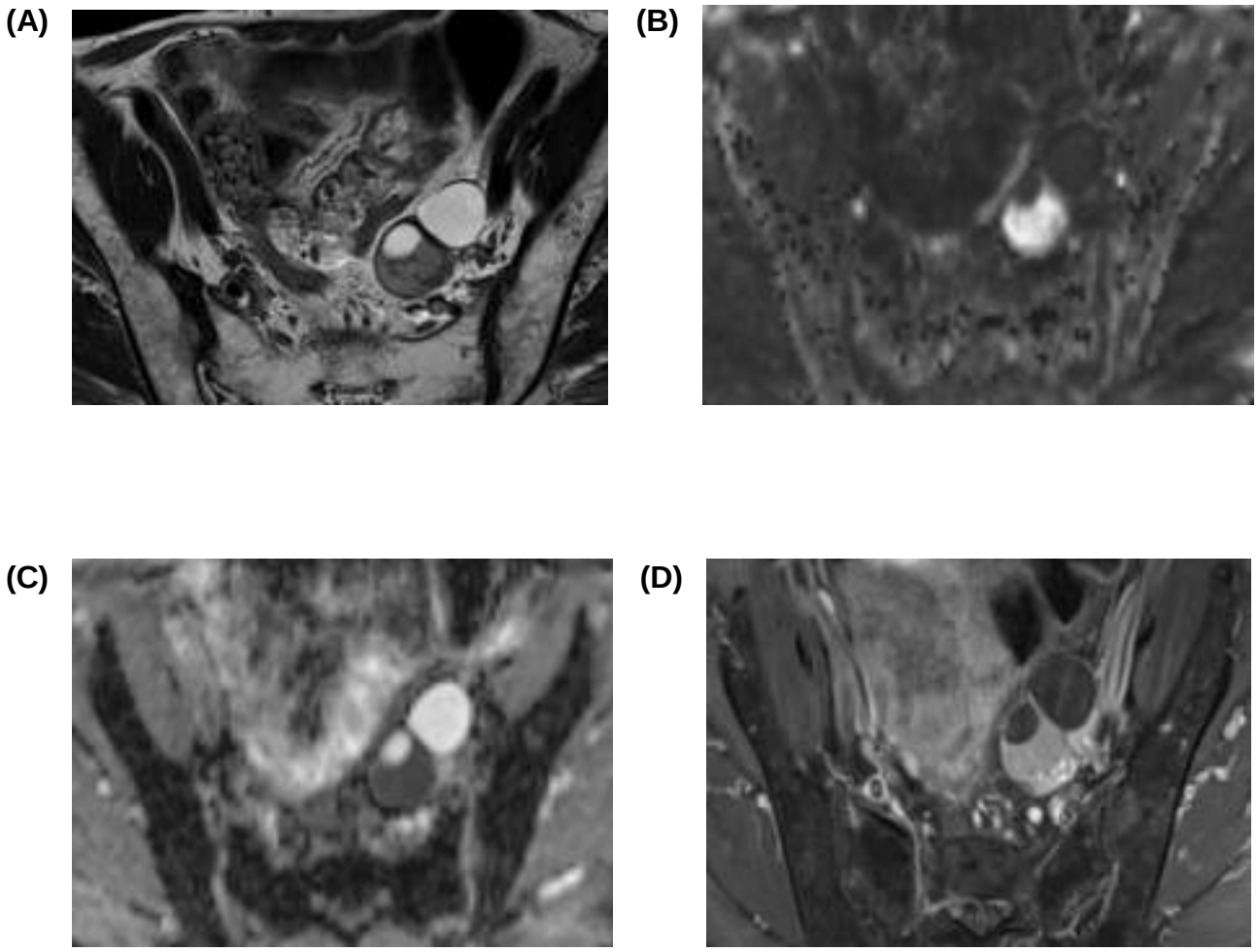

In a 67 year old female, axial T2W image (A) shows a solid-cystic lesion in the left adnexa. The solid component shows intermediate SI on T2WI, and diffusion restriction on DW (B) and ADC (C) images. There is homogeneous enhancement of the solid component on post-contrast T1W fat-saturated image (D).

Case 1 (continued)

(E)

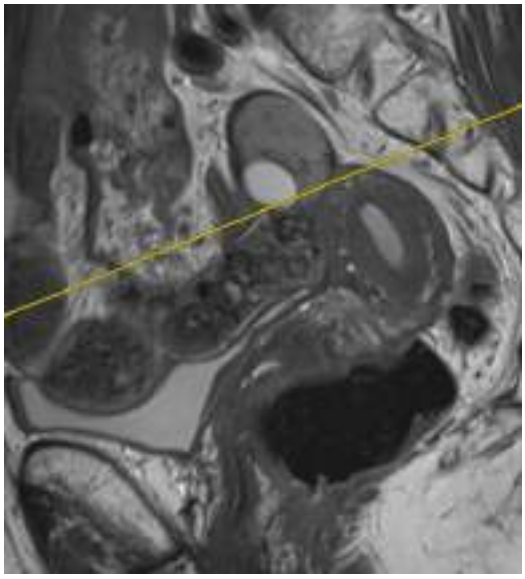

(F)

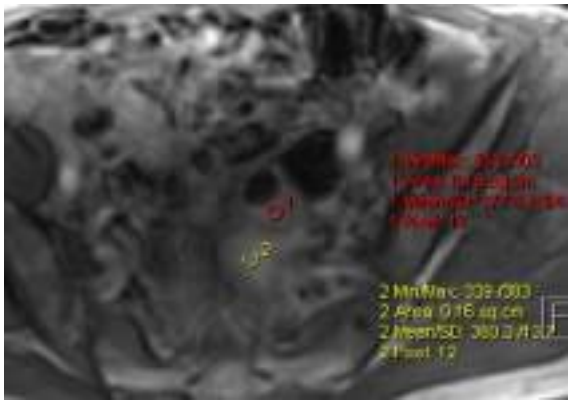

(G)

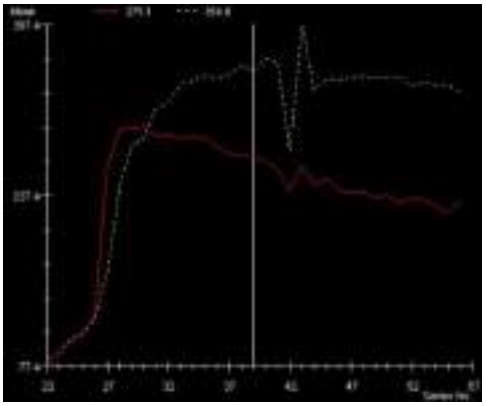

Type III TIC is seen on DCE (F,G). Imaging features are suggestive of a malignant lesion. ROIs for TIC analysis placed in the axial plane (F), with the level marked in the corresponding sagittal T2WI (E). Histopathology revealed a granulosa cell tumor.

(RED Curve: Enhancing component/ thickened septa of the lesion;

YELLOW Curve: Myometrial reference)

Case 2: Metastatic adenocarcinomatous deposits (Krukenberg tumors)

(A)

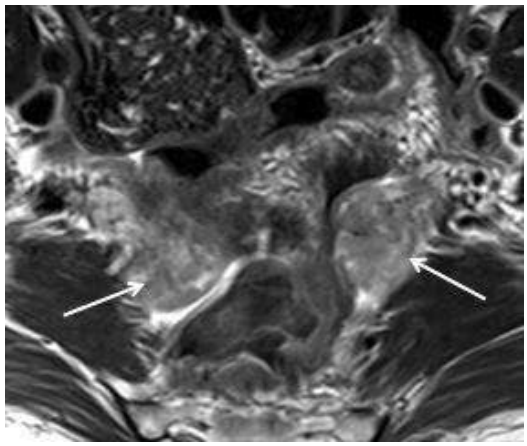

(B)

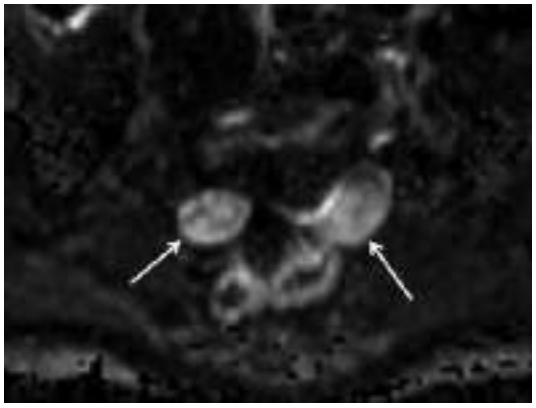

(C)

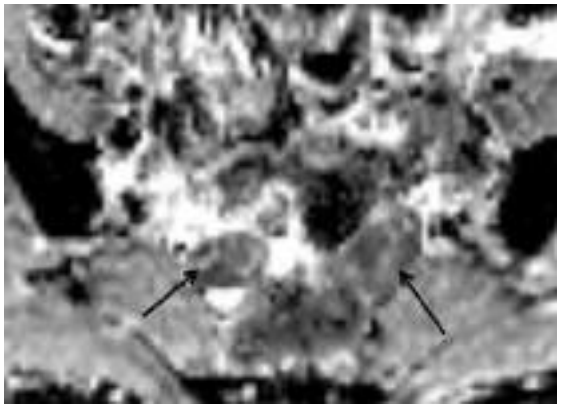

(D)

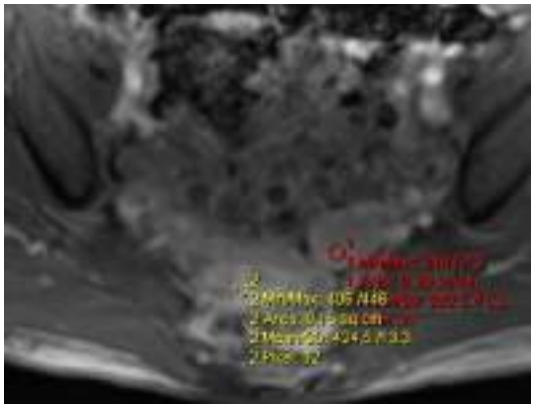

(E)

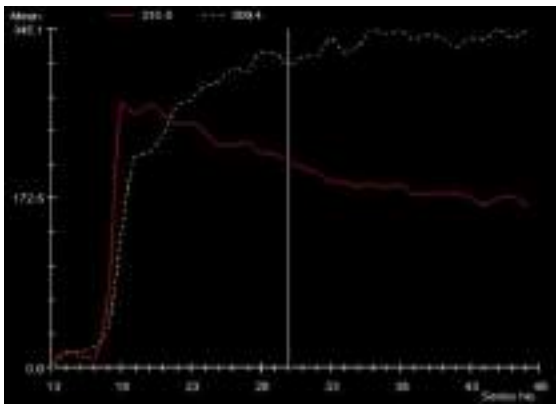

In a 64 year old female with biopsy-proven carcinoma stomach, purely solid lesions of intermediate SI on axial T2WI (A) are seen in bilateral adnexa. These show marked diffusion restriction on DW/ADC images (B,C).Type III TIC is seen in the left adnexal mass on DCE (D,E), suggestive of metastatic ovarian deposits. Histopathology confirmed metastatic adenocarcinomatous deposits (Krukenberg tumor).

Case 3: Actinomycosis

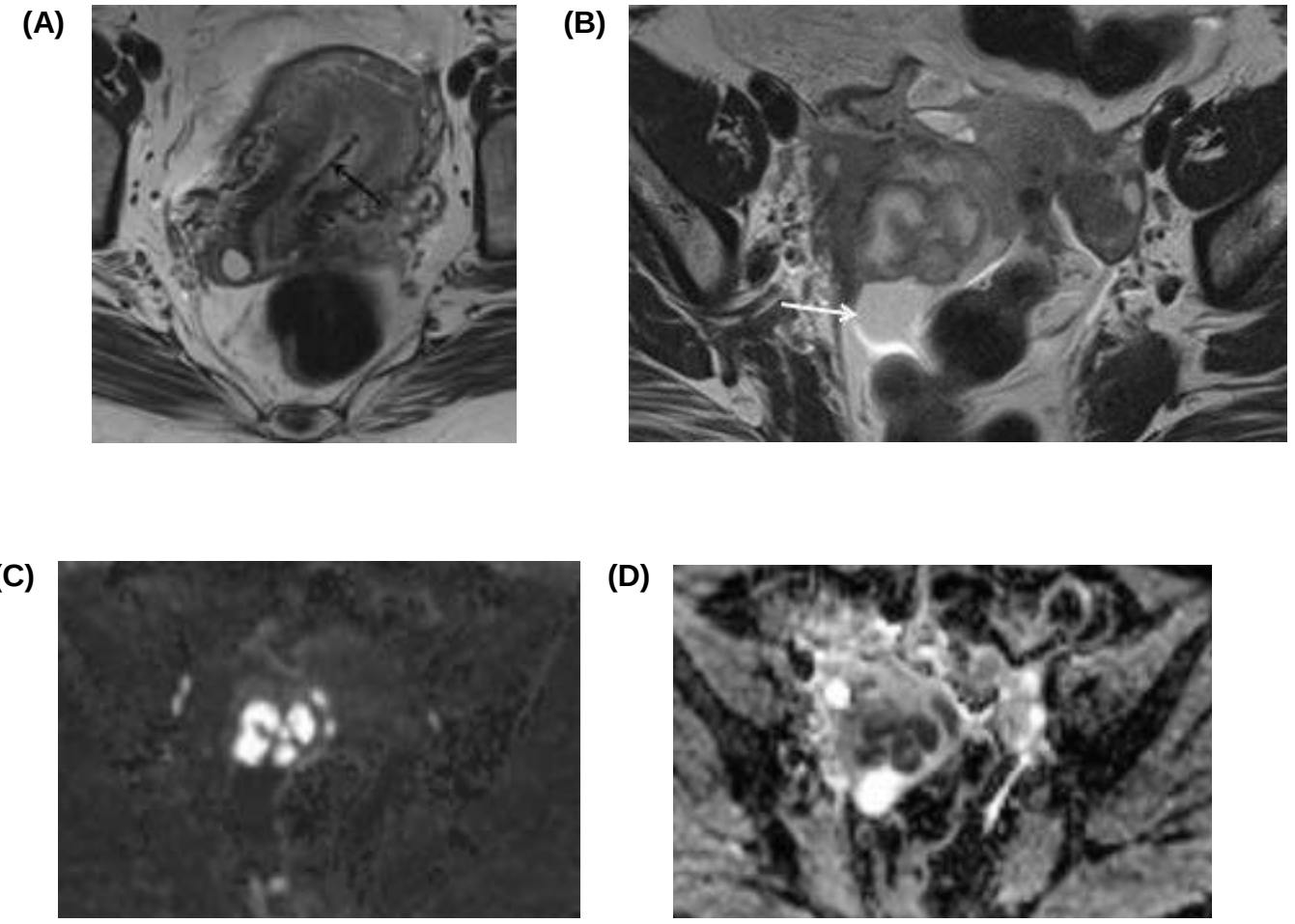

In a 40 year old female with IUCD in-situ (A) and presenting with pelvic pain and fever; Axial T2WI (B) shows a complex solid-cystic lesion with markedly thickened walls and septae in the right adnexa, with marked surrounding inflammatory changes, peritoneal thickening and small ascites (arrow). There is marked diffusion restriction in necrotic component on DW/ADC images suggestive of purulent contents (C,D).

Case 3 (continued)

(E)

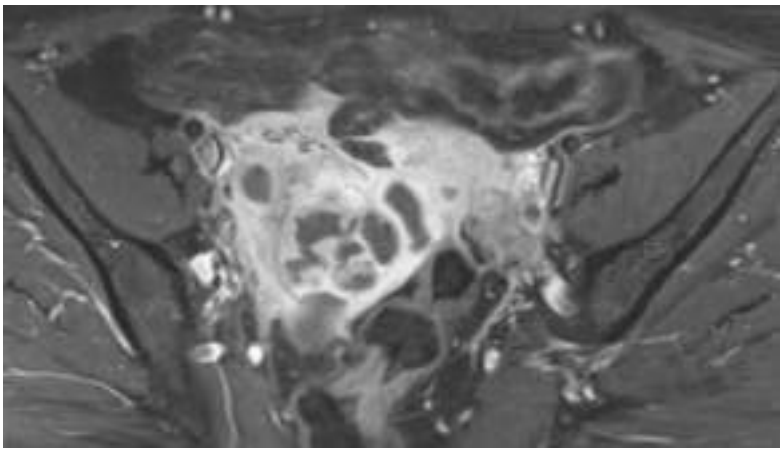

(F)

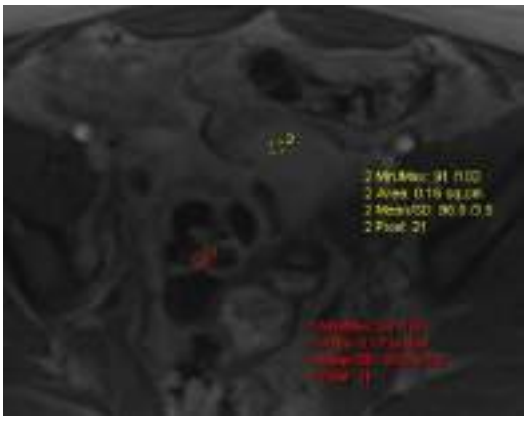

(G)

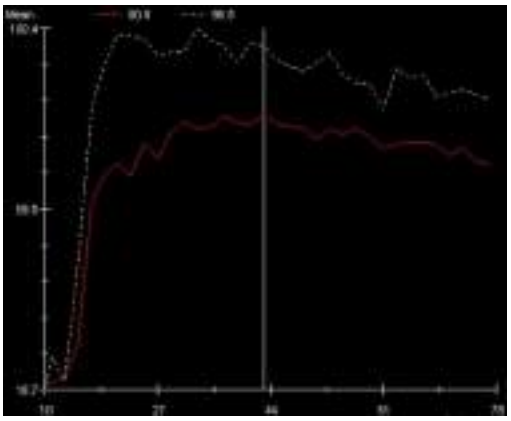

Enhancement of the solid component is seen on post contrast T1W fat-sat image (E) and type II TIC on DCE (F,G). Imaging is suggestive of a tubo-ovarian abscess, possibly actinomycosis. Histopathology confirmed actinomycosis.

Case 4: Subserosal uterine fibroid

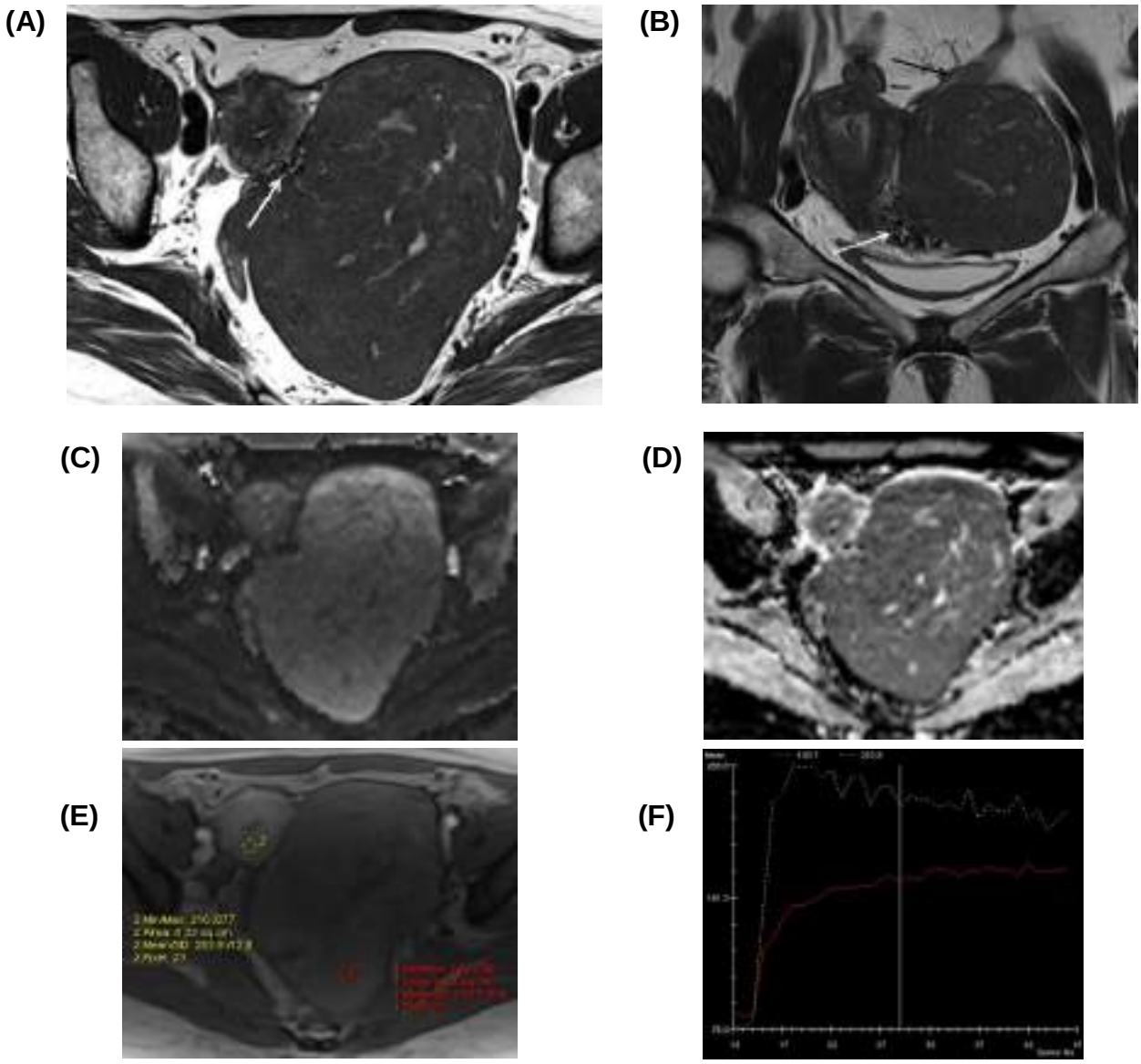

In a 50 year old female with a sonographically detected adnexal mass, axial and coronal T2WI (A,B) show a large hypointense solid mass lesion in the left adnexa, with multiple flow voids at the interface of the lesion with uterus (Bridging vessel sign; white arrow), suggesting a possible uterine origin (black arrow: left ovary). There is no diffusion restriction on DWI/ADC images (C,D), although, signal on ADC images is hypointense, with mean ADC value of 851 x 10^{-6} mm^2/s, suggestive of T2-blackout effect. Type II TIC is seen on DCE (E,F).Imaging is suggestive of a subserosal/broad ligament fibroid. Surgical findings and histopathology confirmed a subserosal uterine fibroid.

Case 5: Endometriotic cyst with endometrioid carcinoma

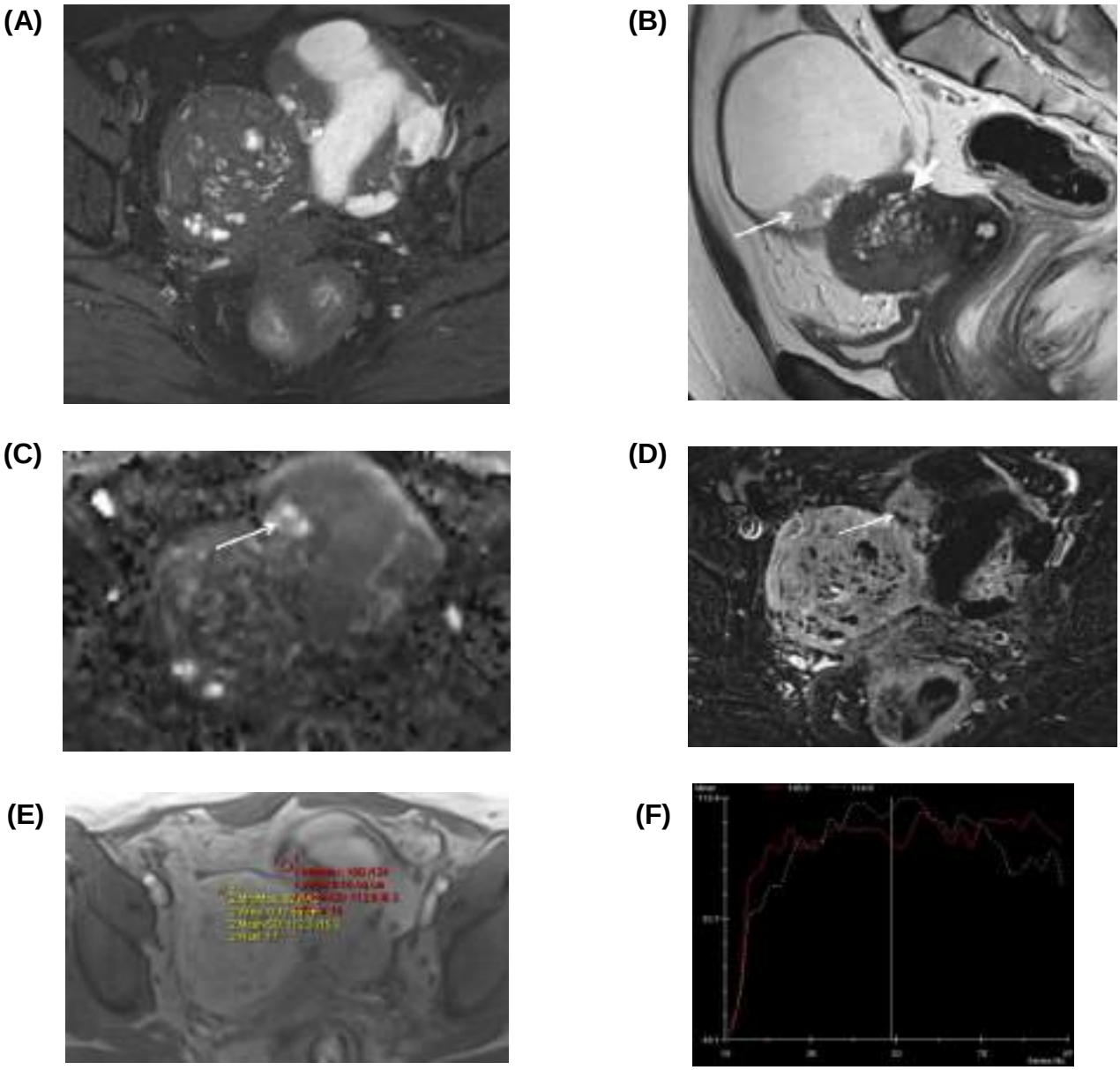

In a 41 year old female, there is a large endometriotic left adnexal lesion with marked hyperintensity on axial T1W fat-sat image (A). Sagittal T2WI (B) shows eccentric papillary projection with intermediate SI (thin arrow). Note deep infiltrative endometriosis of posterior uterus (thick arrow) with multiple T1 and T2 hyperintense foci. The solid component shows diffusion restriction on DWI (C), and enhancement on post-contrast subtraction image (D), and type III TIC on DCE (E,F). Imaging features are suggestive of endometrioid/clear cell carcinoma in a background of endometriosis. Histopathology revealed endometriotic cyst with endometrioid carcinoma.

Case 6: Metastatic ovarian deposit

(A)

(B)

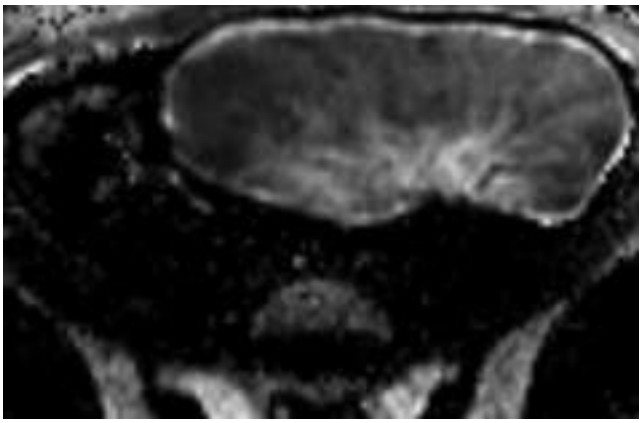

(C)

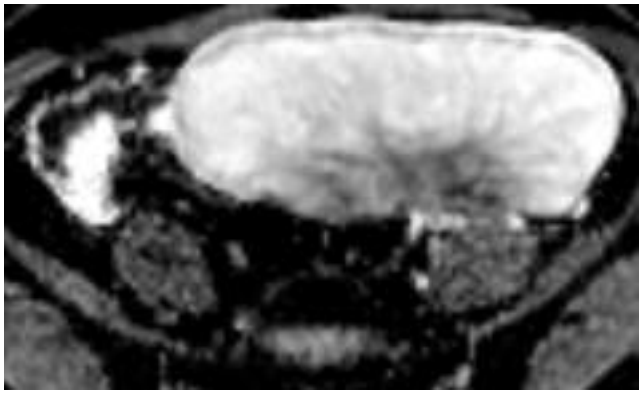

(D)

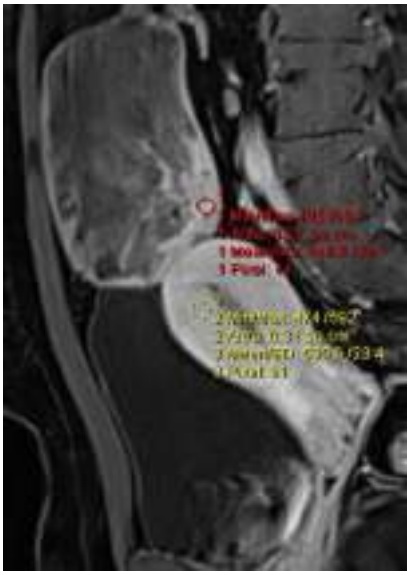

(E)

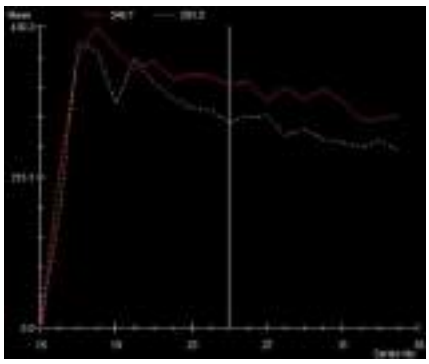

In a 48 year old female with biopsy-proven carcinoma stomach, there is a solid-cystic left adnexal lesion with the eccentric solid component showing intermediate SI on sagittal T2WI (A), diffusion restriction on DWI/ADC images (B,C), type III TIC on sagittal DCE, suggestive of ovarian metastatic deposit (D,E). The lesion showed a significant reduction in size on follow-up CT after chemotherapy.

Case 7: Endometrioid carcinoma

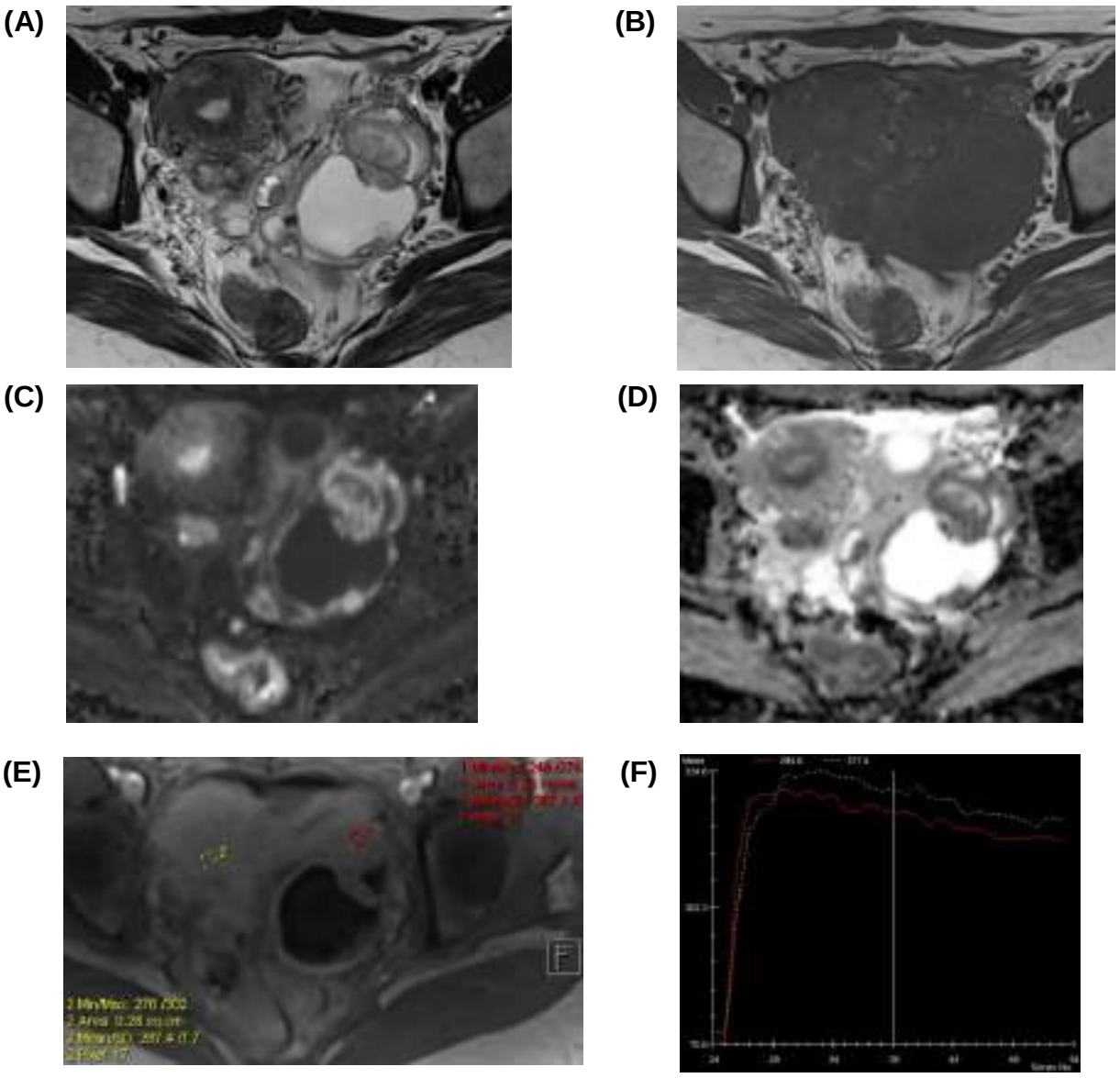

In a 37 year old female, there is a complex solid cystic left adnexal lesion with the solid component showing intermediate SI on T2WI (A), diffusion restriction on DWI/ADC images (C,D) and type III TIC on DCE (E,F). No hyperintense signal is seen on T1WI (B). Imaging is suggestive of a malignant adnexal lesion. Histopathology revealed endometrioid carcinoma.

Case 8: Bilateral endometriotic (chocolate) cysts

(A)

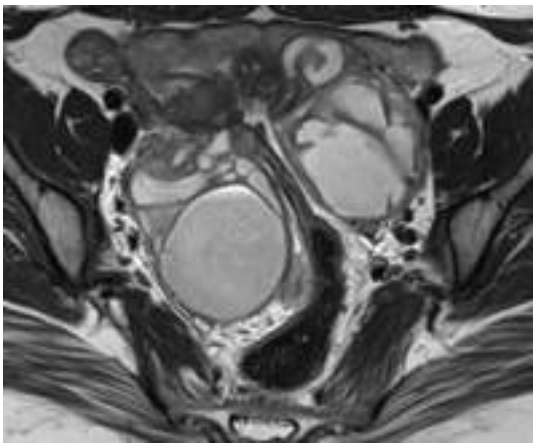

(B)

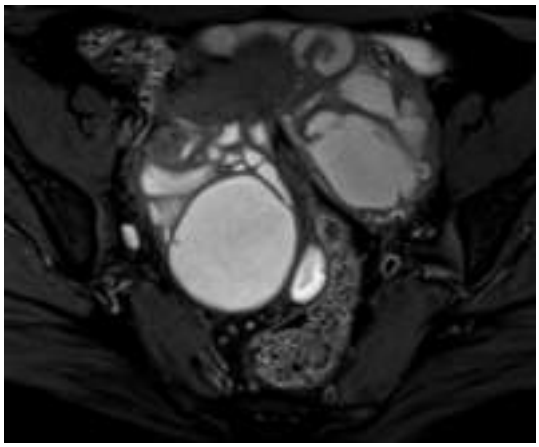

(C)

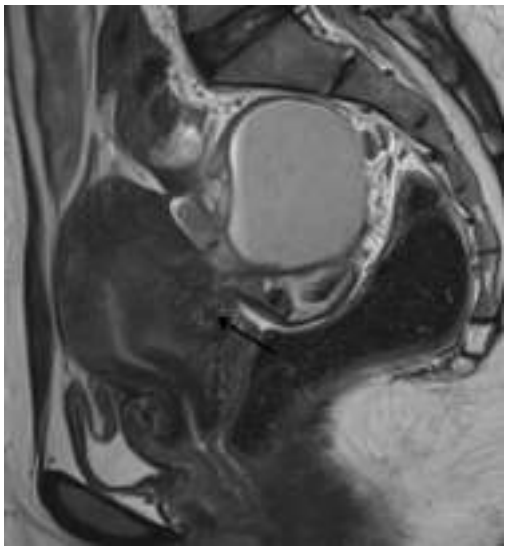

In a 27 year old female, axial T2W (A) and T1W fat-sat (B) images show complex multiseptated bilateral tubo-ovarian endometriotic lesions, with marked T1 fat-sat hyperintense signal. They are retropositioned and adherent to the uterus as well as the rectosigmoid. Note deep infiltrative endometriosis of posterior uterus on sagittal T2WI (C) (black arrow).

Case 8 (continued)

(D)

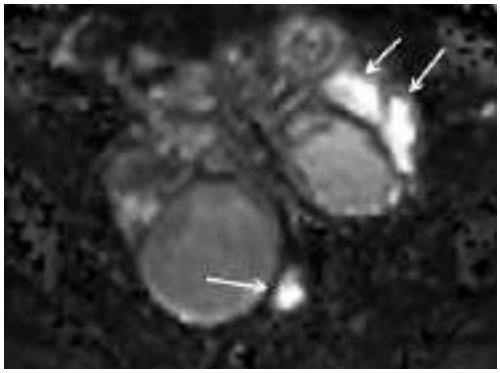

(E)

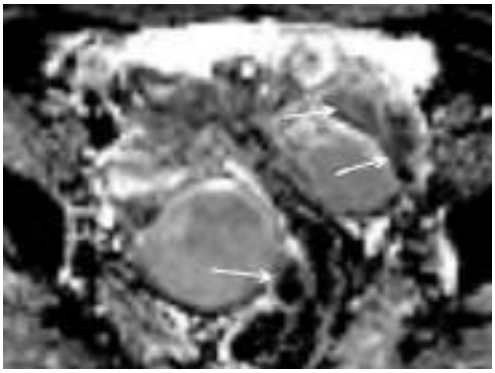

(F)

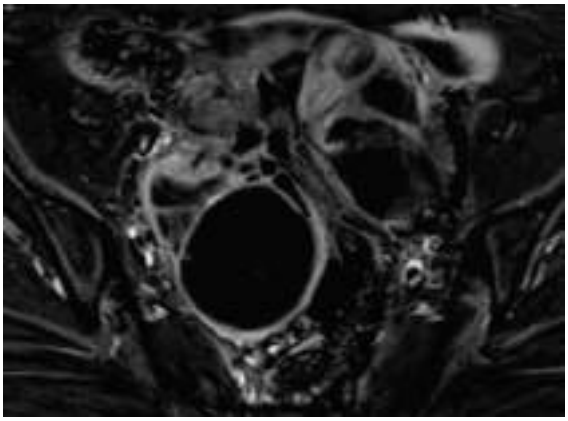

(G)

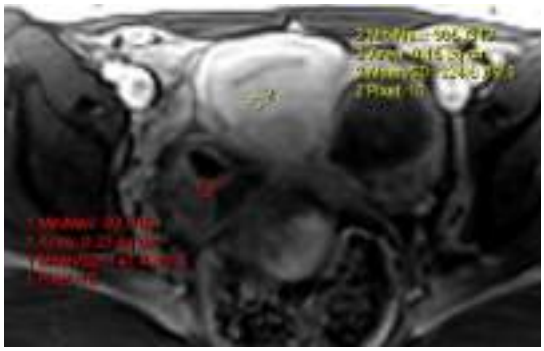

(H)

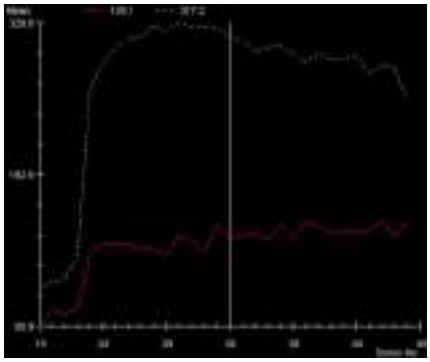

Few of the locules show diffusion restriction on DWI/ADC images (D, E) (white arrows). Thin peripheral and septal enhancement is seen on post-contrast subtraction image (F) with type I TIC on DCE (G, H). Imaging is suggestive of bilateral endometriotic cysts with deep pelvic endometriosis. Histopathology confirmed endometriosis.

Case 9: Endometrioid carcinoma resembling sex cord stromal tumor

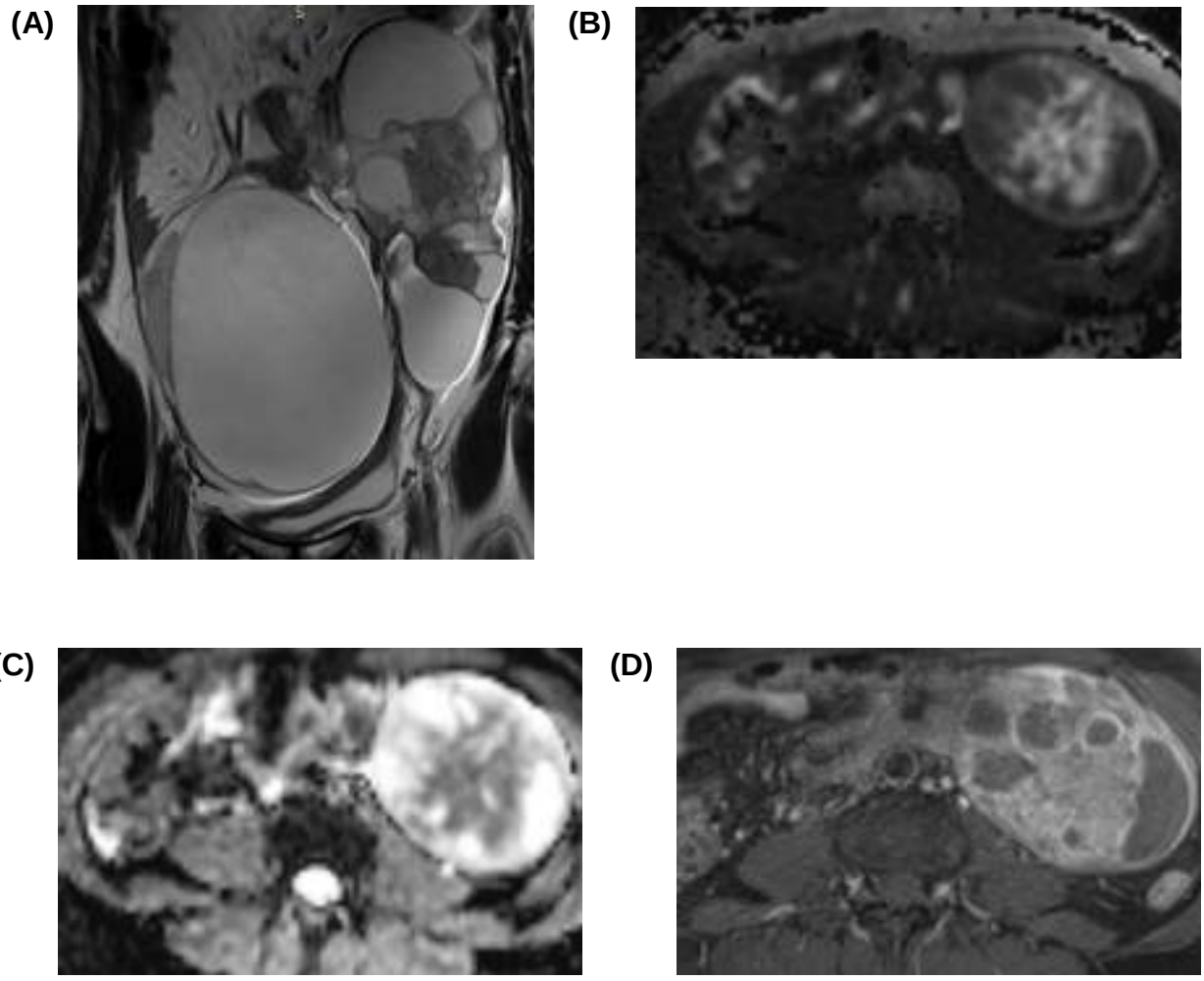

In a 41 year old female, coronal T2WI (A) shows large solid-cystic bilateral adnexal lesions with multiple irregular septations. The solid component as well as thickened septae show intermediate SI, diffusion restriction on DWI/ADC images (B, C), heterogeneous enhancement on post-contrast axial T1W fat-sat image (D).

Case 9 (continued)

(E)

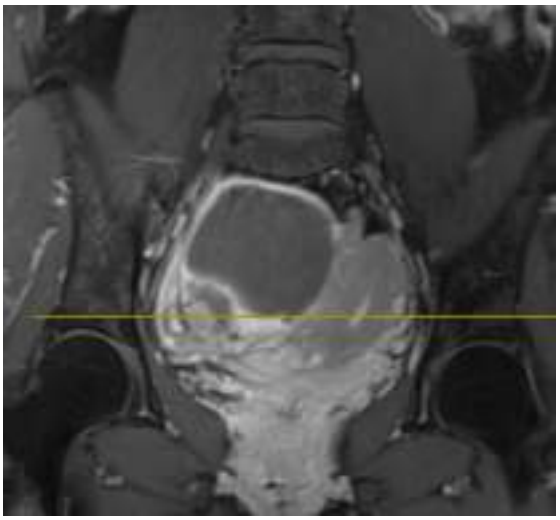

(F)

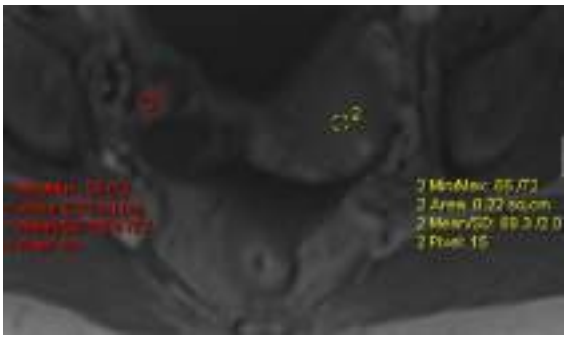

(G)

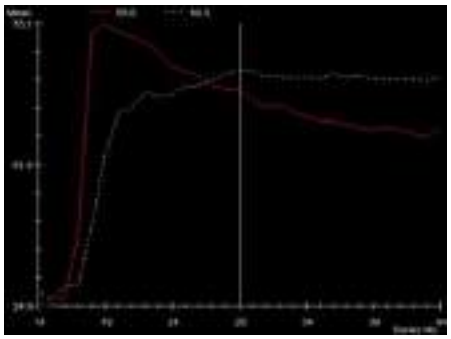

Type III TIC is seen on DCE (F, G). ROI for TIC analysis placed in the solid enhancing component on right side (F) with the level marked in the corresponding coronal post-contrast T1W fat-sat image (E). Imaging features are suggestive of malignant ovarian lesions. Histopathology confirmed endometrioid carcinoma resembling sex cord stromal tumor.

Sr. no	MRD	NAME	AGE	CHIEF COMPLAINTS	CA125	US	SIZE	LARGEST DIMENSION (cm)	BILATERALITY	T2 SI SOLID COMPONENT	MARKED T1 HYPERINTENSITY IN CYSTIC COMPONENT	T2 SHADING	SOLID/CYSTIC
1	843218	AD	60	pain	12.5	complex cyst with echoes & septations	7.8*8*9cm	9	no	NA	yes	no	purely cystic
2	750415	BB	29	pain	15.6	complex adnexal cyst, left hydronephrosis	8.8*5.7cm	8.8	no	NA	yes	yes	purely cystic
3	780057	BB	40	pain, heaviness	10.3	large cystic lesion	7.8*9.4*10.3cm	10.3	no	NA	no	no	purely cystic
4	650935	MS	37	pain, infertility	-	heterogenously hypoechoic lesion	3.8*3.4*3.1cm	3.8	no	hypointense	NA	NA	purely solid
5	843884	M	36	pain, irregular menses	-	multiple cysts with internal echoes	1cm (multiple; avg size)	1	no	NA	yes	yes	purely cystic
6	116436	N	32	pain, irregular menses	51	complex cyst with echoes & septations	Rt:6.5*6.1cm, Lt:6.8*5.6cm	6.8	yes	NA	yes	yes	purely cystic
7	558412	KB	37	dysmenorrhea, menorrhagia	50.5	complex cyst with echoes & septations	5.8*4.3*3.6cm	5.8	no	NA	yes	yes	purely cystic
8	627722	PK	43	pain, heaviness	29.4	large cystic lesion	9.8*7.8cm	9.8	no	NA	no	no	purely cystic
9	732466	SK	30	pain	-	thick walled cyst, minimal ascites	2.1*1.7cm	2.1	no	NA	no	no	purely cystic
10	599674	AD	67	pain, loss of appetite and weight	-	bulky solid appearing ovary	4.2*2.5cm	4.2	no	intermediate	no	no	predominantly solid
11	210823	SW	26	irregular menses	26	multiseptated cystic lesion	5.6*3.0cm	5.6	no	intermediate	no	no	predominantly cystic
12	791239	MS	50	menorrhagia,dysmenorrhea, fever	38.5	B/L complex multicystic lesions	Lt:5.8*5.1cm, Rt:4.1*4.0cm	5.8	yes	NA	yes	yes	purely cystic
13	612486	ZK	36	pain, loss of appetite	53.1	cystic lesion with solid nodular projections	13.3*10.5*18.7cm	18.7	no	intermediate	no	no	predominantly cystic
14	347744	GR	46	pain, heaviness	14.9	cystic lesion with few thin septations	13.4*8*11.9cm	13.4	no	NA	no	no	purely cystic
15	588139	CK	40	pain, irregular menses	-	complex cystic masses, hydrosalpinx	Rt:4.8*4.7cm, Lt:5.3*5.2cm	5.3	yes	NA	yes	yes	purely cystic
16	598935	LK	27	dysmenorrhea	559	multiple cysts with internal echoes	Rt:8.4*5.6cm, Lt:7.0*4.8cm	8.4	yes	NA	yes	yes	purely cystic
17	845818	R	27	pain, dysmenorrhea, menorrhagia	-	subserosal fibroid, torsion	15.7*17.6*9.1cm	17.6	no	hypointense	NA	NA	purely solid
18	8155	KK	49	pain	-	heterogeneous lesion with cystic areas	4.8*4.4cm	4.8	no	NA	no	no	purely cystic
19	491578	SKD	64	K/c/o Ca stomach, incidental adnexal mass	5.6	echogenic adnexal lesion	Rt:2.4*1.5cm, Lt:2.6*2.0cm	2.6	yes	intermediate	NA	NA	purely solid
20	774179	HK	44	fever, discharge per-vaginum	28.2	thick walled lesion with hypoechoic debris	4.5*4.5cm	4.5	no	NA	no	no	purely cystic
21	873435	NS	11	pain	-	cystic lesion with internal debris	4.3*4.0cm	4.3	no	intermediate	no	no	predominantly cystic
22	887692	NS	17	delayed menses, heaviness	81.2	B/L multicystic multiseptated lesions	Rt:7.1*5.6cm, Lt:9.3*5.7cm	9.3	yes	NA	no	no	purely cystic
23	817218	P	18	menorrhagia, heaviness	13.7	large cystic lesion, few septations	21*17*6.7cm	21	no	NA	no	no	purely cystic
24	872968	M	16	pain	21.1	clear cystic lesion	15.4*10.1*7.8	15.4	no	NA	no	no	purely cystic
25	847809	KK	48	irregular menses	184.5	cystic lesion with a septation	5.5*4.6cm	5.5	no	NA	no	no	purely cystic
26	920426	RK	33	fever, discharge per-vaginum	-	thick walled cystic lesion, septae & debris	5.2*5.4*6.0cm	6	no	NA	no	no	purely cystic
27	697152	DI	40	cyclical pain left leg, left foot drop	-	cystic lesion with internal echoes	4.3*3.6cm	4.3	no	NA	yes	yes	purely cystic
28	872472	RS	45	pain, heaviness	-	cystic lesion with few septations	10.9*6.9*5.1cm	10.9	no	NA	no	no	purely cystic
29	622329	BD	59	pain, postmenopausal bleeding	167	solid heterogeneous hypoechoic lesion	9.8*6.8*8.5cm	9.8	yes	intermediate	NA	NA	purely solid
30	852789	SK	47	heaviness	78.7	complex cystic mass, papillary projections	12*10.1*15.1cm	13.1	no	intermediate	yes	yes	predominantly cystic
31	910209	SA	40	pain, fever	-	solid cystic lesion?abscess/endometriotic	6.2*4.0cm	6.2	no	intermediate	no	no	predominantly cystic
32	799437	AD	48	K/c/o Ca stomach, incidental adnexal mass	27.5	solid cystic lesion	15*8*11cm	15	yes	intermediate	no	no	predominantly cystic
33	719525	KK	64	postmenopausal bleeding	30	cystic lesion with few thin septations	15*8*14cm	19	no	NA	no	no	purely cystic
34	582188	SS	44	pain	-	hypoechoic mass lesion	3.3*3.8cm	3.3	no	intermediate	NA	NA	purely solid
35	615794	SK	50	loss of appetite, weight loss	16.1	hypoechoic mass lesion	12.5*10.5*8.9cm	12.5	no	hypointense	NA	NA	purely solid
36	731985	MR	45	pain, irregular menses	8.6	solid cystic lesion	5.4*6.8*7.8cm	7.8	no	NA	yes	yes	purely cystic
37	748559	SC	60	pain	54	solid cystic lesion	4.2*2.7cm	4.2	no	NA	no	no	purely cystic
38	749097	KB	30	pain	20.5	complex cystic lesion	3.3*3.1cm	3.3	no	NA	no	no	purely cystic
39	636184	TK	43	dysmenorrhea, menorrhagia	97	unilocular cyst with internal echoes	Rt:3.3*3.2cm, Lt:5.2*6.3cm	5.2	yes	NA	yes	yes	purely cystic
40	786287	KK	25	dysmenorrhea, menorrhagia	233.4	complex cyst with internal echoes	8.5*4.4*6.7cm	8.5	yes	NA	yes	yes	purely cystic
41	924755	VD	28	infertility evaluation	-	complex cystic masses with calcification	Rt:1.7*1.4cm, Lt:1.8*1.6cm	1.8	yes	NA	yes	yes	purely cystic
42	637025	SKG	37	menorrhagia, heaviness	-	complex cystic lesion	8.2*8.5*9.5cm	9.5	no	intermediate	no	no	predominantly solid
43	848131	SD	45	pain	-	complex cystic mass, irregular septae	11.2*7.2*5.3cm	11.2	no	hypointense	no	no	predominantly cystic
44	666580	MS	66	menorrhagia, irregular menses	-	hypoechoic adnexal lesion ?fibroma	2.6*2.1cm	2.6	no	hypointense	NA	NA	purely solid
45	931228	M	41	heaviness, loss of appetite	93.4	heterogeneous B/l adnexal masses	Rt:12*17*15cm,Lt:18*9*8cm	18	yes	intermediate	no	no	predominantly cystic
46	961461	RR	41	infertility evaluation	289.5	cystic lesion with septations	7.7*8.1*7.2cm	8.1	no	intermediate	yes	yes	predominantly cystic
47	956098	S	27	pain, dysmenorrhea, menorrhagia	-	heterogeneous solid lesion	9.0*5.4*5.0cm	9	no	intermediate	no	no	purely solid

Sr. no	MRD	THICKENED SEPTA	HEMORRHAGE	ASCITES	PAPILLARY PROJECTIONS	DWI HYPERINTENSITY IN SOLID COMPONENT	DWI HYPERINTENSITY IN CYSTIC COMPONENT	ADC HYPOINTENSITY IN SOLID COMPONENT	ADC HYPOINTENSITY IN CYSTIC COMPONENT	MEAN ADC VALUE IN SOLID COMPONENT	MEAN ADC VALUE IN CYSTIC COMPONENT	ENHANCEMENT PATTERN	TYPE OF CURVE	INTERMEDIATE T2 + HIGH DW
1	849218	no	yes	no	no	NA	no	NA	no	-	2406	thin smooth peripheral & septal	1	NA
2	750415	no	yes	no	no	NA	no	NA	no	-	2484	thin smooth peripheral	1	NA
3	780367	no	no	no	no	NA	no	NA	no	-	3016	thin smooth peripheral	1	NA
4	650825	NA	no	yes	no	no	NA	yes	NA	977	NA	homogenous solid	2	no
5	643886	no	yes	no	no	NA	no	NA	yes	-	670	NA	NA	NA
6	139496	no	yes	no	no	NA	no	NA	yes	-	289	thin smooth peripheral	1	NA
7	556412	no	yes	yes	no	NA	no	NA	yes	-	1383	thin smooth peripheral	NA	NA
8	627722	no	no	no	no	NA	no	NA	no	-	2490	NA	NA	NA
9	732686	no	yes	yes	no	NA	no	NA	no	-	2796	thick peripheral enhancement	2	NA
10	559074	no	no	no	no	yes	no	yes	no	748	2904	homogenous solid	3	yes
11	259071	yes	no	no	no	yes	no	yes	no	1288	2856	thin smooth peripheral & septal	2	yes
12	791220	yes	yes	yes	no	NA	yes	NA	yes	-	656	thick peripheral & septal (left side)	2	NA
13	612486	no	no	yes	yes	yes	no	yes	no	1241	2481	NA	NA	yes
14	367364	no	yes	no	no	NA	no	NA	no	-	2722	thin smooth peripheral & septal	NA	NA
15	588039	no	yes	no	no	NA	no	NA	yes	-	854	thin smooth peripheral & septal	NA	NA
16	596935	no	yes	no	no	NA	yes	NA	yes	-	758	thin smooth peripheral & septal	1	NA
17	645818	NA	yes	yes	no	no	NA	yes	NA	882	NA	NA	NA	no
18	9155	no	yes	no	no	NA	no	NA	yes	-	754	thin smooth peripheral & septal	NA	NA
19	491076	NA	no	yes	no	yes	NA	yes	NA	889	NA	homogenous solid	3	yes
20	774179	yes	no	yes	no	NA	yes	NA	yes	-	649	thick peripheral & septal	NA	NA
21	877635	no	no	yes	yes	yes	no	yes	no	1078	2790	NA	NA	yes
22	887682	no	no	no	no	NA	no	NA	no	-	2748	NA	NA	NA
23	817238	no	no	no	no	NA	no	NA	no	-	2689	NA	NA	NA
24	871384	no	no	yes	no	NA	no	NA	no	-	2904	NA	NA	NA
25	847809	no	no	no	no	NA	no	NA	no	-	2783	thin peripheral	1	NA
26	528425	yes	no	yes	no	NA	yes	NA	yes	-	676	thick peripheral & septal	NA	NA
27	697192	no	yes	no	no	NA	yes	NA	yes	-	1068	thin smooth peripheral & septal	NA	NA
28	872372	no	no	no	no	NA	no	NA	no	-	2719	NA	NA	NA
29	622826	NA	yes	no	no	yes	NA	yes	NA	821	2015	heterogeneous solid	2	yes
30	852783	no	yes	no	yes	yes	no	yes	yes	792	1,538	heterogeneous solid	3	yes
31	910209	yes	no	yes	no	no	yes	no	yes	1532	379	thick peripheral & septal	2	no
32	795437	no	no	yes	no	yes	no	yes	no	866	2599	intense enhancement of solid component	3	yes
33	718526	no	no	no	no	NA	no	NA	no	-	2888	thin smooth peripheral & septal	1	NA
34	582089	NA	no	no	no	no	NA	yes	NA	959	NA	homogenous solid	2	no
35	615796	NA	no	no	no	no	NA	yes	NA	851	NA	mild homogenous solid	2	no
36	733085	no	yes	yes	no	NA	no	NA	yes	-	248	thin septal	NA	NA
37	748658	no	yes	no	no	NA	no	NA	yes	-	320	thin smooth peripheral	1	NA
38	743067	no	yes	no	no	NA	no	NA	yes	-	231	thin smooth peripheral	1	NA
39	696184	no	yes	no	no	NA	yes	NA	yes	-	270	thin smooth peripheral	1	NA
40	786267	yes	yes	yes	no	NA	yes	NA	yes	-	554	thick peripheral & septal	1	NA
41	824755	no	yes	no	no	NA	yes	NA	yes	-	966	thin peripheral	1	NA
42	637825	yes	no	yes	no	yes	no	yes	no	952	2804	enhancing solid component & septae	3	yes
43	848131	yes	yes	no	no	no	no	yes	no	453	2270	thin peripheral	1	no
44	666580	NA	no	no	no	no	NA	yes	NA	815	NA	NA	NA	no
45	931228	yes	no	yes	no	yes	no	yes	no	897	2704	enhancing solid component & septae	3	yes
46	981441	no	yes	no	yes	yes	yes	yes	yes	1178	812	enhancing solid component & septae	3	yes
47	956138	NA	no	yes	no	yes	NA	yes	NA	1150	NA	heterogeneous solid	2	yes

Sr. no	MRD	INTERMEDIATE T2+ HIGH DWI+ TYPE 3 TIC	MRI DIAGNOSIS	HISTOPATHOLOGY	FOLLOW UP	FINAL DIAGNOSIS
1	845218	NA	hematosalpinx with deep pelvic endometriosis	NA	medical management, reduction in size	Benign
2	750615	NA	endometriotic cyst with deep pelvic endometriosis	endometriotic cyst	-	Benign
3	780257	NA	benign simple ovarian cyst	simple cyst	-	Benign
4	650905	no	subserosal/broad ligament fibroid left adnexa, multiple uterine fibroids	multiple leiomyomas	-	Benign
5	643884	NA	endometrioma, deep pelvic endometriosis	NA	medical management, reduction in size	Benign
6	116436	NA	B/L endometriomas, hematosalpinx, deep pelvic endometriosis	NA	medical management, reduction in size	Benign
7	556412	NA	Right endometrioma, deep pelvic endometriosis	NA	medical management, reduction in size	Benign
8	627722	NA	benign cystadenoma	serous cystadenoma	-	Benign
9	752486	NA	ruptured corpus luteal cyst with hemoperitoneum	hemorrhagic cyst	-	Benign
10	559674	yes	malignant solid cystic ovarian neoplasm	granulosa cell tumour	-	Malignant
11	339611	no	benign multiseptate cystic lesion	NA	reduction in size on follow up US	Benign
12	791220	NA	B/L adnexal & deep pelvic endometriosis	NA	medical management, reduction in size	Benign
13	612486	NA	malignant ovarian neoplasm	clear cell carcinoma	-	Malignant
14	947748	NA	Large multiloculated cystic lesion/mucinous cystadenoma/inclusion cyst	ovarian stroma, corpus luteum hemorrhagicum, no e/o malignancy	-	Benign
15	589139	NA	B/L endometriomas, deep pelvic endometriosis	endometriosis	-	Benign
16	590935	NA	B/L endometriomas, hematosalpinx, deep pelvic endometriosis	endometriosis	-	Benign
17	645818	NA	Large benign fibrous adnexal lesion with torsion	sex cord stromal tumour: fibrothecoma	-	Benign
18	3155	NA	hemorrhagic ovarian cyst	hemorrhagic cyst	-	Benign
19	481976	yes	B/L solid ovarian lesions, Possibility of Krukenberg tumour	adenocarcinoma, possibly Krukenberg tumour- both ovaries	-	Malignant
20	774179	NA	tuboovarian abscess	salpingo-oophoritis	-	Benign
21	877435	NA	hemorrhagic ovarian cyst	dermoid cyst	-	Benign
22	887692	NA	Ovarian hyperstimulation	NA	medical management, reduction in size	Benign
23	817218	NA	benign cystadenoma	mucinous cystadenoma	-	Benign
24	872966	NA	Large simple paraovarian cyst with torsion	paraovarian cyst	-	Benign
25	847809	NA	benign ovarian cystadenoma	serous cystadeno/fibroma	-	Benign
26	930425	NA	ruptured right tubo-ovarian abscess, moderate ascites, peritonitis	NA	medical management, catheter drainage	Benign
27	697192	NA	right adnexal & deep pelvic endometriosis, deposit along left sciatic nerve	endometriotic deposits	-	Benign
28	872372	NA	peritoneal inclusion cyst	Paratubal cyst	-	Benign
29	622329	no	endometrioid/clear cell carcinoma, background endometriosis	Endometrioid carcinoma	-	Malignant
30	852788	yes	endometrioid/clear cell carcinoma, background endometriosis	Endometrioid carcinoma	-	Malignant
31	910209	no	tuboovarian abscess, possibly pelvic actinomycosis	actinomycosis	-	Benign
32	799437	yes	B/L adnexal metastases	NA	significant reduction in size on chemotherapy	Malignant
33	728525	NA	ovarian cystadenoma	NA	interval stability documented	Benign
34	582169	no	subserosal fibroid	subserosal uterine fibroid	-	Benign
35	625794	no	subserosal/ broad ligament fibroid	subserosal uterine fibroid	-	Benign
36	731985	NA	Endometriotic adnexal cyst, deep pelvic endometriosis	endometriotic cysts	-	Benign
37	748550	NA	hemorrhagic cyst	NA	medical management, reduction in size	Benign
38	743067	NA	hemorrhagic cyst	NA	medical management, reduction in size	Benign
39	636184	NA	B/L adnexal & deep pelvic endometriosis	endometriosis	-	Benign
40	786287	NA	B/L adnexal & deep pelvic endometriosis	endometriosis	-	Benign
41	824755	NA	deep pelvic endometriosis with an endometrioma right side	NA	medical management, reduction in size	Benign
42	697025	yes	solid cystic adnexal mass- malignant	high grade endometrioid carcinoma	-	malignant
43	848131	no	multiseptate cystic lesion with hemorrhage, ovarian torsion	ovarian torsion with hemorrhagic necrosis	-	Benign
44	666580	NA	subserosal uterine fibroid	NA	interval stability documented	Benign
45	981228	yes	B/L solid cystic ovarian masses- malignant	endometrioid carcinoma resembling sex cord stromal tumour	-	Malignant
46	963441	yes	endometrioid/clear cell carcinoma, background endometriosis	Endometrioid carcinoma	-	Malignant
47	956338	no	granulosa cell tumour	granulosa cell tumour	-	Malignant

Baba Farid University of Health Sciences
Sadiq Road
Faridkot-151 203 (Pb). INDIA.
Phone : 01639-256232,256236
Tele/Fax : 01639-256235
Email – Examination@bfuhs.ac.in

No. BFUHS/2K19p-TH/ 1429 Date 9/9/19

The Principal,
DMC, Ludhiana.

Subject: **Approval of Plan of Thesis.**

This is to inform you that the Faculty of Medical Sciences in its meeting held on 29.05.2019 has approved the plan of thesis of **Suryaveer Singh**, a student of your college for **MD Radio-Diagnosis** along with the names of Supervisor/Co-Supervisor as under:-

Topic Plan of Thesis

Role of advanced MRI sequences in the characterisation of adnexal masses

Supervisor
Dr. Kavita Saggar
Prof. & Head,
Dept. of Radio-Diagnosis,
DMCH, Ludhiana.

Co-Supervisor
Dr. Ritu Dhawan Galhotra
Assoc. Prof.,
Dept. of Radio-Diagnosis,
DMCH, Ludhiana.

Dr. Ashima Taneja
Prof. & Head,
Dept. of obst &gynae,
DMCH, Ludhiana.

The student has to submit the four copies of thesis (along with PDF format) , to the Controller of Examinations, BFUHS, Faridkot, at least six months before the commencement of theory examination, if he/she is otherwise eligible to take the examination. He /She must directed to attach a photocopy of this letter with the forwarding letter while submitting thesis to the University along with the letter of approval of University for change of supervisor/Co-Supervisor, change of topic,(if any).

S P Singh
Dr. S P Singh MS(Oph)
Controller of Examinations

Note :

1. *If any discrepancy found regarding topic of thesis or Supervisor/Co-Supervisor, inform undersigned within one month after issue of this letter.*
2. *The student may submit the thesis as per the schedule already conveyed i.e for May/June examination 30th Nov of the preceding the year of examination and for Nov/Dec examinations 31st May of the year of examination.*

ROLE OF ADVANCED MRI SEQUENCES IN THE CHARACTERISATION OF ADNEXAL MASSES

THESIS PROPOSAL

FOR APPROVAL OF SUBJECT OF THESIS TO BE SUBMITTED IN

PARTIAL FULFILMENT OF THE REQUIREMENTS

FOR THE DEGREE OF

MD

In

RADIODIAGNOSIS

OF THE

BABA FARID UNIVERSITY OF HEALTH SCIENCES

FARIDKOT

November, 2018

Dr. Suryaveer Singh

DEPARTMENT OF RADIODIAGNOSIS
DAYANAND MEDICAL COLLEGE AND HOSPITAL
LUDHIANA

ABSTRACT OF PLAN OF THESIS

Title	Role of advanced MRI sequences in the characterisation of adnexal masses
For the degree of	MD (Radiodiagnosis)
Name of the candidate	Dr. Suryaveer Singh
Supervisor	Dr. Kavita Saggar, Professor & Head, Department of Radiodiagnosis, Dayanand Medical College & Hospital
Co-supervisor(s)	Dr. Ritu Dhawan Galhotra, Associate Professor, Department of Radiodiagnosis, DMC&H Dr. Ashima Taneja, Professor & Head, Department of Obstetrics & Gynaecology, DMC&H
Institution	Dayanand Medical College and Hospital, Ludhiana
University	Baba Farid University of Health Sciences, Faridkot

Introduction: The clinical suspicion of an adnexal mass is one of the most frequent indications for gynecologic imaging. Ultrasonography (US) is the first-line imaging technique for adnexal masses but the characterization of complex masses with US alone is difficult. Pelvic magnetic resonance (MR) imaging has clearly been demonstrated to be the best imaging technique to characterise sonographically indeterminate adnexal masses. The accuracy of MRI interpretation to differentiate benign from malignant masses using only the conventional sequences is about 80%. Perfusion and diffusion weighted sequences have been demonstrated to improve diagnostic confidence by about 25% and 15%, respectively, allowing an accuracy of up to 94.6%.

Aim of Study: To assess the role of MRI in characterisation of adnexal masses, into benign and malignant, with reference to histopathological examination wherever possible and to evaluate whether advanced MRI sequences (Diffusion weighted imaging and Dynamic contrast enhanced) have any advantage over conventional MRI sequences in the characterisation of adnexal masses.

Materials & Methods: A prospective study of patients undergoing an MRI for previously detected adnexal masses, at the Department of Radiodiagnosis, Dayanand Medical College & Hospital, during a one year period. The patients will be imaged using a 3 Tesla MRI machine (Magnetom Skyra, Siemens, Germany). The protocol will include T1 weighted, T2 weighted, Diffusion weighted and dynamic contrast enhanced sequences.

Clinical Significance: The characterization of adnexal masses preoperatively is essential for planning surgical strategy, the feasibility of conservative treatment and avoiding unnecessary surgical interventions. Imaging with MRI may therefore help avoid needless removal of benign complex adnexal masses.

Keywords: Magnetic resonance imaging (MRI), Diffusion Weighted imaging (DWI), Dynamic contrast enhanced (DCE) MRI.

(Signature) Candidate | (Signature) Co-supervisor | (Signature) Co-supervisor | (Signature) Supervisor | (Signature) Principal

CERTIFICATE OF FACILITIES AVAILABLE

This is to certify that the facilities for work on the subject of thesis titled **"ROLE OF ADVANCED MRI SEQUENCES IN THE CHARACTERISATION OF ADNEXAL MASSES "** exist in the Department of Radiodiagnosis, DMC&H, Ludhiana and will be provided to the candidate. We will see that the data being included in the thesis is genuine and is collected by the candidate himself under our supervision and guidance.

Supervisor

Dr. Kavita Saggar
Professor & Head
Department of Radiodiagnosis
DMCH, Ludhiana

Co-Supervisor

Dr. Ritu Dhawan Galhotra
Associate Professor
Department of Radiodiagnosis
DMCH, Ludhiana

Dr. Ashima Taneja
Professor & Head
Department of Obstetrics & Gynaecology
DMCH, Ludhiana

Head of Department

Dr. Kavita Saggar
Professor & Head
Department of Radiodiagnosis
DMCH, Ludhiana

Place : DMCH Ludhiana

Date : 17 Dec 2018

APPROVAL PROFORMA
BY
RESEARCH & ETHICAL COMMITTEE
DAYANAND MEDICAL COLLEGE & HOSPITAL, LUDHIANA

Name of candidate	Dr. Suryaveer Singh
Department	Radiodiagnosis
Topic of Thesis	Role of advanced MRI sequences in the characterisation of adnexal masses
Likely date of appearing in PG examination	June 2021
Date of enrollment	10th May, 2018
Name of Head of Department	Dr. Kavita Saggar
1) Supervisor **2) Co-Supervisor(s)**	Dr. Kavita Saggar Dr. Ritu Dhawan Galhotra Dr. Ashima Taneja
Signature of Members of Research Committee with Stamp	**Signature of Members of Ethics Committee with Stamp**
1. HOD Pharmacology	1. HOD Physiology
2. HOD Surgery	2. HOD Pathology
3. HOD Pathology	3. HOD Pharmacology
4. HOD Medicine	4. HOD SPM
5. Dean Academics	5. HOD Medicine
6. Vice Principal	6. HOD Surgery
	7. HOD Obst. & Gynae.
	8. Legal Expert
	9. Secretary, IEC
	10. Dean Academics
	11. Vice Principal
	12. Principal

Approved: Yes / No

Chairperson
Research Committee

Approved: Yes / No

Chairperson
Ethics Committee

Chairperson
Research Committee
Chairperson
Ethics Committee

BABA FARID UNIVERSITY OF HEALTH SCIENCES, FARIDKOT

PROFORMA FOR REGISTRATION OF SUBJECT FOR DISSERTATION

1	NAME OF THE CANDIDATE AND ADDRESS	Dr. Suryaveer Singh, 180 E-Block, Kitchlu Nagar, Ludhiana, Punjab
2	NAME OF THE INSTITUTE	Dayanand Medical College and Hospital, Ludhiana
3	COURSE OF STUDY AND SUBJECT	M.D. Radiodiagnosis
4	DATE OF ADMISSION OF COURSE	10th May 2018
5	TITLE OF THE TOPIC	Role of advanced MRI sequences in the characterisation of adnexal masses

6. BRIEF RESUME OF THE INTENDED WORK

6.1 NEED FOR THE STUDY

Adnexal masses present a special diagnostic challenge when imaging findings cannot convincingly characterise them into benign or malignant.

The preoperative characterization of complex masses is crucial for informing women about surgical strategy and the feasibility of conservative treatment.

The first imaging technique is ultrasonography with Doppler. A large majority of women will not need any other imaging technique for characterization of the adnexal lesion because the lesion either has typically benign features (such as anechoic cyst) or is overtly malignant (such as the presence of peritoneal implants).

Despite ultrasonography being the first-line and most commonly used modality, its limited capability of characterising tissues and significant interobserver variability makes it unsuitable for characterisation of complex adnexal masses.[1]

CT is routinely performed for preoperative evaluation of a suspected ovarian malignancy. CT can identify the size, location, relationship to the other organs and is also very useful in preoperative staging of cancer, but it exposes patients to radiation and is less effective in determining the internal architecture than ultrasound.[2]

Pelvic magnetic resonance (MR) imaging has clearly been demonstrated to be the best imaging technique to characterise sonographically indeterminate or complex adnexal masses due to its excellent tissue contrast and various sequences which can accurately identify hemorrhage, fat and soft tissue. The accuracy of MRI interpretation to differentiate benign from malignant masses

using only the conventional sequences is about 80% according to the published literature. [3]

Dynamic contrast enhanced (DCE) and diffusion-weighted (DW) MR imaging add new criteria to conventional MR imaging to improve the characterization of complex adnexal masses, resulting in an accuracy of 95%.[4-8]

When DCE and DW imaging are added to a conventional MR imaging protocol, there is further reduction in the number of lesions that remain indeterminate at MR imaging and it may help direct more appropriate management [9]. DCE and DW imaging may therefore help women avoid the unnecessary removal of benign complex adnexal masses and help young women who wish to preserve childbearing potential opt for conservative surgery.

6.2 REVIEW OF LITERATURE

Dirk Timmerman et al (1999) [1] evaluated the subjective assessment of ultrasonographic images for discriminating between malignant and benign adnexal masses. One ultrasonographer assessed 300 patients with adnexal masses and the recorded photographic prints were independently assessed by five investigators. The end points were accuracy, interobserver agreement and the possible effect of experience. The accuracy and the level of interobserver agreement are both correlated with experience. About 10% of masses were extremely difficult to classify.

Hricak H et al (2003) [10] conducted MR imaging of the pelvis in 128 consecutive patients with clinically or ultrasonographically detected complex adnexal masses. Histopathologic examination demonstrated 187 masses, 96 of which were malignant. Gadolinium-enhanced MR imaging depicted 176 (94%) of 187 adnexal masses, with an overall accuracy for the diagnosis of malignancy of 93%. The MR imaging findings that were most predictive of malignancy were necrosis in a solid lesion (odds ratio, 107) and vegetations in a cystic lesion (odds ratio, 40).

Another study conducted by S.A. Aslam Sohaib et al (2003) [11] similarly concluded that MR imaging is highly accurate in the characterization of adnexal mass lesions, and the best predictors of malignancy are vegetation in a cystic lesion and ascites.

Thomassin-Naggara I et al (2007) [12] assessed the accuracy of magnetic resonance imaging (MRI), particularly, dynamic MRI, in distinguishing ovarian fibromas from subserous uterine leiomyomas. Fifteen ovarian fibromas and 15 subserous uterine leiomyomas were retrospectively reviewed. Visualization of

arterial vessels was more frequent in uterine leiomyomas than in ovarian fibromas (P= 0.002). The DCE MR enhancement rate was higher for uterine leiomyomas than for ovarian fibromas in terms of both maximal enhancement ($P < 0.001$) and enhancement rate at 30 ($P = 0.009$), 60 ($P = 0.007$), and 90 seconds ($P = 0.0009$). It was suggested that DCE MRI can distinguish ovarian fibromas from uterine leiomyomas and should be used if sonography fails to show the origin of a pelvic mass.

Thomassin-Naggara I et al (2011) [13] evaluated the value of adding perfusion-weighted (PW) and diffusion-weighted (DW) sequences to a conventional magnetic resonance (MR) imaging protocol to differentiate benign from malignant tumors in 87 women who underwent imaging before surgery for complex adnexal masses. The addition of both PW and DW images led to a correct change in the diagnosis in 19% (11 of 57 patients), 23% (13 of 57 patients), and 24% (14 of 57 patients) of cases for readers 1, 2, and 3, respectively, with no incorrect changes. Conventional, PW, and DW MR imaging criteria were combined to generate a decision tree giving an accuracy of 95%.

M. Bazot et al (2013) [14] analysed the morphological magnetic resonance imaging features (MRI) features of borderline ovarian tumours to evaluate whether MRI can be used to differentiate serous from mucinous subtypes. A retrospective study of 72 patients who underwent resection was undertaken. MRI images were reviewed and it was concluded that vegetations and multilocularity are two independent MRI features that can help to distinguish between serous and mucinous borderline ovarian tumors.

Jori S. Carter, MD, MS et al (2014) [15] performed quantitative multi parametric MRI in 37 women with ovarian masses with 3 Tesla MRI. Mean ROI values were compared between benign and malignant masses using generalised estimating equations. Rate constant (kep) was significantly higher in malignant masses, as well as quantitative T2 values (p=0.003), and signal intensity on T2 weighted imaging. Mean ktrans for benign and malignant lesions was 0.06 and 0.10 respectively. Conclusion was made that quantitative parameters from DCE-MRI and T2 mapping can differentiate benign from malignant ovarian masses.

Eman Nasr et al (2014) [16] evaluated the role of DCE MRI in correlation with DWMRI in 30 patients. Pelvic MR with DWI was done for all patients, The mean ADC values for malignant lesions were (0.84 × 10−3 ± 0.1 SD mm2/s), while that for benign lesions were (1.8 × 10−3 ± 0.5 SD mm2/s), with cut off 1.2 × 10−3. Hemorrhagic cysts and endometriomas showed high signal not only on diffusion images but also on corresponding ADC map and ADC values 1.3–1.4 × 10−3 (T2 Shine-through). Sensitivity of MRI was 99.9% while that of DCE-MRI was 60%. The specificity was higher for DCE (91%) compared to conventional MRI sequences (58.3%), as well as the accuracy which was 73.9% for MRI while that of DCE was 77%.

Alpana Karnik et al (2015) [17] evaluated the role of MRI in characterising adnexal masses. Serous cystadenoma shows clear fluid, mucinous cystadenomas are usually multiloculated with different signal intensities. T1W fat suppressed sequences can help in differentiation of hemorrhagic and fat components (dermoid). Solid ovarian tumours include sex cord stromal, germ cell tumors, fibroma and thecoma. Most germ cell tumors are solid cystic,

dysgerminomas can be solid. Malignant tumours usually show solid component/papillary projections/thick septations with post contrast enhancement. Endometrioma show high T1 and T2 signal intensity with T2 shading. Salpingitis with abscess formation can also present as adnexal mass, MRI with contrast will show rim enhancement. Large adnexal masses should be imaged with MRI for better characterisation.

Pourashaf M et al (2015) [18] conducted a study on 56 patients with adnexal masses, who underwent DWI and DCE-MRI examinations, prior to surgery. The mean ADC value was significantly lower in malignant adnexal masses ($p<0.001$). An ADC value<1.20?10-3 mm2/s may be the optimal cutoff for differentiating between benign and malignant tumors. DWI signal intensity, mean ADC value, and TIC type were determined for all the masses and they concluded that DWI, ADC value and TIC type derived from DCE-MRI are all sensitive and relatively specific methods for differentiating benign from malignant adnexal masses. By comparing these functional MR techniques, TIC was found to be more accurate than DWI and ADC.

Kim HJ et al (2016) [19] evaluated the diagnostic performance of diffusion-weighted imaging (DWI) in differentiating malignant from benign ovarian masses. The meta-analysis is based on 21 studies, which reported the findings for 731 malignant and 918 benign ovarian masses. The weighted mean difference (WMD) and corresponding 95% confidence interval (95% CI) were calculated. Subgroup analysis by benign tumor type revealed higher ADC values for cysts, cystadenomas and other benign tumors compared to malignant masses. On the other hand, lower ADC values were observed for endometrioma and teratoma compared to malignant masses. Subgroup

analysis by mass property revealed higher ADC values in cystic tumor types than in solid types for both benign and malignant tumors.

Takeuchi M et al (2016) [20] evaluated the feasibility of diffusion-weighted imaging (DWI) with apparent diffusion coefficient (ADC) measurement in differentiating benign and malignant ovarian tumors. Surgically proven 49 ovarian tumors (39 malignant/borderline malignant and 10 benign) were examined and they found that the solid portion of all 39 malignant tumors showed homogeneous or heterogeneous high intensity on DWI, whereas only 3 of the 10 benign tumors (3 thecomas) showed high intensity. The mean (SD) ADC value in the 39 malignant tumors (1.03 [0.19]) was significantly lower than that in 10 benign tumors (1.38 [0.30]). A relatively low ADC (1.08-1.20) in the 3 thecomas may reflect their abundant cellular nature, and the presence of low intensity on T2-weighted images was suggestive for benign fibrous tumor.

6.3 AIMS AND OBJECTIVES OF THE STUDY

1. To assess the role of advanced MRI sequences (Diffusion Weighted Imaging and Dynamic Contrast Enhanced) in characterisation of adnexal masses, into benign and malignant, with reference to histopathological examination wherever possible.

7. MATERIALS AND METHODS

7.1 Source of Data

A prospective study of patients undergoing an MRI Pelvis for previously detected adnexal masses, at the Department of Radiodiagnosis, Dayanand Medical College & Hospital, during a one year period.

7.2 METHOD OF COLLECTION OF DATA

Patients having previously detected adnexal masses will be included in study. Consent will be obtained from each patient and relevant detailed history will be elicited from all patients. Findings of general physical and systemic examination will be recorded in detail. Before starting the MRI study, the procedure will be explained to the patient in his/her vernacular language to allay the fear and anxiety. Written informed consent will be taken.

Inclusion criteria

- All patients found to have an adnexal mass on MRI

Exclusion criteria

- Any contraindications to MRI (patients with cardiac pacemakers, claustrophobic patients)
- Any contraindications to contrast administration (GFR < 30ml/min)
- Anyone who is unwilling to participate in the study

MR imaging technique

MR imaging will be performed on a 3-T unit (Magnetom Skyra, Siemens, Germany). Following MR imaging sequences to be included:

Sequences	Repetition time (ms)	Echo time(ms)	Flip angle (degree)	Section thickness (mm)	Matrix (mm)	Field of view (mm)
T2 Sag	2800	87	150	3	269x384	230
T1 axial	680	18	150	3	256x320	220
T1 axial FS	600	20	150	3	224x320	220
T2 axial	3100	89	150	3	269x384	220
T2 coronal	2800	87	175	3	269x384	230
DWI	4000	64	-	3	114x114	220
DCE axial	5.08	1.77	15	4	154x192	260
T1 FS PC	600	20	160	3.5	224x320	220

Dynamic Contrast Enhanced MRI

After identification of the abnormal region, Dynamic Contrast Enhanced MRI is performed using the three dimensional volume interpolated breath hold examination (3D VIBE) sequence in the transverse plane.

A rapid bolus of 0.1mmol/kg body weight gadopentetate dimeglumine is to be given through a peripheral vein. A total of 35 measurements are taken and the total acquisition time is 4 minutes 44 seconds.

Enhancement curve calculation: By drawing regions of interest (ROIs) in the dynamic sequence. One ROI will be obtained from the enhancing region of adnexal mass, and another ROI will be obtained from external myometrium, which acts as the internal reference.

Image and data analysis

Tumor size, multilocularity, the presence of loculi with different signal intensities, the presence of a solid and/or cystic component, the presence of

thickened septa, vegetations, and/or a solid portion within a cystic tumor are to be recorded.

DW and ADC images are analysed to look for any diffusion restriction (high signal intensity on high b value DW image with associated low ADC (apparent diffusion coefficient). ADC value will be recorded from the region of diffusion abnormality.

Dynamic enhancement pattern will be evaluated according to a previously established time–signal intensity curve classification.

Time intensity curve of solid tissue in an adnexal mass is compared to that of external myometrium, which acts as the internal reference.

When solid tissue is enhanced with a weak and progressive curve in comparison to the myometrium, the curve is named "type 1."

When solid tissue is enhanced with a moderate enhancement in comparison to myometrium with a plateau, the curve is named "type 2."

When solid tissue is enhanced with a curve steeper than that of myometrium, whatever the intensity of enhancement, the curve is named "type 3"

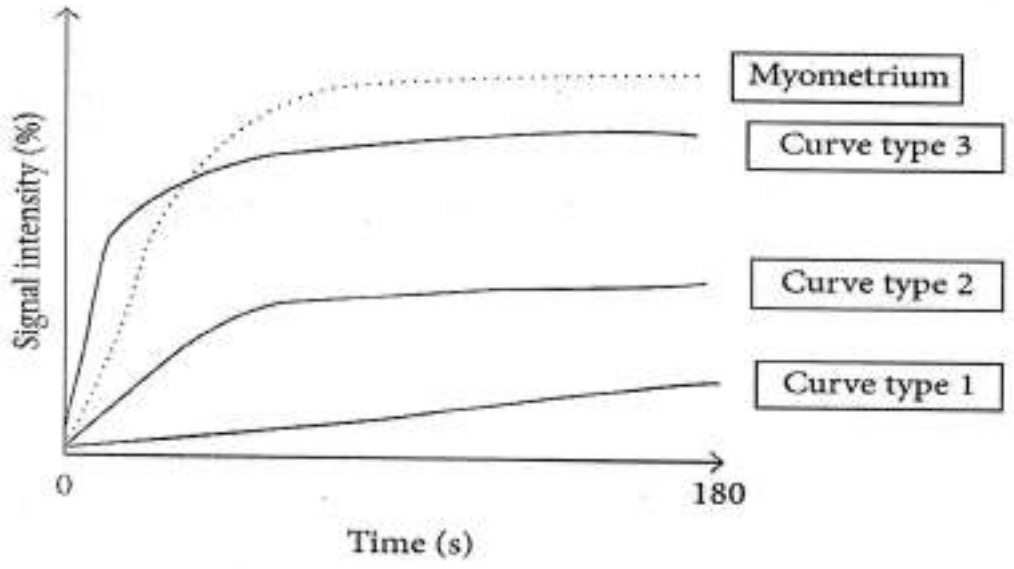

Figure: Time-Intensity Curve[13]

The final objective will be to estimate the sensitivity, specificity, positive predictive value (PPV), negative predictive value (NPV) of the following MRI-based parameters in benign as well as malignant masses, with histopathological examination to be used as the reference standard.

- T2 signal intensity
- Mean ADC
- Type of curve (Time intensity curve)

OUTCOME:

Analysing the MR findings and classifying the adnexal masses into benign and malignant and their correlation with the histopathological findings wherever possible.

Whether there is any added advantage of DWI and DCE over conventional MRI sequences alone in the characterisation into benign and malignant.

STATISTICAL ANALYSIS:

Data will be described in terms of range; mean ±standard deviation (±SD), median, frequencies (number of cases) and relative frequencies (percentages) as appropriate. Comparison of quantitative variables between the study groups will be done using Student t-test and Mann Whitney U test for independent samples for parametric and non-parametric data respectively. For comparing categorical data, Chi square ($\chi 2$) test will be performed and exact test will be used when the expected frequency is less than 5. Sensitivity, specificity, positive and negative predictive values and accuracy of each method and its confidence interval (95% CI) will also be determined, besides the Youden index (probability of correct classification) and determining the area under the ROC curve. A probability value (p value) less than 0.05 will be

considered statistically significant. All statistical calculations will be done using SPSS (Statistical Package for the Social Science) SPSS 21 version statistical program for Microsoft Windows.

7.3 DOES THE STUDY REQUIRE ANY INVESTIGATIONS OR INTERVENTIONS TO BE CONDUCTED ON PATIENTS OR OTHER HUMANS OR ANIMALS? IF SO, PLEASE DESCRIBE BRIEFLY.

The study requires MRI pelvis to be done on patients with adnexal masses. However, the study does not require any intervention to be done on patients, other humans or animals.

7.4 HAS ETHICAL CLEARANCE BEEN OBTAINED FROM YOUR INSTITUTION IN CASE OF 7.3?

Yes, attached herewith

8. LIST OF REFERENCES

1. Timmerman D, Schwärzler P, Collins WP , Claerhout F, Coenen M, Amant F, et al. Subjective assessment of adnexal masses with the use of ultrasonography: an analysis of interobserver variability and experience. Ultrasound Obstet Gynecol. 1999;13:11-6.
2. Sahdev A. CT in ovarian cancer staging: how to review and report with emphasis on abdominal and pelvic disease for surgical planning. Cancer Imaging. 2016;16:19.
3. Foti PV, Attinà G, Spadola S, Caltabiano R, Farina R, Palmucci S, et al. MR imaging of ovarian masses: classification and differential diagnosis. Insights Imaging. 2016;7:21–41.
4. Yamashita Y, Torashima M, Hatanaka Y, Harada M, Higashida Y, Takahashi M, et al. Adnexal masses: accuracy of characterization with transvaginal US and precontrast and postcontrast MR imaging. Radiology. 1995;94:557-65.
5. Thomassin-Naggara I, Toussaint I, Perrot N, Rouzier R, Cuenod CA, Bazot M, et al . Characterization of complex adnexal masses: value of adding perfusion-and diffusion-weighted MR imaging to conventional MR imaging. Radiology. 2011;258:793-803.
6. Mansour S, Wessam R, Raafat M. Diffusion-weighted magnetic resonance imaging in the assessment of ovarian masses with suspicious features: Strengths and challenges. The Egyptian Journal of Radiology and Nuclear Medicine. 2015;46:1279-89.
7. Elzayata WA El-Kalioubiea M Abdel-Nabya MM Abdel-Malekb RR. The role of dynamic contrast enhanced MR imaging in the assessment of

inconclusive ovarian masses. The Egyptian Journal of Radiology and Nuclear Medicine. 2017;48:1159-69.

8. Bakir B, Bakan S, Tunaci M. Diffusion-weighted imaging of solid or predominantly solid gynaecological adnexial masses: is it useful in the differential diagnosis?. Br J Radiol. 2011;84:600-11.
9. Mohaghegh P, Rockall AG. Imaging Strategy for Early Ovarian Cancer: Characterization of Adnexal Masses with Conventional and Advanced Imaging Techniques. Radiographics. 2012;32:1751-73.
10. Hricak H, Chen M, Coakley FV, Kinkel K, Yu KK, Sica G, et al. Complex adnexal masses: detection and characterization with MR imaging--multivariate analysis. Radiology. 2000;214:39-46.
11. Sohaib SA, Sahdev A, Van Trappen P, Jacobs IJ, Reznek RH. Characterization of Adnexal Mass Lesions on MR Imaging. AJR Am J Roentgenol. 2003;180:1297-304.
12. Thomassin-Naggara I, Daraï E, Nassar-Slaba J, Cortez A, Marsault C, Bazot M. Value of Dynamic Enhanced Magnetic Resonance Imaging for Distinguishing Between Ovarian Fibroma and Subserous Uterine Leiomyoma. J Comput Assist Tomogr 2007;31:236-42.
13. Thomassin-Naggara I, Balway D, Rockall A, Carrete MF, Ballester M, Darai E, et al. Added Value of Assessing Adnexal Masses with Advanced MRI Techniques. Biomed Res Int. 2015;2015:785206.
14. Bazot M, Haouy D, Daraï E, Cortez A, Dechoux-Vodovar S, Thomassin-Naggara I. Is MRI a useful tool to distinguish between serous and mucinous borderline ovarian tumours? Clin Radiol. 2013;68:e1-8.

15. Carter JS, Koopmeiners JS, Kuehn-Hajder JE, Metzger GJ, Lakkadi N, Downs LS Jr, et al. Quantitative multiparametric MRI of ovarian cancer. J Magn Reson Imaging. 2013;38:1501-9.
16. Nasra E, Hamed I, Abbas I, Khalifa NM. Dynamic contrast enhanced MRI in correlation with diffusion weighted (DWI) MR for characterization of ovarian masses. The Egyptian Journal of Radiology and Nuclear Medicine. 2014;45:975-85.
17. Karnik A, Tembey RA, Mani S. Value of MRI in Characterizing Adnexal Masses. J Obstet Gynaecol India. 2015;65:259–66.
18. Malek M, Pourashraf M, Mousavi AS, Rahmani M, Ahmadinejad N, Alipour A, et al. Differentiation of benign from malignant adnexal masses by functional 3 tesla MRI techniques: diffusion-weighted imaging and time-intensity curves of dynamic contrast-enhanced MRI. Asian Pac J Cancer Prev. 2015;16:3407-12.
19. Kim HJ, Lee SY, Shin YR, Park CS, Kim K. The Value of Diffusion-Weighted Imaging in the Differential Diagnosis of Ovarian Lesions: A Meta-Analysis. PLoS One. 2016;11:e0149465.
20. Takeuchi M, Matsuzaki K, Nishitani H. Diffusion-weighted magnetic resonance imaging of ovarian tumors: differentiation of benign and malignant solid components of ovarian masses. J Comput Assist Tomogr. 2010;34:173-6.

PROFORMA

S.No. MRD No.

Name Age

Address

Contact no.

Date of admission Date of discharge

Chief complaints

Systemic examination

Clinical diagnosis

Laboratory investigations

- hemogram
- LFTs
- RFTs
- CA125

Sonographic findings and diagnosis

MRI findings

- Size
- Solid components
- Cystic
- Mixed
- Wall thickness

Signature of Candidate **Signature of Supervisor**

- Septations
- Calcifications
- Necrosis
- Papillary projections
- Tumor vessels
- Lymph nodes
- Peritoneal/omental implants

DWI

- Focal signal hyperintensity on DWI
- Focal signal hypointensity on ADC map
- ADC value

Dynamic contrast enhanced MRI

- Pattern of enhancement
- Washout pattern
- Type of curve

MRI Diagnosis:

PET-CT Findings (if any):

Intra-operative findings:

Report of histopathology:

Follow-up findings (3-6 monthly follow-up):

Signature of Candidate **Signature of Supervisor**

INFORMED PATIENT CONSENT

Date: _____

I.....D/o, W/o, S/o..... .....am willing to participate in the study **"ROLE OF ADVANCED MRI SEQUENCES IN THE CHARACTERISATION OF ADNEXAL MASSES"** The procedure with its complications has been explained to me in local vernacular language. I have fully understood that no special tests and extra expenditure in any form, merely for the purpose of thesis is being carried out. I am free to opt out the study any time without assigning any reason.

.....
Signature of the Witness

Name:

.....
Signature of the patient

Signature of Candidate

Signature of Supervisor

मरीज अनुमति फार्म

तिथि _____

मैं _____ पत्नी/पुत्र/पुत्री _____

निवासी _____

इस शोधकार्य **"ROLE OF ADVANCED MRI SEQUENCES IN THE CHARACTERISATION OF ADNEXAL MASSES"** में भाग लेने के लिए सहमत हूँ। मैं इस शोधकार्य में भाग लेने के लिए अपनी स्वेच्छा से तैयार हूँ। मैं पुष्टि करता/करती हूँ की यह स्वीकृति देने के लिए मुझे कोई आर्थिक प्रलोभन नहीं दिया गया और न ही दबाव डाला गया है। मुझे इस शोधकार्य का उद्देश्य स्पष्ट कर दिया गया है और मुझे यह विश्वास है की यह विज्ञान और मानवता के लाभ के लिए है। मुझे इस शोधकार्य में होने वाले जोखिम के बारे में समझा दिया गया है और मेरी समझ में यह जोखिम बहुत मामुली है।

मैं इस शोधकार्य में भाग लेने के सम्बन्ध में किसी भी समय अपनी अस्वीकृति व्यक्त कर सकता/सकती हूँ और मेरे अस्वीकृति व्यक्त करने का मेरे इलाज पर कोई प्रभाव नहीं पड़ेगा।

_____ _____

गवाह के हस्ताक्षर रोगी के हस्ताक्षर/अंगूठे का निशान

नाम: नाम:

_____

अन्वेषक के हस्ताक्षर

_____

विद्यार्थी के हस्ताक्षर

ਮਰੀਜ਼ ਰਜ਼ਾਮੰਦੀ ਫਾਰਮ

ਮਿਤੀ_____

ਮੈ_____ਪਤਨੀ/ਪੁੱਤਰ/ਪੁੱਤਰੀ_____

ਵਾਸੀ _____

"ROLE OF ADVANCED MRI SEQUENCES IN THE CHARACTERISATION OF ADNEXAL MASSES" ਤੇ ਚਲ ਰਹੀ ਖੋਜ ਵਿਚ ਹਿੱਸਾ ਲੈਣ ਲਈ ਰਜ਼ਾਮੰਦ ਹਾਂ। ਇਸ ਖੋਜ ਕੰਮ ਵਿਚ ਹਿੱਸਾ ਲੈਣ ਲਈ ਮੈ ਆਪਣੀ ਮਰਜ਼ੀ ਨਾਲ ਤਿਆਰ ਹਾਂ। ਮੈ ਇਹ ਦਸਣਾ ਚਾਹੁੰਦਾ ਹਾਂ/ ਚਾਹੁੰਦੀ ਹਾਂ ਕੇ ਇਹ ਰਜ਼ਾਮੰਦੀ ਦੇਣ ਵਾਸਤੇ ਮੈਨੂ ਕਿਸੇ ਵੀ ਤਰਾਂ ਦਾ ਲੋਭ-ਲਾਲਚ ਨਹੀ ਦਿੱਤਾ ਗਿਆ ਅਤੇ ਨਾ ਹੀ ਕੋਈ ਦਬਾ ਪਾਇਆ ਗਿਆ ਹੈ। ਮੈਨੂ ਇਸ ਖੋਜ ਦਾ ਮਨੋਰਥ ਸਮਝਾ ਦਿੱਤਾ ਗਿਆ ਹੈ ਅਤੇ ਮੈਨੂ ਇਹ ਭਰੋਸਾ ਦਵਾਇਆ ਗਿਆ ਹੈ ਕੇ ਇਹ ਖੋਜ ਵਿਗਿਆਨ ਅਤੇ ਮਾਨਵਤਾ ਦੀ ਭਲਾਈ ਲਈ ਹੈ। ਮੈਨੂ ਇਸ ਖੋਜ ਵਿਚ ਹੋਣ ਵਾਲੇ ਖਤਰੇ ਬਾਰੇ ਸਮਝਾ ਦਿੱਤਾ ਗਿਆ ਹੈ ਅਤੇ ਮੈਨੂ ਇਹ ਯਕੀਨ ਹੈ ਕੇ ਇਹ ਖਤਰਾ ਬਹੁਤ ਮਾਮੂਲੀ ਹੈ। ਮੈਨੂ ਇਸ ਖੋਜ ਕੰਮ ਵਿਚ ਹਿੱਸਾ ਲੈਣ ਦਾ ਢੰਗ – ਤਰੀਕਾ ਸਮਝਾ ਦਿੱਤਾ ਗਿਆ ਹੈ।

ਮੈ ਇਸ ਖੋਜ ਕੰਮ ਵਿਚ ਹਿੱਸਾ ਲੈਣ ਬਾਰੇ ਆਪਣੀ ਰਜ਼ਾਮੰਦੀ ਕਿਸੇ ਵੀ ਸਮੇ ਵਾਪਸ ਲੈ ਸਕਦਾ ਹਾਂ/ ਸਕਦੀ ਹਾਂ ਅਤੇ ਮੇਰੀ ਰਜ਼ਾਮੰਦੀ ਵਾਪਸ ਲੈਣ ਦਾ ਮੇਰੇ ਇਲਾਜ ਤੇ ਕੋਈ ਅਸਰ ਨਹੀ ਹੋਵੇਗਾ।

_____ _____

ਗਵਾਹ ਦੇ ਹਸਤਾਖਰ ਮਰੀਜ਼ ਦੇ ਹਸਤਾਖਰ

ਮਿਤੀ_____ ਮਿਤੀ_____

ਪਤਾ _____ ਪਤਾ _____

_____

ਨਿਰੀਖਕ ਦੇ ਹਸਤਾਖਰ

_____

ਸਿਖਿਆਰਥੀ ਦੇ ਹਸਤਾਖਰ